

# **EVALUATION OF BEHAVIOUR FACTORS OF STEEL MOMENT RESISTING FRAMES**

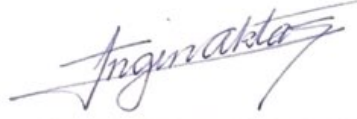
**A Thesis submitted to  
Graduate School of Engineering and Science of  
İzmir Institute of Technology  
in Partial Fulfillment of the Requirements for the Degree of  
MASTER OF SCIENCE  
in Civil Engineering**

**by  
İbrahim BARAN**

**July 2019  
İZMİR**

We approve the thesis of İbrahim BARAN

**Examining Committee Members:**



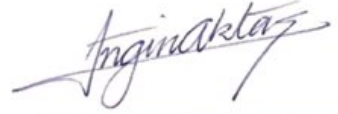
**Assoc. Prof. Dr. Engin AKTAŞ**  
Department of Civil Engineering, İzmir Institute of Technology



**Assoc. Prof. Dr. İzzet ÖZDEMİR**  
Department of Civil Engineering, İzmir Institute of Technology

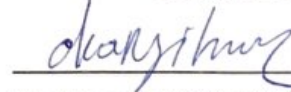


**Assoc. Prof. Dr. Emre ERCAN**  
Department of Civil Engineering, Ege University

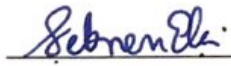


**Assoc. Prof. Dr. Engin AKTAŞ**  
Supervisor,  
Department of Civil Engineering  
İzmir Institute of Technology

12 July 2019



**Dr. Alper KANYILMAZ**  
Co-supervisor, Architecture, Built  
Environment and Construction  
Engineering  
Politecnico di Milano



**Prof. Dr. Şebnem ELÇİ**  
Head of the Department of  
Civil Engineering

**Prof. Dr. Aysun SOFUOĞLU**  
Dean of the Graduate School of  
Engineering and Sciences

## **ACKNOWLEDGMENTS**

I would like to express my gratitude to my supervisor Assoc. Prof. Dr. Engin AKTAŞ for sharing his valuable knowledge, friendly attitude, strong motivation and support during this study.

I am also very glad and thankful for having met and worked with my co-advisor Dr. Alper KANYILMAZ, from the Architecture, Built Environment and Construction Engineering Department at Politecnico di Milano, and for his interest, valuable comments, and contributions throughout this study.

I would like to express my thanks to my all undergraduate and graduate instructors from Civil Engineering Department of İzmir Institute of Technology (İYTE) for their advice and guidance.

I would like to thank the love of my life Sadiye AKKILIÇ, for her endless patience, strong motivation and for making hard things easier.

Finally, I am grateful to my family for their unconditional support and endless love throughout my life.

# ABSTRACT

## EVALUATION OF BEHAVIOUR FACTORS OF STEEL MOMENT RESISTING FRAMES

Builders of structures throughout the history of civilizations have been challenged with various threats. Earthquakes, which may be considered as the most critical challenge of the built environment have been one of the main concerns of builders at all times especially in regions with high earthquake risk.

In this study, Response Modification Factor, (also known as 'R' or 'q' factor) which is used by seismic codes to determine force demand considering the ductile behaviour of the structure during the earthquake, has been analyzed. Steel frames (36 frames) with a different number of stories (3,6,9) and bays (3 to 8) were designed with normal ductility (18 frames) and high ductility (18 frames) moment resisting steel frames.

The Turkish Building Earthquake Code-2018 (TBEC 2018) was followed for the seismic design process. All frames were assumed to be constructed in a region with the highest seismic demand defined in the web-based Hazard Map in TBEC 2018. The performance evaluation of the designed frames is completed using non-linear static analyses following FEMA, ATC-40 and NEHRP guidelines.

The non-linear static analyses were implemented with SAP2000 v20.2 commercial software. Static pushover analysis as well as the capacity curve graph, known as the N2 method, has been obtained, and the position of the frame capacity in the spectral acceleration graph has been determined and presented visually.

The results were summarized and the R factors obtained from these analyses were compared with the values given in the Turkish Building Earthquake Code.

Key words: behaviour factor, nonlinear analysis, moment resisting steel frames.

# ÖZET

## MOMENT AKTARAN ÇELİK ÇERÇEVELERDE DAVRANIŞ KATSAYISININ DEĞERLENDİRİLMESİ

Medeniyet tarihi boyunca yapıları inşaa edenler çeşitli tehditlere karşı yapıları güvenli kılmak için uğraş vermişlerdir. Yapılı çevre için en önemli meydan okuyucu olarak düşünülebilecek olan deprem, özellikle deprem riski yüksek olan bölgelerde her zaman ana kaygılardan biri olmuştur.

Bu çalışmada, deprem kodlarının deprem talebini belirlemede yapının sünek davranışını hesaba katmak için kullandıkları 'R' veya 'q' katsayısı olarak bilinen Taşıyıcı Sistem Davranış Katsayısı incelenmiştir. Bu çalışmada incelenen çelik çerçeveler (36 çerçeve) farklı kat adetleri (3,6,9) ve farklı açıklıklarda (3'ten 8'e kadar) olmak üzere süneklik düzeyi normal (18 çerçeve) ve süneklik düzeyi yüksek (18 çerçeve) olan moment aktaran çelik çerçeveler olarak tasarlanmıştır.

Sismik tasarım sürecinde, Türkiye Bina Deprem Yönetmeliği-2018 (TBDY 2018) esas alınmıştır. Tüm çerçevelerin TBDY 2018'de yer alan Risk Haritası'ndaki en yüksek deprem talebi bulunan bölgede yapılacağı varsayılmıştır. Tasarlanan çerçevelerin performans değerlendirmesi, FEMA, ATC-40 ve NEHRP yönergelerindeki lineer-olmayan statik analizler kullanılarak gerçekleştirilmiştir.

Doğrusal-olmayan analizler SAP2000 v20.2 ticari yazılımı ile uygulanmıştır. Statik itme analizi yanı sıra N2 metod olarak bilinen kapasite eğrisi grafiği de elde edilmiş olup, çerçeve kapasitesinin spektral ivme grafiğindeki yeri de belirlenmiş ve görsel olarak sunulmuştur.

Yapılan analizler sonucunda her çerçeve için elde edilen R katsayısı Türk Bina Deprem Yönetmeliği'nde verilen değerleri ile kıyaslanarak değerlendirilmiştir.

Anahtar Sözcükler: davranış katsayısı, doğrusal olmayan analiz yöntemi, moment aktaran çelik çerçeveler.

# TABLE OF CONTENTS

LIST OF FIGURES .....	ix
LIST OF TABLES.....	xi
LIST OF ABBREVIATION.....	xii
CHAPTER 1 INTRODUCTION .....	1
1.1 Objective and Scope.....	3
1.2 Thesis Organization .....	4
CHAPTER 2 GENERAL INFORMATION.....	6
2.1 Steel Structures In Seismic Zones.....	6
2.2 System Reliability and Structural Design .....	9
2.3 System Limit States.....	10
2.4 Lateral Load Resisting Systems .....	12
2.4.1 Moment Resisting Steel Frames .....	14
2.4.2 Special Moment Frames (SMF).....	15
2.4.3 Ordinary Moment Frames (OMF) .....	16
CHAPTER 3 RESPONSE MODIFICATION FACTORS.....	17
3.1 Historical Evaluation and Formulation of R Factor.....	18
3.1.1 Chia-Ming Uang, 1991 [31].....	19
3.1.2 Whittaker et al., 1999 [23].....	21
3.1.3 Patel and Sahah, 2010 [33] .....	23
3.1.4 Ferraioli et al., 2012 [21] .....	24
3.1.5 Castiglioni et al., 2017 [35] .....	25
3.2 Overstrength Factor.....	27
3.2.1 Previous Studies of Overstrength Factor .....	27
3.3 Ductility Factor .....	28
3.3.1 Previous Studies of Ductility Factor .....	30

3.4	Redundancy Factor.....	31
3.4.1	Previous Studies of Redundancy Factor .....	32
CHAPTER 4	NONLINEAR STATIC ANALYSIS .....	34
4.1	Pushover Analysis.....	35
4.2	Capacity Spectrum Method.....	36
4.2.1	Previous Studies of Capacity Spectrum Method .....	37
CHAPTER 5	METHOD OF ANALYSIS .....	45
5.1	Frame Type .....	45
5.2	Frame Design .....	45
5.2.1	Equivalent Lateral Load Analysis.....	46
5.2.2	Gravitational Load Analysis .....	48
5.2.3	Load Combinations.....	50
5.2.4	Sample Design .....	50
5.3	Nonlinear Static Analysis.....	53
5.4	Analysis Results .....	54
5.4.1	Pushover Analysis.....	56
5.4.2	Capacity Spectrum.....	57
5.4.3	The Idealization of Pushover Graph .....	59
5.4.4	Evaluation of R Factors .....	60
CHAPTER 6	RESULTS OF ANALYSIS AND FURTHER REMARKS.....	64
CHAPTER 7	SUMMARY OF ANALYSIS AND CONCLUSIONS .....	70
7.1	SUMMARY OF RESULTS.....	70
7.2	CONCLUSIONS.....	71
7.3	SUGGESTIONS .....	72
REFERENCES	.....	74
APPENDICES		
APPENDIX A	FRAME SECTIONS.....	79

APPENDIX B PUSHOVER AND SPECTRAL CAPACITY CURVES .....	1033
APPENDIX C SUPERIMPOSING CAPACITY CURVES FOR OMRF AND SMRF.....	139

# LIST OF FIGURES

<b><u>Figure</u></b>	<b><u>Page</u></b>
Figure 2.1 Steel structure surrounded by ruins in Tokyo .....	8
Figure 2.2 Cross-Sectional Member Damage Limits .....	11
Figure 2.3 Common configurations of Concentrically Braced Frames (CBF).....	13
Figure 2.4 Typical configurations of Eccentrically Braced Frames (EBF) .....	13
Figure 2.5 Plastic Hinge Deformation .....	14
Figure 2.6 Anticipated sideways mechanisms in SMF.....	15
Figure 3.1 General structure response .....	19
Figure 3.2 Sample base shear force versus roof displacement relationship .....	21
Figure 3.3 Definition of the response reduction factor .....	23
Figure 3.4 Base shear versus roof displacement relationship.....	24
Figure 3.5 Transition of load-transfer mechanisms: (a) the prototype structure; (b) flexural load transfer mechanism; (c) tensile load mechanism .....	33
Figure 4.1 Pushover analysis of an eight-story MRSF designed according to Eurocode 3 and Eurocode 8.....	37
Figure 4.2 Typical capacity curve.....	39
Figure 4.3 Capacity spectrum conversion.....	40
Figure 4.4 Response spectrum conversion .....	40
Figure 4.5 Typical elastic acceleration ( $S_{ae}$ ) and displacement spectrum ( $S_{de}$ ) for 5 percent damping normalized to 1.0g peak ground acceleration.....	41
Figure 4.6 Ductility-dependent reduction factor $R_{\mu}$ versus period (T).....	42
Figure 4.7 Demand spectra for constant ductilities in ADRS format.....	42
Figure 4.8 The relative effectiveness of strengthening.....	43
Figure 4.9 Determination of performance point .....	43
Figure 4.10 Performance point .....	44
Figure 5.1 Lateral elastic design acceleration spectrum .....	47
Figure 5.2 Gravity load distribution on slab (a), on beam (b) and equivalent distribution.....	49
Figure 5.3 Gravity load distribution on beam (two adjacent slabs).....	50
Figure 5.4 3x3 Moment resisting frame (SAP2000).....	51
Figure 5.5 Normal ductility level moment resisting frame design properties	

	(SAP2000) .....	51
Figure 5.6	High ductility level moment resisting frame design properties (SAP2000) .....	52
Figure 5.7	Auto plastic hinge defining properties for the beam (SAP2000) .....	53
Figure 5.8	Defined plastic hinge boundaries for the beam (SAP2000) .....	53
Figure 5.9	Auto plastic hinge defining properties for column (SAP2000).....	54
Figure 5.10	Interaction diagram properties for column (SAP2000) .....	54
Figure 5.11	Plastic hinge formations for OMRF .....	55
Figure 5.12	Plastic hinge formations for SMRF .....	55
Figure 5.13	Pushover curve for both normal (a) and high (b) ductility level 3x3 frames.....	56
Figure 5.14	Spectral capacity curve for both normal (a) and high (b) ductility level 3x3 frames (SAP2000).....	57
Figure 5.15	Spectral capacity curve for both normal (A33R4) and high (A33R8) ductility level 3x3 frames .....	58
Figure 5.16	Idealized pushover curve for normal (A33R4) ductility level 3x3 frame ..	59
Figure 5.17	Idealized pushover curve for high (A33R8) ductility level 3x3 frame .....	60
Figure 5.18	Representation of R value component's parameters for A33R4 frame.....	63
Figure 5.19	Representation of R value component's parameters for A33R8 frame.....	63
Figure 6.1	R Values for Ordinary Moment Resisting Frames .....	66
Figure 6.2	R Values for Special Moment Resisting Frames.....	66
Figure 6.3	Response Modification Factor (R) for each story (3-6-9) vs. bays (3-4-5-6-7-8) ( $R_{design}=4$ ).....	67
Figure 6.4	Response Modification Factor (R) for each bay (3-4-5-6-7-8) vs. stories (3-6-9) ( $R_{design}=4$ ) .....	67
Figure 6.5	Response Modification Factor (R) for each story (3-6-9) vs. bays (3-4-5-6-7-8) ( $R_{design}=8$ ).....	68
Figure 6.6	Response Modification Factor (R) for each bay (3-4-5-6-7-8) vs. stories (3-6-9) ( $R_{design}=8$ ) .....	68
Figure 6.7	Superimposing pushover curve of OMRF and SMRF .....	69
Figure 6.8	Superimposing capacity curve of OMRF and SMRF .....	69

## LIST OF TABLES

<b><u>Table</u></b>	<b><u>Page</u></b>
Table 3.1. $\alpha$ & $\beta$ coefficient proposed by Lai and Biggs [25] .....	31
Table 3.2. Draft Redundancy Factor .....	32
Table 5.1. Local ground impact coefficients for short period [4] .....	48
Table 5.2. Local ground impact coefficients for 1 second period [4] .....	48
Table 5.3. Frame names and expressions .....	52
Table 5.4. Design force $V_{te}$ .....	60
Table 5.5. R factor and its parameters .....	61
Table 6.1. Calculated R factors .....	64
Table 6.2. R values for both OMRF and SMRF .....	65

## **LIST OF ABBREVIATION**

ADRS	Acceleration-Displacement Response Spectrum
ASCE	American Society of Civil Engineers
ATC	Applied Technology Council
ANSI	American National Standards Institute
AISC	American Institute of Steel Construction
FEMA	Federal Emergency Management Agency
TBEC	Turkish Building Earthquake Code
NEHRP	National Earthquake Hazards Reduction Program
SEI	Structural Engineering Institute
SEOAC	Structural Engineers Association of California
UBC	Uniform Building Code

# CHAPTER 1

## INTRODUCTION

Each year, several thousands of earthquakes occur around the world. Although most of these earthquakes have low severity and do not cause any damage to the buildings, some of them are severe and cause major damage in buildings. The casualties are the common aftermath of the severe earthquakes. In order to minimize the damage caused by an earthquake, the demand of earthquakes on structures are estimated, and design is carried out. It is not easy to determine the earthquake a structure may experience but codes provide design earthquakes that a design engineer can design against. Designing a structure to behave elastically during an earthquake with a 10% probability of exceedance in 50 years would be uneconomical. Therefore the capability of a structure to resist such an earthquake with some damage without jeopardizing overall stability of structure is utilized. In short, the aim of design is not for buildings to survive the severe earthquakes without damage, but to dampen the earthquake's energy on the building done by showing the building's post-elastic behaviour. In other words, the aim is to design buildings to be ductile under the effect of an earthquake. Therefore, structural non-linear load-bearing capacity was used instead of linear elastic capacities in earthquake load design.

Earthquakes may be considered as one of the most critical challenges facing built environments. In the past, it has been experience accumulated through the years which has been relied on to construct safer structures against various threats. As improvements in theory and understanding of earthquake demands on structures, structures' responses to seismic actions, and limits on materials with these demands on them allow developed approaches for design and construction of structures in more rational sense. Modern codes would allow structural designers to estimate the expected earthquake demand considering the location's seismicity and structure itself. Earthquakes generate dynamic effects on structures, but codes permit designers to handle structures with an equivalent static loading to attain similar effects without involving dynamic analysis. The analysis are linear elastic for this simple design

approach, but designing for an elastic system at this level of demand would be costly. So, codes allow modifying the demand considering the capability of the structure beyond the elastic limit. Regulations define the earthquake demand considering some predefined parameters. The use purpose of the building, the property of the building's lateral load resisting system and the static-dynamic characteristics of the load bearing system are the main parameters in determining the earthquake's demand.

After the mid-1980's the non-linear (plastic) analysis started to get more attention instead of linear analysis. This trend is encouraged by codes and computer softwares. In design, once analysis of forces is completed, then member and joint details are checked for conformance with the design code. The conformance check is repeated for the modification of inadequate and over-designed elements until the capacities are close enough to the requirements.[1]

Non-linear response was assumed during design earthquakes for the seismic design of buildings for the 1990's codes and guidelines, such as the Uniform Building Code (UBC) 1997 [2] and the NEHRP Recommended Provisions for the Development of Seismic Regulations for New Buildings (FEMA 1997b) [3]. The design in these guidelines is based on elastic (force-based) analysis rather than plastic (displacement-based) analysis. It was known that structural damage can be measured by component deformations and floor displacements.

Under the effect of design earthquakes and considering the non-linear behaviour of the system, the expected load demand is determined by a reduction factor ( Response Modification Factor ) that reduces elastic earthquake load demand. Thus the non-linear post elastic behaviour of the structure under lateral load is included in the linear design calculations. The Seismic Load Reduction Factor,  $R_a(T)$  factor, defined as a function of the fundamental period of the structural system is determined according to structure type and its ductility level in Turkish Building Earthquake Code - 2018 (TBEC 2018) [4].

Many seismic codes allow a reduction in design loads, taking advantage of the fact that the structures have an important reserve capacity and the capability to dissipate energy. This reserve capacity originally comes from ductility of systems and over designed strength of systems. These parameters are incorporated into the structural design by a force reduction factor.

The response modification factor allows engineers to perform a simple and rapid linear analysis, accounting for the structure's non-linear behaviour. The determination

of the true R-value in the building will be a highly assertive approach, especially under an earthquake's complex dynamic effect.

## **1.1 Objective and Scope**

The main objective of this thesis is to evaluate the performance of moment resisting steel frames designed according to TBEC 2018 [4] with non-linear static analysis (pushover analysis) based on their lateral load-bearing capacities and evaluate the relevant behaviour factors based on the definition in previous studies. In this context, the redundancy factor, overstrength factor and ductility reduction factors are evaluated by pushover analysis of the frames with the help of SAP2000, a computer modeling software. The pushover curve of frames has been converted to a bilinear curve to better identify the aforementioned factors. Since the main aim is to show the variability of the R factor, the details are not overly studied, such as connection details. The section assignments in the design process are carried out by SAP2000.

In the earthquake resistant design, the structure may face both structural and non-structural damages, but it should resist earthquake effects without collapse. These damages should be within acceptable limits defined by codes. The damage levels are classified as invisible damages, repairable damages, and irreparable damages. Even if the damage received is in irreparable limits, the overall collapse of building is not desired.

In the design phase of this thesis, seismic zone, soil group, building importance factor and gravity loads are kept constant for all design cases. The main variations are ductility level, story number and the span number of the system.

Hinge points and their properties are defined to perform pushover analysis. In this incremental static analysis, the performance curve of the system is evaluated. To reach the ultimate capacity of the system, the pushover analysis is run until the system becomes mechanism that is unstable. The capacity curve of the system is also evaluated in an Acceleration-Displacement Response Spectrum (ADRS) format (at spectral acceleration and spectral displacement conversion). The plastic hinges are defined and pushover analysis is performed according to the American Society of Civil Engineers (ASCE 41-13) [5], and the capacity spectrum is performed according to Applied Technology Council (ATC-40) [6] by SAP2000 v20.2.

Steel member design is carried out according to Load and Resistance Factor Design (LRFD). The design sections are defined by a SAP2000 auto list that consists of European sections, IPE, and HE sections.

## **1.2 Thesis Organization**

### *Chapter 1: Introduction*

In the first chapter, a brief introduction about response modification factor, R factor, and the importance of non-linear behaviour consideration in design of frames are provided. Further, the objective and scope of this study are summarized.

### *Chapter 2: General Information*

In chapter two of this thesis, general information about steel structures in seismic zones, system reliability and structural design, system limit states, and lateral load resisting frames have been provided. Further, the historical background of each has been provided.

### *Chapter 3: Response Modification Factors*

In the third chapter, the response modification factor is determined, along with its components overstrength, redundancy and ductility. The historical background of each factor is explained with their references.

### *Chapter 4: Nonlinear Static Analysis*

In this chapter of the thesis, the emergence, and development of non-linear analysis is provided. Pushover analysis and capacity spectrum methods, which are based on non-linear analysis, are also included.

### *Chapter 5: Method of Analysis*

In this chapter, non-linear analysis has been applied to the case study. Descriptions of frames have been provided. Two identical frames with the same story and same spans, but different in ductility level, are studied. As an example of the application of the procedure, a 3 story - 3 span frame has been chosen, and the results for others are provided in appendices.

*Chapter 6: Results of Analysis and Further Remarks*

In this chapter, the results of the designed frames are provided with their graphs.

*Chapter 7: Summary of Results and Conclusions*

In this chapter, the summary, and conclusions of the study have been provided. Suggestions for future studies are given.

## CHAPTER 2

### GENERAL INFORMATION

#### 2.1 Steel Structures In Seismic Zones

Earthquakes usually occur when under ground rock suddenly breaks along a fault releasing great amount of energy. Seismic waves causing ground shaking occur with this sudden energy release. The earth's structures are affected by this ground shaking. Studies have been carried out for many years to minimize the effects of the earthquake on structures. This study focuses on steel structures.

Earthquakes can occur anywhere, however, most intensities observed along zones of weakness in the earth's crust, which are called faults, where many earthquakes are experienced. Faults are categorized as a type of activity and also categorized based on their types of slip. The categorization accordance of activity is divided into two groups which are active, that if geologic evidence suggests that movement has occurred along a fault in the past 11.000 years, and inactive, that if have not produced earthquakes in this time period. Categorization of earthquakes according to their slip are also in two groups which are strike-slip faults, that has movement consisting of horizontal displacement, and normal faults that have movement consist of vertical slip along the fault. [7]

Size and severity of an earthquake measured as the magnitude of the earthquake. Magnitude is the size of an earthquake that represents the amount of energy released by an earthquake. Richter, who developed the earliest magnitude scales that reflect magnitude on the basis of seismic wave measuring a standard location with respect to original earthquake occurred place, created a logarithmic magnitude scale ranging from 0 to 9, from release negligible energy to large energy release for an earthquake. Increasing 1 unit on the scale represents increase approximately 32 times in the amount of energy released. [7]

Each year, several thousand earthquakes occur in the world. Most of earthquakes occur frequently, small magnitude which causes no damage. The large scale

earthquakes occur rarely, magnitude 8 or larger earthquake occurring once every 10 years in average. [7]

The complex behaviour of the earthquake requires structural elements to be resistant to complex effects. The actual behaviour of an individual member will depend on the forces acting on it. The value of the acting force enforces the element to the plastic range. The state of behaviour of a structure during an earthquake is judged in condition of its ductility. This condition is directly related with ability of the structure to figure out large plastic deformations without losing the strength. The importance of steel structures is better understood at that point where non-linearity is important.

As supposed by Gioncu and Mazzolani, 2014 [8] there is a myth, it is generally accepted that steel is a perfect material for structural applications, especially in seismic zones, due to large absorption displacement capacities. Gioncu stated this myth based on the very good strength and ductility performance of steel. Unlike other building materials, it can withstand significant inelastic deformation without losing its strength. The good performance of steel structures gives confidence in the design methods developed for recent years. [8]

In the 1906 San Francisco earthquake, the large portion of the city, the oldest buildings made of masonry and timber are damaged. Despite the large damage in many portions of the city, the steel structures behaved very well. The result of this earthquake showed that the behaviour of steel buildings proved the reliability of steel material for buildings in seismic zones. [8]

In the 1923 Kanto earthquake, nearly half of the buildings were severely damaged or collapsed. The use of steel was relatively new at the time of this earthquake occurred. The large buildings made out of steel were faced almost no damage in structures but serious damages occurred to the non-structural elements. This good performance of these steel buildings during earthquake placed in some historical photos (Figure 2.1).[8]

1957 Mexico City earthquake results aftermath supports good behaviour of steel structures in seismic areas. When a lot of the buildings around a steel tower collapsed, it held its condition. The main reason for the good behaviour of this building is that it was well designed.[8]

The good behaviour myth of steel structures under earthquake was started to change with Northridge (1994) earthquake. Despite it showed better performance compared to reinforced concrete buildings, serious damage was recorded in beam to

column connection points. This damage was noticed for the first time, because a near-source earthquake affected a steel structure for the first time. The reason for this degree damage was considered as poor workmanship on the one hand, and on the other hand, it was related to the characteristic of the earthquake. [8]



Figure 2.1 Steel structure surrounded by ruins in Tokyo  
(Source: Gioncu and Mazzolani, 2014 [7])

Another earthquake that the steel structures surprised the public is the Kobe (1995) earthquake. The ground motion was associated with the presence of a thick alluvial soil layer, which caused intense liquefaction on the area of the Kobe port area. In this earthquake, it was observed that the energy absorption capacity of structure

reduced due to deformations of overall buckling of braced members. But generally, despite some structural members failed, the structure had maintained its status without collapse.[8]

The good behaviour measurement of a structure during a strong earthquake depends on its ductility. Ductility is the resistance of large plastic deformation without losing strength. Although knowing less information about ductility behaviour of steel structure, the general opinion was that it is a perfectly good material for lateral load resisting structures at the mid 20<sup>th</sup> century. [8]

Between 1985 and 1995, called seismic decade, the result of some earthquakes showed that the using steel material is not enough alone to obtain full performance of steel, besides that the detailing also should be considered to attain desirable performance.[8]

## 2.2 System Reliability and Structural Design

Structural design engineers have always advocated the need for a “factor of safety” to take into account uncertain and uncontrollable factors that may negatively affect the performance of structure during its lifetime. The degree of reliability of the system is evaluated by the factor of safety.

As detailed in Galambos, 1988 [1] report that structural design specifications and load codes make several explicit concessions to systems reliability [1]:

- 1) *Connection elements have reliability larger than required.*
- 2) *‘The importance factor’ in load code judge to be more important with an increase in the reliability index.*

The conventional structural design assumes that when one element has reached its limit state, the structure also has reached. Limit state of stability of the entire structure is sublimated the design of individual members. [1]

The optimal design considered as all elements are close enough to limits as possible. If we lay down as a condition that the system fail when any limit state reached then “the reliability of the total is less than the reliability of its elements”. But that is known that a structural system is more reliable than any of its elements. [1]

As detailed in Galambos, 1988 [1] report;

*“ there is some reason why the series system reliability not supported by evidence:*

1. *Generally, the structures tend to be overdesigned as a consequence of the following:*
  - a. *Step jump in member sizes*
  - b. *Maintenance of uniform depth for the sake of appearance or convenience of connection or transportation*
  - c. *Availability of shapes*
  - d. *Conservative modeling for the purposes of analysis*
  - e. *Conservative load assignments*
2. *Structural modeling for purposes of analysis does not generally account for the strengthening and stiffening effects of nonstructural cladding elements and structural elements not counted part of the main load-bearing system.*
3. *Many structural elements are controlled by serviceability criteria and so their reliability against an ultimate limit state is quite high.*
4. *Forces due to dynamic loads, such as wind, are reduced by the energy absorption mechanism in the structure and these are not included in the analytical model.*
5. *Critical elements in the structure ( such as column or hanger rods) or important connections receive special care during design, fabrication, and construction so that some of the randomnesses is eliminated.*
6. *Many member limit states produce no or little damage to the member.*
7. *Limit states in steel structures are ductile, they do not shed capacity once the limit state condition is reached. This facilitates many avenues of force redistribution so that more load can be carried by the system, this is called redundancy.*
8. *The structural system does not fail when one element reaches the limit state.*
9. *Framed structures are generally designed for the limit state of the first hinge formation or for a drift limit but none of them involves damage.”*

### **2.3 System Limit States**

The limit state can be explained as the capacity state of the structural element (or structural system) no longer satisfies the performance target. The limit states are defined in TBEC-2018[4] shown in Figure 2.2.

Due to the need to built structures in seismic areas, the special design philosophy has started to develop. The basic principle of this philosophy is designing all structures to overcome the strongest ground motion without any damage is not economically feasible in a seismic area. However, it may be reasonable to expect that the moderate earthquake overcome without damage but the damage may be accepted in the severe earthquake if the collapse prevented. [9]

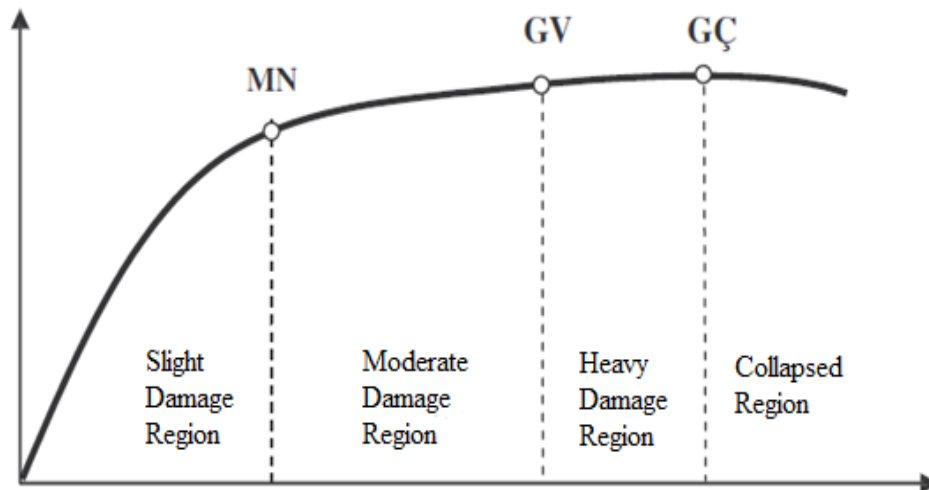


Figure 2.2 Cross-Sectional Member Damage Limits  
(Source: Turkish Building Earthquake Code, 2018 [4])

The determination of performance explained as followed levels according to Mazzolani and Gioncu, 2000 [9] studies:

Life Safety, that is the primary requirement. The collapse of building components causes the loss of lives and serious injuries. The number of deaths and injuries cannot be considered as economic damage in an optimization process.

Collapse Prevention, that can be directly related to the prevention of loss of lives. The structure must stand after major earthquakes.

Reparable Damage, the distinction between reparable or irreparable damage of structural or non-structural component.

The limit states explained according to Galambos, 1988 [1] as life safety is the most important issue of design in the event of a severe earthquake and the limit states explained as:

*“the built resist in minor earthquake without damage, resist moderate earthquakes without significant structural damage but with some non-structural*

*damage, and resist major or severe earthquakes without major failure of the structural framework or its component members and maintain life safety. (the first two can be considered serviceability limit states and last item as an ultimate limit state).”*

Following some large scale earthquakes (United States, Japan, etc.), the old principles for seismic design had to be converted as the view of designer against earthquake was preventing the collapse of the buildings, the new rules are based on some acceptable damage levels. In this principle, two limits appeared: service and ultimate limit states. [8]

#### Serviceability Limit States:

The structure should be able to withstand the actions expected to reach maximum design level it has been exposed to several times in its life cycle and should resist the damage of these actions at acceptable levels. The serviceability limit state design criteria reduce the structural motion as a tolerable level. The permissible damage must be repairable and visible damage level should not inconvenience humans.

The structural system must stay in the elastic range. The frequent low degree earthquakes should not cause any damage at non-structural elements. The interaction between structural and non-structural elements evaluated remain in elastic limits.

#### Ultimate Limit States:

The ultimate limit state can be called a survivability limit state. At the condition of this limit state, the non-structural elements are completely damaged and the global mechanism is formed under severe earthquakes.

Despite the structure might experience the extreme magnitude action with small probability in its lifetime it should be prepared and it should maintain life safety.

## **2.4 Lateral Load Resisting Systems**

Chosen criteria of the type of seismic resistant structure should be the fulfillment of the required stiffness and strength and robust enough. The basic typologies of seismic-resistant (lateral load resistant) dissipative structural systems classified as followed according to Mazzolani and Gioncu, 2000 [9] study:

- *Moment Resisting Frames (MRF)*
- *Centrically Braced Frames (CBF)*
- *Eccentrically Braced Frames (EBF)*

In moment resisting frames, the beams and columns are connected linearly and rigidly. The lateral stiffness and strength sources are provided by the bending rigidity and strength of the frame elements. The energy dissipative zones are formed by plastic hinges that placed at the ends of the members. Moreover, moment resisting frames are also preferred by architectures since they do not include diagonal members and allow large openings.

Centrally braced frames resist lateral loads primarily by developing high axial forces in diagonal members. Diagonals designed as high axial forces resistant. The dissipative zones are represented by tensile diagonals, because of assumption usually made that the compression ones buckle. The presence of diagonal bracing members ensure high elastic stiffness. The typical configurations of concentrically braced frames are shown in Figure 2.3.

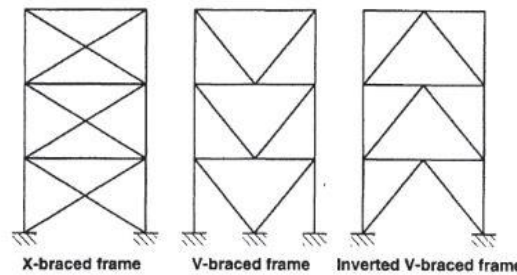


Figure 2.3 Common configurations of Concentrically Braced Frames (CBF)  
(Source: Mazzolani and Gioncu, 2000 [9] )

Eccentrically braced frames can be assumed as both moment resisting frames and concentrically braced frames because of including the individual advantages of both. They assure high elastic stiffness, good ductility, and energy dissipation capacity. As shown in Figure 2.4, this type of frames are formed by diagonals eccentrically located in moment-resisting frames.

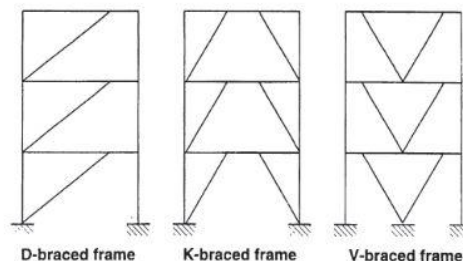


Figure 2.4 Typical configurations of Eccentrically Braced Frames (EBF)  
(Source: Mazzolani and Gioncu, 2000 [9] )

## 2.4.1 Moment Resisting Steel Frames

Structural steel can be considered as an ideal material for dealing with earthquake effect. The tolerance of larger displacement may cause higher damage levels of non-structural damage. However, the non-structural damages are more acceptable than structural damages at recent manuals. Steel structures have performed well because they have a high level of ductility and energy absorption.

The resistance of moment frames are developed mainly through the bending strength of the beam and column. A frame may develop plastic hinges, with appropriate proportions and details that absorb energy. The plastic hinges may allow the frame to withstand real displacements greater than elastic based design. [5]

In this study, the moment resisting frame system is studied. Moment resisting frames are defined in codes for low-rise structures in seismic zones as the lateral force resisting systems. Moment resisting frame design for high rise buildings can be heavy and become uneconomical in developing the design stiffness requirements.

Moment resisting frames have stable hysteretic behaviour and excellent ability to dissipate earthquake energy. This energy dissipating behaviour is mostly met with in-elastic deformation at the beam to column joint. The strong column-weak beam design approach is desirable for the safety of building (see Figure 2.5). In this design philosophy, the beams are designed weaker than columns and the formation of plastic hinges on beams are desired rather than columns. The strength of the column should be higher than the overstrength of the adjoining beams at each joint. [10]

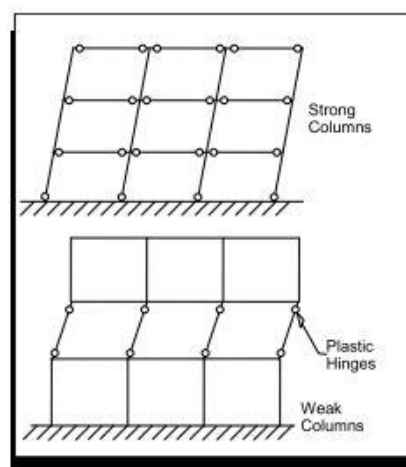


Figure 2.5 Plastic Hinge Deformation  
(Source: ASCE/SEI 41-13, 2013 [5])

As mentioned in Guidelines for Nonlinear Structural Analysis for Design of Buildings, 2017 [12] the beams in moment resisting frames are often acted compositely with the floor deck, that can affect the lateral stiffness, beam hinging, beam buckling and connection response.

## 2.4.2 Special Moment Frames (SMF)

Beams and columns of SMF should be seismically compact and connections must be full strength. Strong column- weak beam criteria must be fulfilled. Column webs should provide more strength than beams in the panel zone to improve the expected flexural strength of the beams. [7]

In special moment frames, locations of the maximum moment are designed to maintain inelastic behaviour associated with plastic hinge over many cycles and the load reversals. [5]

SMFs should be able to maintain a large inelastic demand without failure or significant loss of strength. The post elastic deformations are concentrated on the compact sections to withstand the deformations without torsional buckling and without strength loss. An effective value of behaviour factor,  $R$ , is permitted to use for these frames. The member size selection of these frames is mainly controlled by limiting inter-story drift.[7]

Configured frames in this manner can be able to develop plastic mechanism consisting of the plastic hinges in beams, close to connection and on the base or top of the columns as shown in Figure 2.6.

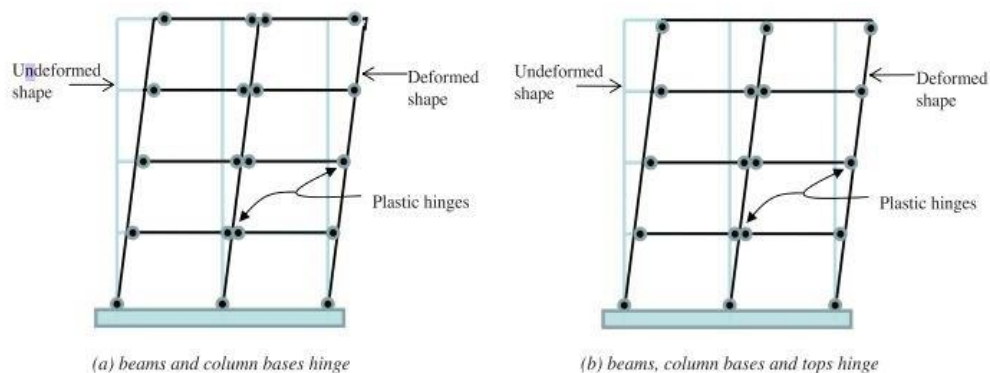


Figure 2.6 Anticipated sideways mechanisms in SMF  
(Source: Hamburger, 2009 [7])

### **2.4.3 Ordinary Moment Frames (OMF)**

This type of frame has relatively fewer limitations on the configuration of the designs or details. The connections can be designed for both partially and fully restrained connections.

The building code requires a relatively low value of behaviour factor, because of the less design and details requirements to withstand significant inelastic deformation. The designing of these types of frames are controlled by strength rather than drifts. [7]

OMF is expected to provide a minimum inelastic deformation capacity. To satisfy this low level of ductility, the OMF is designed to provide a larger lateral force than SMF. The design basis of the OMF provides a minimum in-elastic deformation capacity to avoid non-ductile behaviour in its response to lateral load. [13]

Design requirements for ordinary moment frames are given in regulations, such as UBC [2], FEMA 356 [11], NEHRP [15], FEMA 273 [3], ASCE/SEI 7-05 [14], ANSI/AISC 341-16 [13], FEMA P695[16], ASCE/SEI 41-13[5] etc..

## CHAPTER 3

### RESPONSE MODIFICATION FACTORS

The response modification factor firstly introduced in ATC-3-06,1978 [17], to reduce the base shear force calculated by elastic analysis. In this concept, %5 damped acceleration response spectrum ( $S_{a5}$ ) was used for calculation design base shear ( $V_b$ ).[18]

The performance of the structure cannot be predicted at traditional force-based design approach. In fact, it is possible to enter the non-linear region during the earthquake ground motion. Response modification factor is defined in codes in order to take non-linear effect into account in linear analysis. It is the design base force reduction factor that accounts non-linear effects. In other words, the design action of inelastic behaviour of the structure is approximately defined. Response Modification Factor,  $R$ , is defined as ‘structural quality factor’ or ‘the system performance factor’ in Structural Engineers Associations of California (SEOAC) guidelines, 1999 [20]. [21]

Response modification factor is defined in TBEC 2018 [4] as Load Bearing System Behaviour Factor and represented by letter ‘ $R$ ’.

Response modification factors have remained in the center of seismic force formulation since the early development of seismic design codes. The main purpose of using this factors is to simplify the analysis process. Thus, the elastic methods can be used to take in account the expected inelastic demands in a structure system.

It is inevitable that seismic design methodology in the existing code will be started to change. Performance-based design approach moves forward on becoming a preference and in this manner damage control started to come fore. This concept based on non-linear analysis into the seismic design methodology. On the upshot, the most suitable approach seems to be the non-linear static (pushover) analysis. [22]

The most commonly used procedure, Equivalent Static Lateral Force Method, has been used for many years. There are some reasons using this procedure; there is no need for a deep understanding of the structural dynamics, providing estimates actions of regular buildings, and developing preliminary component and element sizes of a

structural systems.[23]

Based on past earthquake observations, the structures can resist earthquake forces larger than for what they were designed. This is because of the considerable energy damping capacities of structures. This reserve energy dissipation capacity is taken into account with the response modification factor that includes system inherent ductility, overstrength, and redundancy factors. The description of R factor in NEHRP is “*an empirical response modification (reduction) factor intended to account for both damping and ductility inherent in a structural system at displacements great enough to approach the maximum displacement of the system.*”[3]. The ductility component of the R-factor is the most dominant one in the non-linear design provisions.[23]

The numerical values given with codes for various types of structural systems were obtained by expert engineers, not rigorous analysis and experimentation. There were many different approaches stated in different international codes and regulations and articles, which are still under discussion.[24]

### 3.1 Historical Evaluation and Formulation of R Factor

The formulation of Response Modification Factor at Informative Attachment 4A in TBEC 2018 [4] defined as follows:

$$\frac{R}{I} = \mu \cdot D \quad (3.1)$$

where  $\mu$  and  $D$ , refer to ductility coefficient and overstrength factors respectively and defined as following equations:

$$\mu = \frac{u_{max}}{u_y} \quad (3.2)$$

$$D = \frac{V_y}{V_d} \quad (3.3)$$

Period dependent ductility factor is defined as follows:

$$R_y(\mu, T) = \mu \quad T > T_B \quad (3.4a)$$



As all components are shown at the Figure 3.1, and the R factor defined as follows:

$$R = \frac{C_{eu}}{C_s} = \frac{C_{eu} C_y}{C_y C_s} = R_\mu \cdot \Omega \quad (3.5)$$

R factor at UBC allowable-stress design format:

$$R = \frac{C_{eu}}{C_w} = \frac{C_{eu} C_y}{C_y C_s} \frac{C_s}{C_w} = R_\mu \cdot \Omega \cdot Y \quad (3.6)$$

The displacement amplification factor  $C_d$ :

$$C_d = \frac{\Delta_{max}}{\Delta_s} = \frac{\Delta_{max} \Delta_y}{\Delta_y \Delta_s} \quad (3.7)$$

$\frac{\Delta_{max}}{\Delta_y}$  is the structural ductility factor

$$\frac{\Delta_y}{\Delta_s} = \frac{C_y}{C_s} = \Omega \quad (3.8)$$

$$C_d = \mu_s \cdot \Omega \quad (3.9)$$

$\mu_s$  is the structural ductility factor

$R_\mu$  is the ductility factor

$\Omega$  is the overstrength factor

$Y$  is the allowable stress factor

$C_w$  is the design force level

$C_s$  significant yield level

$C_y$  is the actual structural yield level

$C_{eu}$  is the required elastic strength

$\Delta_{max}$  is maximum deformation demand

$\Delta_y$  is yield deformation level

$\Delta_s$  is significant yield deformation level

### 3.1.2 Whittaker et al., 1999 [23]

The main aim of using R factor in this study is explained as the estimation of the effect of non-linear response quantities in linear analysis and the reason for using elastic analysis is sorted as:

- *Avoid the designer to go into details of structural dynamics.*
- *Provide the estimation component actions of sufficient accuracy for the design of low-rise, regular buildings.*
- *Develop the preliminary sizes of components and elements of a structural system.*
- *Provide the designer with a simple order of magnitude check on the results of the dynamic analysis.*

To achieve these aims, R factor used to reduce base shear force for design. The usage of R factor formulated as follows and component of the formulation shown in Figure 3.2 :

$$V_b = \frac{V_e}{R} = \frac{S_{a5} \cdot W}{R} \quad (3.10)$$

$V_b$  is the design base shear

$V_e$  is the elastic base shear

$S_{a5}$  is the %5 damped acceleration response spectrum

$W$  is the structural weight

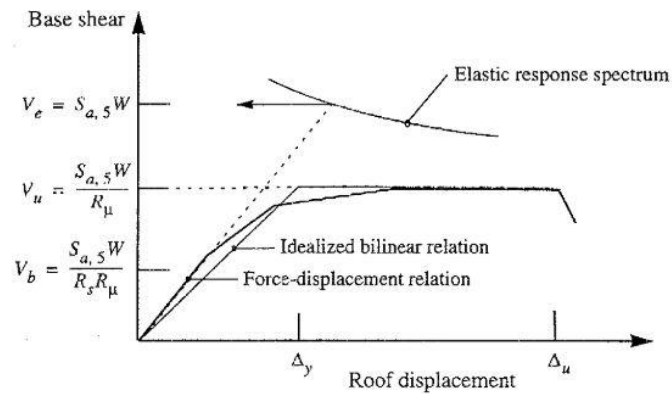


Figure 3.2 Sample base shear force versus roof displacement relationship  
(Source: Whittaker et al., 1999 [19])

The Berkeley researchers describe the R factor product of reserve strength, ductility and added viscous damping:

$$R = R_S \cdot R_\mu \cdot R_\xi \quad (3.11)$$

The strength factor  $R_S$  calculated as maximum base shear force ( $V_u$ ) divided by the design base shear force ( $V_b$ )

The ductility factor  $R_\mu$  calculated as base shear for an elastic response ( $S_{a5}$ ) divided by maximum base shear force ( $V_u$ )

The damping factor was set equal to 1.0.

According to this study, the R factor formulation developed (Freeman, 1990) and supported by ATC 1995a [32]. New formulation expressed as:

$$R = (R_S \cdot R_\mu) \cdot R_R \quad (3.12)$$

$R_S$  is the period-dependent strength factor

$$R_S = \frac{V_y}{V_d} \quad (3.13)$$

$R_\mu$  is the period-dependent ductility factor (evaluated according to Krawinkler and Nassar Equation)

$$R_\mu = [c(\mu - 1) + 1] \left[ \frac{1}{c} \right] \quad (3.14)$$

$$c = \frac{T^{[a]}}{1+T^{[a]}} + \frac{b}{T} \quad (3.15)$$

$$\mu = \frac{d_u}{d_y} \quad (3.16)$$

where;  $\mu$  is ductility coefficient,  $T$  is period,  $d_u$  is ultimate displacement and  $d_y$  is yield displacement.

The regression parameters  $a$  and  $b$  were obtained for different values of the ratio of postyield stiffness to elastic stiffness ( $\alpha$ ). For  $\alpha$  ranging between 0 and 0.10,  $a = 1.00$  and  $b$  ranges between 0.42 and 0.29.

$R_R$  is the redundancy factor and taken as equal 1

### 3.1.3 Patel and Sahah, 2010 [33]

The response reduction factor is defined in this particular study as a combined effect of over strength, ductility and redundancy factors which are shown in Figure 3.3.

$$R = R_S \cdot R_R \cdot R_\mu \quad (3.17)$$

The R factor components are explained as:

The strength factor is a measure of base shear at the design level ( $V_d$ ) and yielding ( $V_y$ ),

$$R_S = \frac{V_y}{V_d} \quad (3.18)$$

The ductility factor is a measure of roof displacement at yielding ( $d_y$ ) and at code specified limit ( $d_u$ ),

$$R_\mu = \frac{\mu - 1}{\Phi} + 1 \quad (3.19)$$

$$\mu = \frac{d_u}{d_y} \quad (3.20)$$

$$\Phi = 1 + \frac{1}{12T - \mu T} - \frac{2}{5T} \exp \left[ -2 \left( \ln T - \frac{1}{5} \right)^2 \right] \quad (3.21)$$

where;  $\Phi$  is soil dependent coefficient, T is period,  $\mu$  is ductility coefficient

The redundancy factor depends on the number of vertical framing participated in seismic resistance.

$$R_R = 1 \quad (3.22)$$

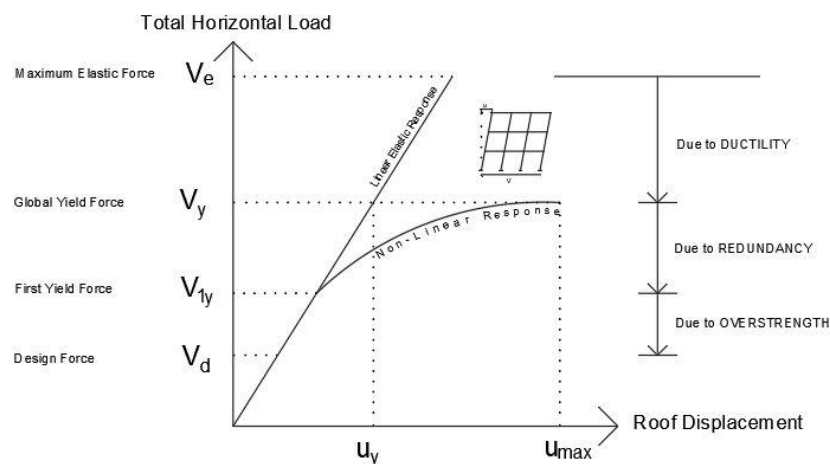


Figure 3.3 Definition of the response reduction factor  
(Source: Patel and Sahah, 2010 [18])

### 3.1.4 Ferraioli et al., 2012 [21]

Behaviour factor modifies the linear system accounting approximately the non-linear effects in force based seismic design. The definition of the R factor according to this study is based on a component of ductility dependent, overstrength dependent and damping dependent as shown in the following formula:

$$R = R_S \cdot R_\mu \cdot R_\xi \quad (3.23)$$

$R_S$  is the strength reduction factor

$R_\mu$  is the ductility reduction factor

$R_\xi$  damping reduction factor, generally taken 1.0 as in generally assumed that the damping ratio for linear and nonlinear response is the same.

The strength factor expressed as:

$$R_S = R_p \cdot R_\Omega \quad (3.24)$$

$R_p$  is the redundancy factor: the ratio of the collapse mechanism instant to the first yield in the structure.

$R_\Omega$  is the overstrength factor: the ratio between first plastic hinge and design shear value.

The base shear - roof displacement response curve obtained from the pushover analysis that idealized by a bilinear curve is shown in Figure 3.4:

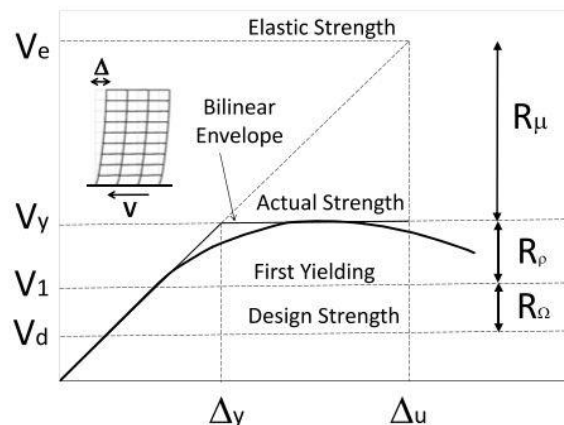


Figure 3.4 Base shear versus roof displacement relationship  
(Source: Ferraioli et al., 2012 [13])

$$R = \frac{V_e}{V_d} = \frac{V_e}{V_y} \cdot \frac{V_y}{V_1} \cdot \frac{V_1}{V_d} = R_\mu \cdot R_\rho \cdot R_\Omega \quad (3.25)$$

$V_e$  is the elastic base shear

$V_d$  is the design base shear

$V_y$  is the yield base shear

$V_1$  is the first yield base shear

### 3.1.5 Castiglioni et al., 2017 [35]

The process of the design of statically indeterminate structure requirements are divided into three phases in this study. The first phase, the pre-design phase, is the identification initial size of the structural load carry members based on engineer experience or similarity of other existing structures of similar typologies. The second phase, the analysis phase, is leading to the assessment of the demand under external actions. Axial load, bending moment, shear, torque, and displacements or rotations in joints are taken into consideration in this phase. The third phase, capacity phase, is verifying the capacity in terms of both strength and ductility. Especially ductility is the important property for the seismic design because of energy dissipation by plastic deformations.

The structural analysis is considered in two alternative methods in this study:

*Nonlinear dynamic analysis*

*Linear elastic response spectrum analysis*

The use of the nonlinear dynamic analysis method and its application is harder to use in daily practice because of its complexity. It is motivated by certain situations related to the importance of the building and its function. The linear elastic response spectrum analysis method performed by means of linear elastic analysis but considering indirectly the nonlinear structural behaviour with the use of behaviour factor (called “q factor” according to Eurocode).

The behaviour factor defined in this study as the ratio of the peak ground acceleration producing the collapse of the structure to the first yield point.

This study is carried out to explain the two main shortcomings of the available behaviour factors that defined in codes. The first one is that the validation of available q values is for a limited number of structural typologies and the non-compliance in

applying to different structural types. Besides, several case studies show that the real ductility of structures is far from the assumed values. The second reason is design force defined in current codes caused over-designed structures because of simplification and generalizing.

The formulation of the  $q$  factor in this study is based on definition of FEMA P-695 [16] as a product of overstrength  $q_{\Omega}$ , ductility  $q_{\mu}$ , and redundancy factor  $q_{\xi}$  :

$$q = q_{\Omega} \cdot q_{\mu} \cdot q_{\xi} \quad (3.26)$$

$q_{\Omega}$  is an over-strength dependent factor, the function of the non-linear structural response

$q_{\mu}$  is ductility dependent factor, the function of the displacement ductility

$q_{\xi}$  is a damping dependent factor, equal to 1.0 when assuming that the same damping ratio holds for both elastic and inelastic analysis

The overstrength factor formulated as:

$$q_{\Omega} = \frac{F_y}{F_1} \quad (3.27)$$

$F_y$  is the strength corresponding to the knee-point of the idealized bilinear elastic-plastic behaviour curve.

$F_1$  is the strength corresponding to the first significant yielding of the structure.

The ductility factor formulated with an expression of Newmark and Hall, as a function of the system ductility, that related to the natural period of vibration as follows:

$$q_{\mu} = 1 \quad (T < 0.03 \text{ sec}) \quad (3.28a)$$

$$q_{\mu} = \sqrt{2\mu - 1} \quad (0.03 < T < 0.5 \text{ sec}) \quad (3.28b)$$

$$q_{\mu} = \mu \quad (T > 0.5 \text{ sec}) \quad (3.28c)$$

$$\mu = \frac{d_m}{d_y} \quad (3.29)$$

$d_m$  is the displacement corresponding to the maximum strength

$d_y$  is the displacement corresponding to the knee-point of the idealized bilinear elastic-plastic behaviour curve

## 3.2 Overstrength Factor

Generally, the maximum lateral strength of a building ( $V_u$ ) exceeds its design lateral strength because of minimum design criteria and the tendency of material suppliers produce high strength materials to secure themselves. As mentioned above, the response modification formulation part, the overstrength factor is one of the main parameters of the R factor which deal with the over-design.

The defined strength at the building by the designer is considered as *yielding strength* and *strength capacity*. The strength capacity is usually larger than the strength that is designed according to both steel and reinforcement codes. For example in the Turkish Steel Structure Code [36], the design strength of steel is obtained by dividing the characteristic strengths over ‘ $\Omega$ ’ coefficient ( $\Omega=1.67$ ). Also, the steel and concrete suppliers tend to produce high strength materials to secure themselves.

Overstrength factor formulated as follows:

$$\Omega_d = \frac{V_y}{V_d} \quad (3.30)$$

where  $V_y$  is the yield force and  $V_d$  is the design force

The ratio of  $V_y$  to  $V_d$  vary as a function of different zones and building height and other specification of the frame system. Differences in regional construction will also affect the value of the strength factor.

### 3.2.1 Previous Studies of Overstrength Factor

Osteras and Krawinkler, 1990 [37] divide the overstrength factor into two groups which are local overstrength and global overstrength. Local overstrength is leads larger and stronger components than required. The sources of local overstrength are listed as implied code strength, controlling design condition, actual vs nominal yield strength, actual vs design loads, code minimum requirements, discrete size selection, uniformity of constructability and architectural considerations. Global overstrength was defined as developing of the overall response of the structure to lateral loading. It was primarily related with redistribution of internal forces in the inelastic range. It was

defined as the difference between resistance at first plastic hinge formation and resistance at mechanism occurrence. The sources of global ductility were listed as: structural elements not considered in design (neglected lateral strength and stiffness of the structure, only certain portions of the structure designed as part of lateral load system) and non-structural elements (negligible contribute to lateral strength effect of non structural elements such as partitions, cladding, elevator shafts, stairways, etc.). Osteras and Krawinkler, 1990 [37] reported strength factor range 2.1-6.5 for distributed moment frames, range 1.8-3.5 for perimeter moment frames and range 2.2-2.8 for concentrically braced frames.

Barakat et al., 1996 [38] report the overstrength factors after the analysis of their study case as obtained 3.04 in seismic zone 4, 7.87 in seismic zone 1 for a four storey building; 2.56 in zone 4, 7.26 in zone 1 for six-story building and 2.24 in seismic zone 4, 5.68 in seismic zone 4 for eight-story building.

The main sources of overstrength factor is listed in Elnashai and Mwafy's (2002) [39] special study as, difference between actual and design material strength, design procedure requirements, load factors, accidental torsion consideration, serviceability limit state provisions, effect of non-structural elements, not considering participation of some structural elements in lateral load capacity (slab width etc.), exceedance of minimum reinforcement and member sizes that defined in design requirements, redundancy capacity, strain hardening, actual confinement effect and utilize the elastic period to obtain design forces. Although the study basically based on reinforced concrete structure, the source of overstrength was clearly explained with its parameters.

Arslan and Erkan, 2011 [40] associated the overstrength factor with some reasons as; minimum design criteria, tendency of material suppliers secure themselves, etc., The result of their case study shows the average overstrength factor is 2.74 for 4 stories, 2.73 for 6 stories and 2.80 for 8 stories at difference seismic zones and different soil groups.

### **3.3 Ductility Factor**

Ductility is a property that allows some structural elements and systems made up of these elements to maintain their load-carrying capacity when strained beyond their

elastic limit. Ductility is an important parameter for seismic resistance because it supply the design of structures that do not have adequate strength to resist strong earthquake elastically, continue to overcome this earthquake shaking in inelastic behaviour. Ductility coefficient defined as ratio of ultimate displacement ( $du$ ) to yield displacement ( $dy$ ), and formulated as follows:

$$\mu = \frac{du}{dy} \quad (3.31)$$

Ductility factor,  $R_\mu$ , is originated from two variables that displacement ductility ratio and period of the structure. The first component that displacement ductility factor defined as the ratio of the  $F_y$  ( $\mu=1$ , the yield strength of elastic demand) to the  $F_y$  ( $\mu= \mu_i$ , the yield strength of inelastic demand) as formulated followed:

$$R_\mu = \frac{F_y(\mu=1)}{F_y(\mu=\mu_i)} \quad (3.32)$$

Another variable of ductility reduction factor is period dependence of structure and defined as:

$$R_\mu = R_\mu (T, \mu_i) \quad (3.33)$$

The ductility reduction factor is regardless of the period of the structure for elastic behaviour ( $\mu_i = 1$ ) equal to 1:

$$R_\mu = R_\mu (T, \mu=1 ) =1 \quad (3.34)$$

The factor is equal to 1 for rigid systems that natural periods goes to zero ( $T \sim 0$ );

$$R_\mu = R_\mu (T=0, \mu_i ) =1 \quad (3.35)$$

The factor is equal to the displacement ductility ratio for very flexible systems where the natural period goes to infinity ( $T \sim \infty$ );

$$R_\mu = R_\mu (T= \infty , \mu_i ) = \mu \quad (3.36)$$

### 3.3.1 Previous Studies of Ductility Factor

Newmark and Hall, 1994 [25] observed that in their studies;

*In the low-frequency and medium frequency spectral regions:* an elastic and an inelastic system have approximately the same maximum displacement.

*In the extremely high-frequency region:* an elastic and an inelastic system have the same force.

The strength reduction factor defined as follows for each spectral region;

$$R_{\mu} = 1 \quad 0 \leq T < \frac{T_1}{10} \quad (3.37a)$$

$$R_{\mu} = \sqrt{2\mu - 1} \left[ \frac{T_1}{4T} \right]^{2.513 \left[ \frac{1}{\sqrt{2\mu - 1}} \right]} \quad \frac{T_1}{10} \leq T < \frac{T_1}{4} \quad (3.37b)$$

$$R_{\mu} = \sqrt{2\mu - 1} \quad \frac{T_1}{4} \leq T < T_1' \quad (3.37c)$$

$$R_{\mu} = \frac{T \cdot \mu}{T_1} \quad T_1' \leq T < T_1 \quad (3.37d)$$

$$R_{\mu} = \mu \quad T_1 \leq T < T_2 \quad (3.37e)$$

$$R_{\mu} = \mu \quad T_1 \leq T < 10.0s \quad (3.37f)$$

Limiting periods are determined as:

$$T_1 = 2\pi \frac{\Phi_{ev} \cdot V}{\Phi_{ed} \cdot A} \quad T_1' = T_1 \frac{\mu}{\sqrt{2\mu - 1}} \quad T_2 = 2\pi \frac{\Phi_{ed} \cdot D}{\Phi_{ev} \cdot V} \quad (3.38)$$

A, V and D are the maximum ground acceleration, velocity, and displacement

$\Phi_{ea}$ ,  $\Phi_{ev}$ , and  $\Phi_{ed}$  are factors applied to give the ordinates of the elastic design spectrum in acceleration, velocity and displacement spectral regions.

Miranda's, 1994 [25] study based on 124 ground motions performed on rock, alluvium and soft soil conditions during various earthquakes in order to study the influence of local site conditions on strength reduction factors. The followed expressions proposed to estimate the reduction factor:

$$R_{\mu} = \frac{\mu - 1}{\phi} + 1 \geq 1 \quad (3.39)$$

$$\Phi = 1 + \frac{1}{10T - \mu T} - \frac{1}{2T} \exp \left[ -\frac{3}{2} \left( \ln T - \frac{3}{5} \right)^2 \right] \quad \text{for rock sites} \quad (3.40a)$$

$$\Phi = 1 + \frac{1}{12T - \mu T} - \frac{2}{5T} \exp \left[ -2 \left( \ln T - \frac{1}{5} \right)^2 \right] \quad \text{for alluvium sites} \quad (3.40b)$$

$$\Phi = 1 + \frac{T_s}{3T} - \frac{3T_g}{4T} \exp \left[ -3 \left( \ln \frac{T}{T_g} - \frac{1}{4} \right)^2 \right] \quad \text{for soft soil sites} \quad (3.40c)$$

Where the  $\Phi$  is a function of  $\mu$ ,  $T_g$  is the predominant period of the ground motion.

Lai and Biggs, 1994 [25] support their study with 20 artificial ground motion. The analyses carried on for 50 natural periods between 0.1 second and 10 seconds on a logarithmic scale.

$$R_\mu = \alpha + \beta (\log) T \quad (3.41)$$

$\alpha$  and  $\beta$  values are listed in Table 3.1:

Table 3.1.  $\alpha$  &  $\beta$  coefficient proposed by Lai and Biggs [25]

Period Range	Coefficient	$\mu=2$	$\mu=3$	$\mu=4$	$\mu=5$
0.1 < T < 0.5	$\alpha$	1.6791	2.2296	2.6587	3.1107
	$\beta$	0.3291	0.7296	1.0587	1.4307
0.5 < T < 0.7	$\alpha$	2.0332	2.7722	3.3700	3.8336
	$\beta$	1.5055	2.5320	3.4217	3.8323
0.7 < T < 4.0	$\alpha$	1.8409	2.4823	2.9853	3.4180
	$\beta$	0.2642	0.6605	0.9380	1.1493

### 3.4 Redundancy Factor

Redundancy can be defined as the needlessness or the excess of necessity but it is vital importance in structural analysis. It is reconciled with alternative load paths in structural analysis. In a redundant system the new path of load distribution can occur when a member fails but in a non-redundant system, the failure of a member means failure of the entire system. The static indeterminacy and alternative load paths terms are should be explained to defining redundancy factor clearly.

*Static indeterminacy* is related with geometric stability of the structure and the form and connectivity of a structure in the intact state at the state of exposed on specific loadings. In classically, the degree of indeterminacy is equal to the difference between the number of unknown reaction forces and the independent equilibrium equations.

*Alternative load paths* mean ability or availability of alternative ways to carry loads that previously carried by failed portions of system. The existence of alternative load paths delays the whole collapse of the building.

Both redundancy and alternative load path are generally accepted as synonyms. Redundancy is the ability redistribute of stresses the structural system to among its member. Nonredundant structures may fail immediately under local damage. Redundancy provides availability of warning prior to system failure.

In some previous studies, such as Barakat et al.,1996 [38], Chia-Ming Uang,1991 [31], and Castiglioni et al., 2017 [35], the redundancy factor defined as a component of the overstrength factor but in this study, it is defined as a separate component of the behaviour factor. The redundancy factor is referred to tolerance of structure after the first yield point to maximum load capacity. The formulation is as followed:

$$R_R = \frac{F_y}{F_1} \tag{3.42}$$

where  $F_y$  is the maximum load capacity and  $F_1$  is the first yield (first plastic hinge) force.

### 3.4.1 Previous Studies of Redundancy Factor

Whittaker et al., 1999 [23] suppose that the seismic frame system should be consist of multiple alternative lines that are transfer earthquake-based internal forces to the foundation. The relation between lines and redundancy factor given in Table 3.2. In the study supposed that the reliability of the frame system will be higher than the reliability of each individual member of the system.

Table 3.2. Draft Redundancy Factor (Whittaker et al. 1999 [23])

Lines of vertical seismic framing <sup>a</sup> (1)	Draft redundancy factor (2)
2	0.71
3	0.86
4	1.00
<sup>a</sup> Frames to be stiffness- and strength-compatible. In each principal direction of building.	

Z.X.Fang and H.T.Fan, 2011 [41] study the importance of redundancy explained with a case study. According to this study, there is two expectation from the structure through the life-span; firstly, expect to withstand loads reliably under normal situations and pristine state and secondly, the structure or major part of it should remain stable under accidental situations and local damage state. At the reliability level, redundancy contributes to the safety margin of a structure in its intact state; at the robustness level, redundancy assists in mitigating the sensitivity of the structure to accidental scenarios.

Structural redundancy relies on member sizes, material properties, member connection properties, applied loads and load sequence.

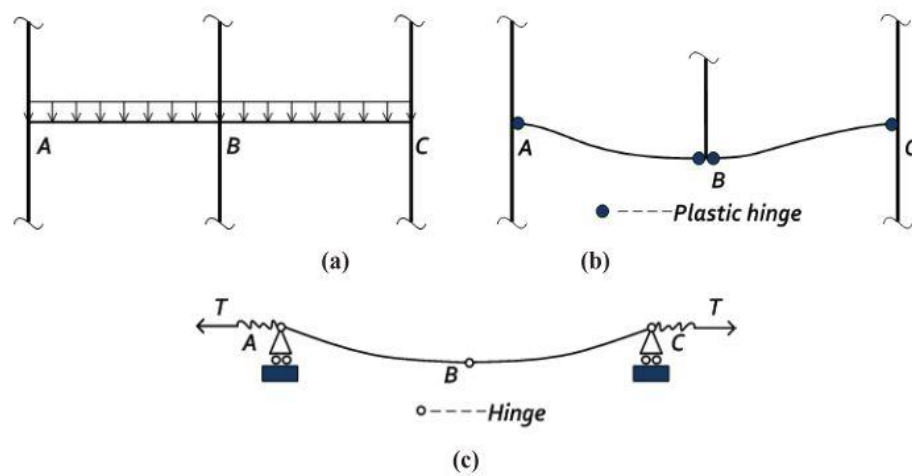


Figure 3.5 Transition of load-transfer mechanisms: (a) the prototype structure; (b) flexural load transfer mechanism; (c) tensile load transfer mechanism (catenary action). (Source: Z.X.Fang, H.T.Fan (2011) [41])

Assume Figure 3.6a is an example of a system with a strong column/weak beam design. When the center column removed at the lower floor, the part which is supported in the intact frame begins to deflect downward under vertical load. The damaged structure will carry the load until plastic hinges develop at the beam ends, see Figure 3.6b. As damage widespread and plastic hinges turn to ordinary hinges, the damaging structure may continue to carry external loads, see Figure 3.6c. This process represents the ideal redundancy of a frame.

Godinez-Dominguez and Tena-Colugna, 2016 [42] associated the redundancy with plastic hinges. A static non-linear pushover analysis represented the earthquake loading to describe the number of plastic hinges of the structural system.

## CHAPTER 4

### NONLINEAR STATIC ANALYSIS

Nonlinear static analysis is generally more informative than linear static analysis in defining the characteristics of the performance of a structure. Non-linear static analysis subjected to monotonically increasing lateral displacement that represents earthquake until a target displacement is exceeded. Target displacement represents the possible maximum displacement in the design earthquake.

As described in FEMA 356 (Federal Emergency Management Agency)[11], if the non-linear static analysis performed for seismic analysis, a model directly incorporating the non-linear load-deformation characteristics of elements of the building should be exposed to increased lateral loads. The force-displacement behaviour of all components should be explicitly incorporated into the model using full backbone curves which include strength degradation and residual strength. The lateral load distribution methods classified in FEMA according to the total mass participation percentage in the fundamental mode in the direction under consideration.

The non-linear analysis cannot be considered apart from plastic hinges. Plastic hinges can be defined as a form of cross-section that represents the performance after elastic limits. The plastic hinges occurs when an element reaches the elastic limit and it can continue to resist against exposed load with another formation (plastic form). For example, if a beam (having sufficient strength against the shear) that influenced larger cases of the moment, the cross section continues to lengthen up to the moment carrying capacity is reached. If the moment still continues to be increased from this boundary condition, the cross section continues to rotate (shape changes continue), provided that the moment carried by section is still constant. In this case, the material remains elastic at the close to the neutral axis, plasticizations occur on the outer parts which are away from the neutral axis (the most elongation and shortening occurred at outer parts ). In other words, plasticization means that the deformations in the outer fibers occur as elasto-plastic. It is useful to remind that, in the elastic behaviour the material returned to its original state when force removed, in elasto-plastic behaviour the material does not

return to its original state, permanent shape changes occur when force removed. It can be said that the plasticization is formed intensively on the beam support region and at the lower ends of the columns. One thing to keep in mind is that if a plastic joint is formed, damage also caused in that part.

## 4.1 Pushover Analysis

The pushover analysis procedure is mainly used to estimate the strength and drift capacity of structures. This procedure supported by several guidelines and design codes as ATC-40 [6], FEMA 356 [11], Eurocode 8 [19] for the last decade. The procedure can be performed as either force-controlled or displacement-controlled depending on behaviour expected from the structure. The accuracy of pushover results is affected by the selection of lateral load patterns and the identification of failure mechanisms for an estimate of target displacement.

The pushover analysis is a static incremental push analysis method for obtaining the force-displacement capacity curve of the building. The first step of this method is determining the horizontal load form to be used in push analysis. For this purpose, the horizontal loading form that will affect the structure is considered to be compatible with the first mode shape in the direction of analysis of the structure.

Pushover analysis is the method available to understand the behaviour of the structure subjected to earthquake forces. The purpose of this analysis is to evaluate the expected performance of structural systems in design earthquakes. The evaluation is based on the global drift, inter-story drift, inelastic element deformations, element and connection forces. The inelastic static pushover analysis can be seen as a method for predicting the effect of seismic force on the structural system.

The importance of pushover analysis listed as follows, at Krawinkler,1998 [43];

- “ *This analysis gives realistic force demands results such as axial force demands on columns, moment and force demands on connections, shear demands of beams and piers, etc.*
- *The deformation demands for elements that deform inelastically in order to dissipate seismic energy can be estimated.*
- *Effect of strength deterioration of each element on the structural system can be observed.*

- *Identification of the critical regions in which the deformation demands are expected to be high and that have become the focus of thorough detailing.*
- *Strength discontinuities in plan and elevation, which lead to changes in the dynamic characteristics of the system in the inelastic range, can be identified.*
- *The inter-story drifts that account for strength and stiffness discontinuities that used to control damage and evaluate P-delta effects can be estimated.*
- *Completeness and adequacy of load path all detail of the structural system can be verified. ”*

Some computer software (Seismostruct, DRAIN-2DX, SAP2000, ANSYS) can directly perform the pushover analysis and obtain a capacity curve of structural.

## **4.2 Capacity Spectrum Method**

The capacity spectrum method is a performance-based analysis technique. This method is derived from the intersection of pushover curve and response spectra of the structure. The performance-based seismic analysis gives a realistic assessment of structure behaviour when subjected to an earthquake ground motion. The capacity spectrum method is a procedure that can be applied to performance-based seismic design.

As pointed at Freeman et al., 2004 [44], study, The Capacity Spectrum Method (CSM) first introduced in the 1970s as a rapid evaluation procedure in a pilot project for assessing seismic vulnerability of buildings at the Puget Sound Naval Shipyard. In the 1980s ATC version, it was used to find a correlation between earthquake motion and building performance. “Seismic Design Guidelines for Essential Buildings” manual [45] that designed verification procedure for Tri-services, it was the initial drafts of the CSM procedure, (Army, Navy and Air Force) developed the method.[44]

The capacity spectrum curve obtained by converting the base shears and roof displacements from a pushover analysis to equivalent spectral accelerations and displacements than superimposing with earthquake demand curve. The earthquake demand curve represented by the different level of viscous damping of response spectra. In other words, the CSM method requires that both capacity and demand curve converted in response spectral ordinates. Initially, the 5% damped linear elastic response spectrum used to characterize the seismic demand and reduced the spectrum to

reflects the effects of energy dissipation to estimate the inelastic displacement demand. The intersection of the capacity and reduced response curve represents the performance point at which capacity and demand are equal to each other.

#### 4.2.1 Previous Studies of Capacity Spectrum Method

L. Sanchez-Ricart and A. Plumier, 2008 [46] explain the CSM in their related article, “Parametric study of ductile moment-resisting steel frames. The first step for Eurocode 8 calibration.”. Figure 4.1 shows the elastic behaviour and the pushover analysis of a structural system designed according to the structural code’s gravity and seismic loads.

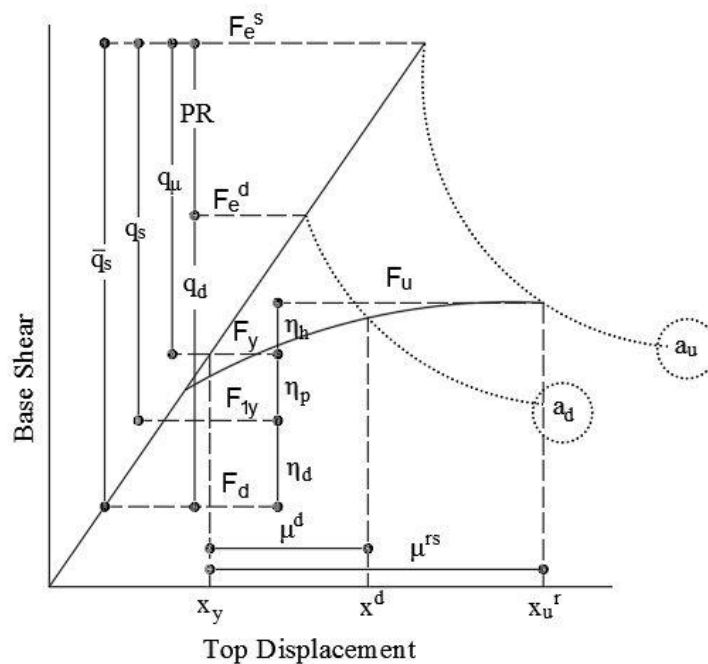


Figure 4.1 Pushover analysis of an eight-story MRSF designed according to Eurocode 3 and Eurocode 8 (Source: L. Sanchez-Ricart and A. Plumier, 2008 [46])

The dashed lines represent the constant values of Peak Ground Acceleration (PGA),  $a_d$  is the design PGA that represent the demand or requirement and  $a_u$  is the maximum value of PGA which represent supply or capacity.  $F_e^d$  and  $F_e^s$  are the base shears induced in the equivalent elastic structural system by the elastic spectrum of the seismic code for a value of PGA equal to  $a_d$  and  $a_u$ , respectively.

$F_{1y}$  is the base shear at first yield, first plastic hinge occurred point,  $F_d$  is the seismic demand or requirement,  $F_y$  is the base shear when the structure yields at globally and  $F_a$  is the base shear related ultimate capacity of the structure.

Applied Technology Council (ATC-40) [6] is the earliest developed guideline that goes in details of seismic evaluation and retrofit of concrete buildings designed and constructed.

The procedure followed by ATC-40 for the capacity spectrum method is as:

- *Obtain the pushover curve*
- *Convert the pushover curve to the capacity diagram*
- *Convert the elastic response spectrum from the standard pseudo-acceleration versus natural period format.*
- *Plot the demand diagram and the capacity diagram together and determine the displacement demand. Performance point (intersection point of demand and capacity diagram) evaluated.*
- *Convert the displacement demand determined in the previous step to global (roof) displacement and individual component deformation and compare them the limiting values for specified performance goals.*

The Capacity Spectrum Method (CSM) is based on obtaining the capacity spectrum curve. Capacity spectrum curve is defining two separate curves in one base. These curves are a non-linear static curve (pushover) and response spectrum curve. The capacity spectrum curve for the structure is obtained by transforming the capacity curve from lateral force (V) vs. lateral displacement (d) to spectral acceleration ( $S_a$ ) vs. spectral displacement ( $S_d$ ) coordinates. The demand response spectra curve is obtained by transforming the spectral acceleration ( $S_a$ ) vs. period (T) to spectral acceleration ( $S_a$ ) vs. spectral displacement ( $S_d$ ) coordinates. Spectra plotted in this format are known as Acceleration-Displacement Response Spectra (ADRS) and this method called the N2 method.

The basis of this approach is based on ATC in the 1980s. It was used as a procedure to find a correlation between earthquake ground motion and building performance. The method was also developed into a design verification procedure for Army, Navy and Air Force services in ‘Seismic Design Guidelines for Essential Buildings’ manual [45].

According to *Retrofit Strategies (chapter 6) part of ATC-40* [6] the capacity spectrum is derived from a pushover analysis. After obtaining pushover grap, the capacity curve is developed for related frame or building. This capacity curve is

obtained by total lateral shear demand 'V' against the incremental lateral displacement 'D' of the building at roof level. A capacity curve showed in the Figure 4.2.

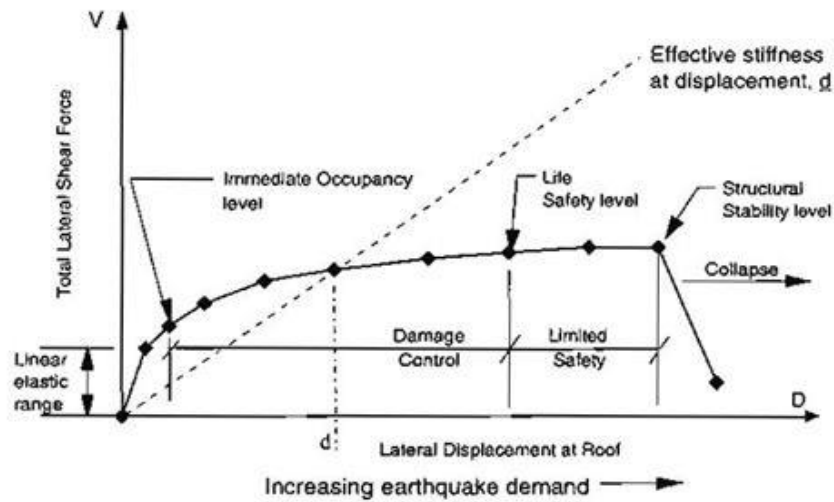


Figure 4.2 Typical capacity curve  
(Source: ATC-40 [6])

In the curve presentation, the cumulative effects of damage sustained at each level of individual events, and the overall behaviour of structure pointed as increasing lateral displacement. It is possible that to determine and indicate on the capacity curve those total structural lateral displacements that represent a limit on the various structural performance levels.

According to commentary part of ATC 40 [6], the process of defining lateral deformation points on the capacity (pushover) curve, at which specific structural performance levels may be said to have occurred, requires the exercise of considerable judgment on the part of the engineer. The global system response limits as acceptance criteria for the individual structural elements defined for each of structural performance levels. These acceptance criteria generally consist of limiting values of element deformation parameters, such as plastic chord rotation of a beam. These limitation values have been selected as reasonable approximate estimates of the average deformations at which certain types of element behaviour such as cracking, yielding may be expected to occur. The point of exceedance permissible deformation of the first element in structure does not represent the point of the structure as a whole reaches that structural performance. The structure performance levels may be said to be reached at which level of whole and consider the importance of damage occurred for the various elements on the overall behaviour of the building.

ATC 40 [6] explain the capacity curve in the ‘Capacity Spectrum Conversion’ concept (part 6-8). In this basis, in order to develop the capacity spectrum from the pushover curve, it is necessary to do a point by point conversion to first mode spectral coordinates. The conversion of base shear ‘V’ and roof displacement ‘ $\Delta_{roof}$ ’ to spectral acceleration ‘Sa’ and spectral displacement ‘Sd’ respectively according to the following formulation at Figure 4.3:

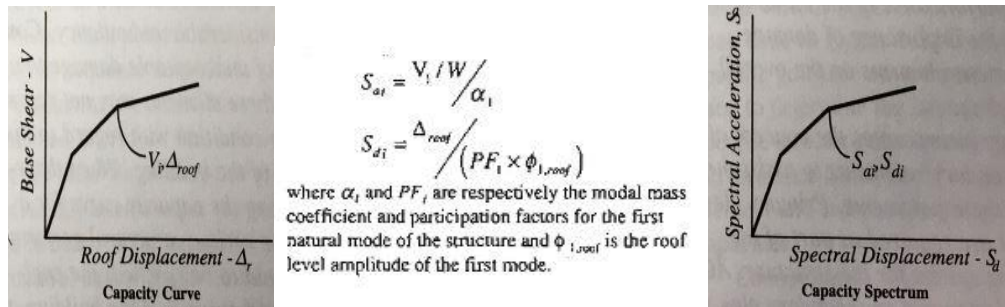


Figure 4.3 Capacity spectrum conversion  
(Source: ATC-40 [6])

The response spectra help in obtaining the peak structural responses under linear range, which can be used for obtaining lateral forces developed in structure due to the earthquake. The damping must be presented or else the response will be infinite. In codes even in Turkish seismic code specified damping ratio is 5%. This accounts for incidental damping from hysteretic behaviour, which is not explicitly modeled during response spectrum analysis.

The elastic spectrum should also be exposed to the conversion procedure. This conversion procedure explained in ATC-40 as ADRS conversion. To convert ‘Sa’ vs ‘T’ format to ‘Sa’ vs ‘Sd’ is a need to convert between ‘T’ and ‘Sd’ defined with the following formulation in Figure 4.4:

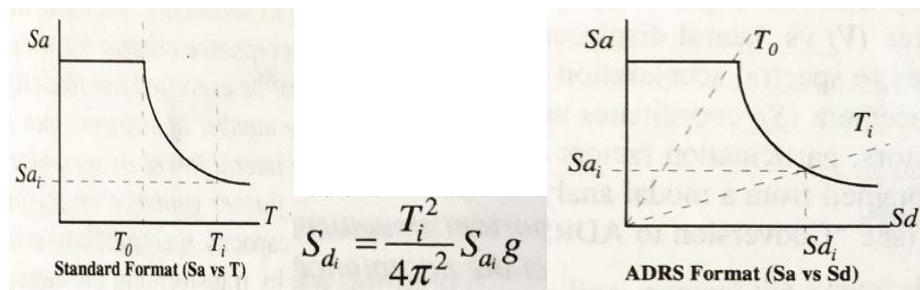


Figure 4.4 Response spectrum conversion  
(Source: ATC-40 [6])

P.Fajfar, 1999 [47] graphed the typical smooth elastic acceleration spectrum for 5% damping, normalized to peak ground acceleration of 1.0g and the corresponding elastic displacement spectrum in Figure 4.5:

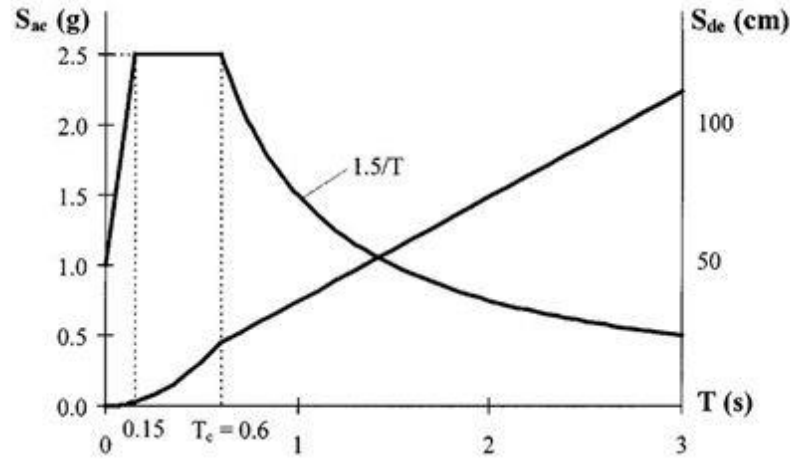


Figure 4.5 Typical elastic acceleration ( $S_{ae}$ ) and displacement spectrum ( $S_{de}$ ) for 5 percent damping normalized to 1.0g peak ground acceleration (Source: P.Fajfar, 1999 [47])

The acceleration spectrum ( $S_a$ ) and displacement spectrum ( $S_d$ ) determined with following formulas for an inelastic SDOF system with a bilinear force-displacement relationship:

$$S_a = \frac{S_{ae}}{R_\mu} \quad (4.2)$$

$$S_d = \frac{\mu}{R_\mu} S_{de} = \frac{\mu}{R_\mu} \frac{T^2}{4\pi^2} S_{ae} = \mu \frac{T^2}{4\pi^2} S_a \quad (4.3)$$

$\mu$  is the ductility factor: ratio of maximum displacement to the yield displacement.

$R_\mu$  is the reduction factor due to ductility

In the P.Fajfar,1999 proposal, the Vidic et al.,1994 formula for reduction factor is used. The formulas determined as followed and graphed in Figure 4.6 [48]:

$$R_\mu = (\mu - 1) \frac{T}{T_o} + 1 \quad T \leq T_o \quad (4.4a)$$

$$R_\mu = \mu \quad T \geq T_o \quad (4.4b)$$

$$T_o = 0.65 \mu^{0.3} \qquad T_c \leq T_c \qquad (4.5)$$

$T_c$  is the characteristic period of the ground motion.  $T_o$  is a transition period and depends on the ductility and it should be smaller than  $T_c$ .

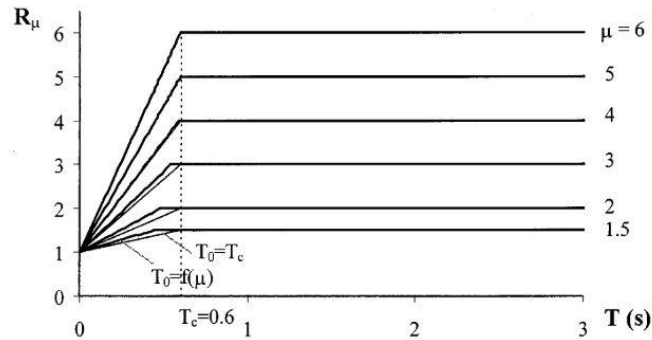


Figure 4.6 Ductility-dependent reduction factor  $R_\mu$  versus period ( $T$ )  
(Source: P.Fajfar, 1999 [48])

The effect of changing the value of the ductility factor  $\mu$  on the elastic design spectra is presented in Figure 4.7:

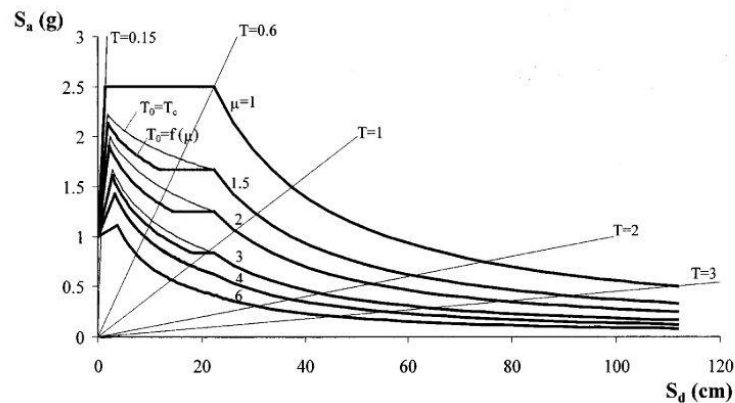


Figure 4.7 Demand spectra for constant ductilities in ADRS format  
(Source: P.Fajfar, 1999 [47])

The last step of this procedure is presented by both capacity and spectral curves in the same base. According to ATC 40 (Chapter-8) [6] the capacity spectrum method, a nonlinear static procedure that provides a graphical representation of the global force-displacement capacity curve of the structure and compares it to the response spectra representations of the earthquake demands. The graphical representation provides a clear provision of how a building responds to earthquake ground motion and it provides

the view of how to intervene strategies such as adding stiffness or strength will impact the response of the building to earthquake demands. Figure 4.8 which is taken from IABSE ‘Working Group 7: Earthquake Resistant Structures’s, 2015 [49] presentation will support ATC-40’s thought:

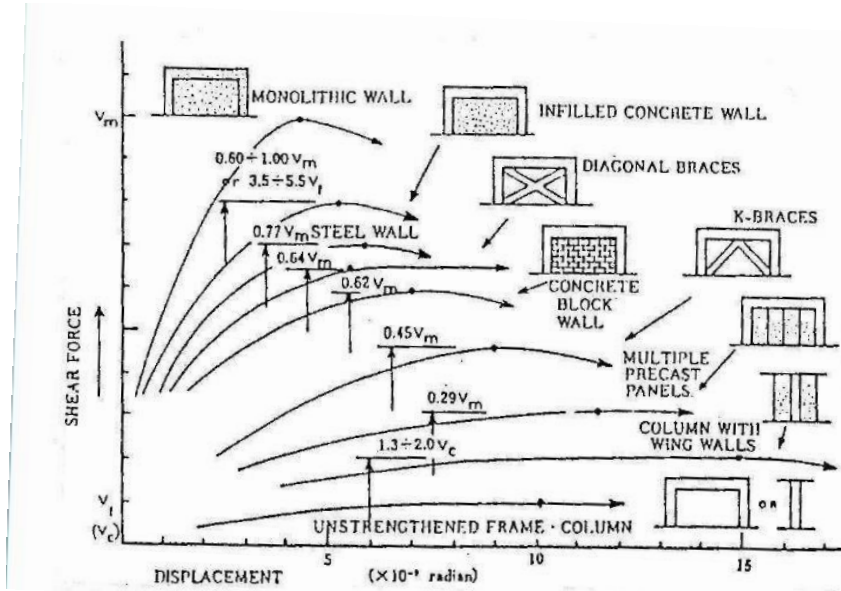


Figure 4.8 The relative effectiveness of strengthening  
(Source: IABSE ‘Working Group 7: Earthquake Resistant Structures’s 2015 [49])

If we go back to our last step, Figure 4.9 illustrates both the capacity spectrum and response spectrum:

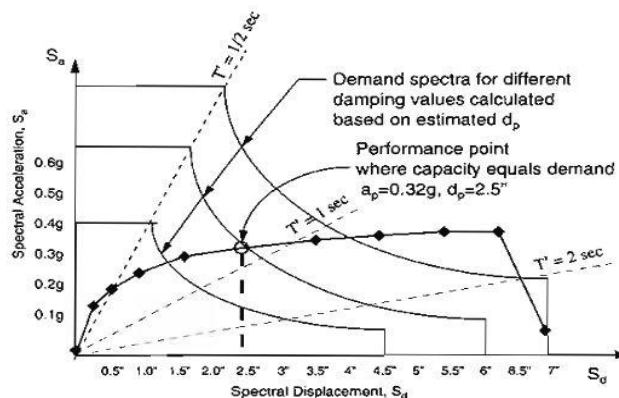


Figure 4.9 Determination of performance point  
(Source: ATC-40 [6])

As pointed at ATC-40 [6], extend initial stiffness line up to intersect elastic response spectrum give elastic spectral displacement (ordinate of intersection). The performance point determined as the equal displacement approximation. This

approximation estimates that the inelastic spectral displacement is the same as that which occur if the structure remained perfectly elastic.

The demand displacement in the capacity spectrum method occurs at a point on the capacity spectrum called the performance point. This performance point represents the condition for which the seismic capacity of the structure is equal to the seismic demand imposed on the structure by the specific ground motion. The determination of 'performance point' is an approximate approach to determining the nonlinear response of a building to given ground motion. To find the point where demand and capacity are equal, the engineer selects a point on the capacity spectrum as an initial estimate. Using the spectral acceleration and displacement defined by this point, then, reduction factor can be calculated to apply 5% elastic spectrum to account for the hysteretic energy dissipation, or effective damping, associated with the specific point. If the reduced demand spectrum intersects the capacity spectrum or near the initial assumed point then it is the solution for the unique point where capacity equal demand. If the intersection is not close enough to the initial point, the new point should be assumed and the procedure repeated. After defining performance point, the demand spectra obtained by 3 different procedure which are called Performance Point Calculation Procedure A, B, C explained at ATC-40 (Chapter 8) [6].

Also, as an alternative and more practical, these all steps can be performed by the computer software SAP2000. Already known that the pushover curve is obtained by computer software for years. Additionally, the new versions of software can obtain performance curve based on ATC-40 procedures.

Figure 4.10 taken from SAP2000 v20.2 software. As seen in the figure, the performance point and demand curve obtained according to ATC 40.

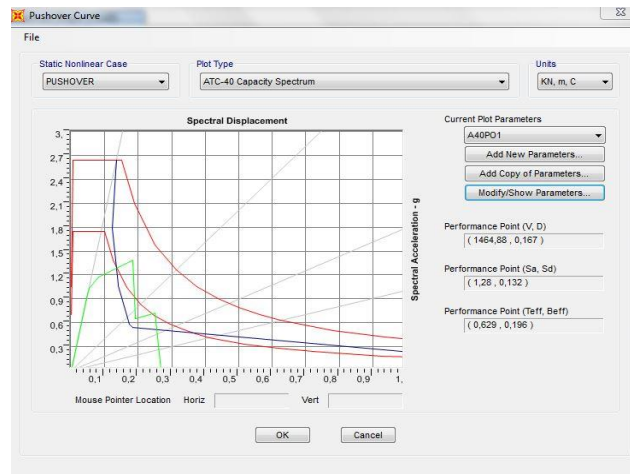


Figure 4.10 Performance point

## **CHAPTER 5**

### **METHOD OF ANALYSIS**

The analysis stages will be explained in this section. Linear and nonlinear analysis methods are performed according to TBEC 2018 and Turkish Steel Regulation. The analyses were performed by SAP2000 v20.2 computer software. It has provided great convenience in this version because of including the new Turkish Building Earthquake Code (TBEC 2018) requirements. Especially, in non-linear analysis method, defining automatically the hinge properties according to ASCE-41 [5] provides great convenience. Further, in addition to the force-displacement curve (pushover) as a result of the analysis, giving the capacity curve together with the performance point makes things even easier.

#### **5.1 Frame Type**

Only moment resisting steel frames are used in the case analyses. In this thesis which examines the variability of R factor, different spans and stories were chosen to provide this. The story heights were taken standard 3 meters and spans were taken standard 5 meters. The number of stories was selected as 3-6-9 and the spans were selected as 3-4-5-6-7-8. A total of 36 frames were analyzed in 18 different frames and two different ductility levels (high and normal ductility levels) for each.

#### **5.2 Frame Design**

Two separate analyses were made for each frame type with high ductility level and normal ductility level in frame design. The high ductility moment resisting frames defined in the SMRF (Special Moment Resisting Frames) category and the normal ductility moment resisting frames defined in the OMRF (Ordinary Moment Resisting

Frames) category in SAP2000. The sections used in the frames are automatically assigned in SAP2000 with automatic section identification. The AISC 360-16 [50], same base as Turkish Steel Structure Code [36], and TBEC 2018 [4] were taken into consideration in section assignments. The criteria determined by the earthquake code is taken into consideration in the automatic section designation such as system R factor, overstrength factor, etc.

The number of floors is limited to 9 stories because the new earthquake code requires some enforcement for nonlinear analysis for floors with a total height of more than 28 meters.

### 5.2.1 Equivalent Lateral Load Analysis

The base shear force to be used in design according to earthquake regulation is determined as a followed formula:

$$V_{tE} = m_t \cdot S_{aR}(T_p^{(x)}) \geq 0.04 \cdot m_t \cdot I \cdot S_{DS} \cdot g \quad (5.1)$$

$m_t$  : total seismic mass of the structure

$S_{aR}(T_p^{(x)})$  : reduced spectral acceleration of the natural period of the structure

$I$  : building importance factor (used as 1)

The total seismic mass of structure determined in the TSC18 as:

$$w_j = w_{Gj} + n \cdot w_{Qj} \quad ; \quad m_j = \frac{w_j}{g} \quad (5.2)$$

$n$  : live load participation factor ( taken as 0.3)

$w_j$  : total load that affect the story

$w_{Gj}$  : dead load

$w_{Qj}$  : live load

$m_j$  : mass of story

Reduced the design Spectral Acceleration defined as a followed formula:

$$S_{aR}(T) = \frac{S_{ae}(T)}{R_a(T)} \quad (5.3)$$

$S_{ae}(T)$  : lateral elastic design acceleration spectrum

$R_a(T)$  : earthquake load reduction factor

Lateral elastic design acceleration spectrum (Figure 5.1) defined as followed formulas:

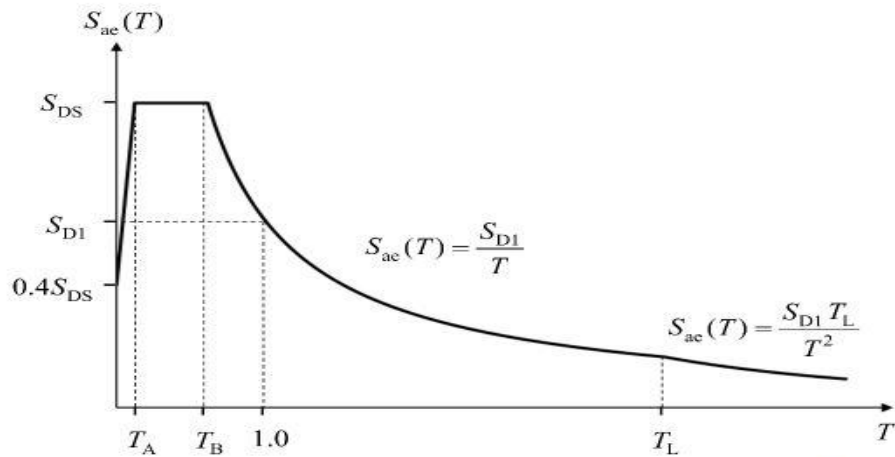


Figure 5.1 Lateral elastic design acceleration spectrum  
(Source: Turkish Building Earthquake Code-2018 [4])

$$S_{ae}(T) = \left(0.4 + 0.6 \frac{T}{T_A}\right) S_{DS} \quad (0 \leq T < T_A) \quad (5.4a)$$

$$S_{ae}(T) = S_{DS} \quad (T_A \leq T < T_B) \quad (5.4b)$$

$$S_{ae}(T) = \frac{S_{D1}}{T} \quad (T_B \leq T < T_L) \quad (5.4c)$$

$$S_{ae}(T) = \frac{S_{D1} \cdot T_L}{T^2} \quad (T_L \leq T) \quad (5.4d)$$

Where  $T_A$ ,  $T_B$  and  $T_L$  defined as:

$$T_A = 0.2 \frac{S_{D1}}{S_{DS}} ; T_B = \frac{S_{D1}}{S_{DS}} ; T_L = 6 \text{ s} \quad (5.5)$$

$$S_{D1} = S_1 \cdot F_1 \quad (5.6)$$

$$S_{DS} = S_s \cdot F_s \quad (5.7)$$

$S_1$  and  $S_s$  defined in attachment list of TBEC for every location of Turkey.

$F_s$  and  $F_1$  defined at the followed tables from TBEC - 2018 (Table 5.1 and Table 5.2):

Table 5.1. Local ground impact coefficients for short period [4]  
(Source: Turkish Building Earthquake Code-2018 [4])

Local Ground Class	Local Ground Impact Coefficients for Short Period $F_s$					
	$S_s \leq 0.25$	$S_s = 0.50$	$S_s = 0.75$	$S_s = 1.0$	$S_s = 1.25$	$S_s \geq 1.50$
ZA	0.8	0.8	0.8	0.8	0.8	0.8
ZB	0.9	0.9	0.9	0.9	0.9	0.9
ZC	1.3	1.3	1.2	1.2	1.2	1.2
ZD	1.6	1.4	1.2	1.1	1.0	1.0
ZE	2.4	1.7	1.3	1.1	0.9	0.8
ZF	Site-specific ground behaviour analysis should be conducted.					

Table 5.2. Local ground impact coefficients for 1 second period [4]  
(Source: Turkish Building Earthquake Code-2018 [4])

Local Ground Class	Local Ground Impact Coefficients for 1.0 second Period $F_1$					
	$S_1 \leq 0.10$	$S_1 = 0.20$	$S_1 = 0.30$	$S_1 = 0.4$	$S_1 = 0.5$	$S_1 \geq 0.6$
ZA	0.8	0.8	0.8	0.8	0.8	0.8
ZB	0.8	0.8	0.8	0.8	0.8	0.8
ZC	1.5	1.5	1.5	1.5	1.5	1.4
ZD	2.4	2.2	2.0	1.9	1.8	1.7
ZE	4.2	3.3	2.8	2.4	2.2	2.0
ZF	Site-specific ground behaviour analysis should be conducted.					

Seismic load reduction factor defined as:

$$R_a(T) = \frac{R}{I} \quad T > T_B \quad (5.8a)$$

$$R_a(T) = D + \left(\frac{R}{I} - D\right) \frac{T}{T_B} \quad T \leq T_B \quad (5.8b)$$

Where  $I$  is building importance factor and taken as 1 and the  $R$  and  $D$  coefficients are given in the table at TBEC 2018 at Table 4.1

## 5.2.2 Gravitational Load Analysis

Gravitational load values are obtained from the Design Loads for Buildings (TS-498) [51]. The load distributions are defined into two groups which roof and floor level loads.

For frame load distribution following procedure applied (Figure 5.2):

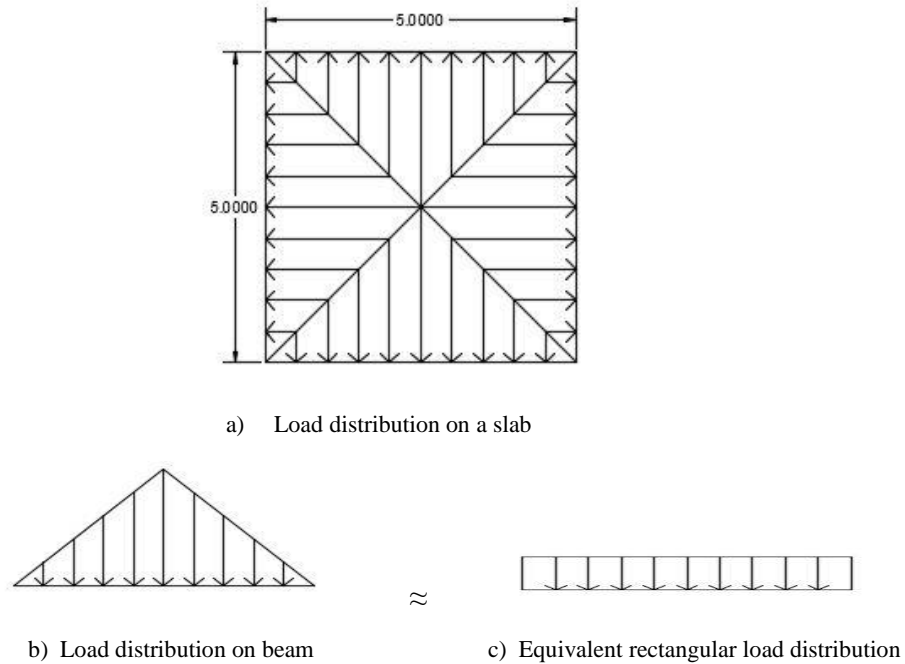


Figure 5.2 Gravity load distribution on slab (a), on beam (b) and equivalent distribution(c)

The transformation from triangle to uniform distribution achieved with followed formula:

$$P_e = \frac{1}{3} P_d l_s \quad (P_e \text{ refers to rectangular distributed load})$$

Roof:

$$\text{Dead} = 3 \text{ kN/m}^2 \quad P_e = \frac{1}{3} * 3 * 5 = 5 \text{ kN/m} \quad (2D \text{ Frame distribution})$$

$$\text{Wall (dead)} = 0.2 \text{ kN/m}^2 \quad P_e = \frac{1}{3} * 0.2 * 5 = 0.33 \text{ kN/m} \quad (2D \text{ Frame distribution})$$

$$\text{Snow} = 0.75 \text{ kN/m}^2 \quad P_e = \frac{1}{3} * 0.75 * 5 = 1,25 \text{ kN/m} \quad (2D \text{ Frame distribution})$$

$$\text{Live} = 2 \text{ kN/m}^2 \quad P_e = \frac{1}{3} * 2 * 5 = 3.33 \text{ kN/m} \quad (2D \text{ Frame distribution})$$

Floor:

$$\text{Dead} = 4 \text{ kN/m}^2 \quad P_e = \frac{1}{3} * 4 * 5 = 6.67 \text{ kN/m} \quad (2D \text{ Frame distribution})$$

$$\text{Wall (dead)} = 0.8 \text{ kN/m}^2 \quad P_e = \frac{1}{3} * 0.8 * 5 = 1.33 \text{ kN/m} \quad (2D \text{ Frame distribution})$$

$$\text{Live} = 5 \text{ kN/m}^2 \quad P_e = \frac{1}{3} * 5 * 5 = 8.33 \text{ kN/m} \quad (2D \text{ Frame distribution})$$

The frames loads take the two times that calculated so that take in consideration as mid frames (Figure 5.3):

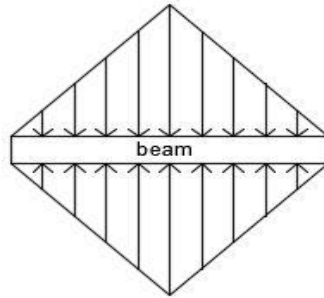


Figure 5.3 Gravity load distribution on beam (two adjacent slabs)

### 5.2.3 Load Combinations

The load combinations defined according to TBEC 2018 section 4.4.2 [4] and Turkish Steel Specifications Code part 5.3.1 [36]:

$$1.4G$$

$$1.2G + 1.6Q + 0.5S$$

$$1.2G + Q + 1.6S$$

$$1.2G + Q + 0.2S + (\pm E + 0.3Ez)$$

$$0.9G + (\pm E - 0.3Ez)$$

Where

G : Dead Load

Q : Live Load

S : Snow Load

E : Earthquake Load (assigned for one way because of 2D frame)

Ez : Earthquake (Vertical) Load (added to code with 2018 update)

### 5.2.4 Sample Design

A sample frame is presented to clearly illustrate the process. This sample frame analyzed for both high ductility level and normal ductility level. The sample frame has 3 bay (each 5m), and 3 stories (each 3m) as shown in Figure 5.4.

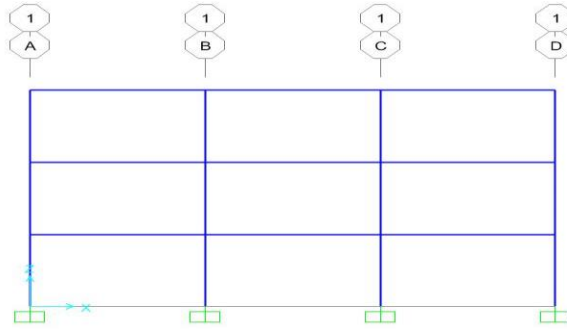


Figure 5.4 3x3 Moment resisting frame (SAP2000)

All properties that used and specified for this case study is valid for all frame analysis. The most critical region of Turkey taken into consideration for seismic analysis. The location chosen in the web-based Hazard Map in TBEC 2018 has longitude: 41.05, latitude: 39.35 (Bingöl). The used values in the list is that possibility of exceedance 10% in 50 years which  $S_s$  and  $S_1$  are 2.0 and 0.529 respectively;  $F_s$  and  $F_1$  are 1.2 and 1.471 respectively;  $S_{D1}$  and  $S_{D5}$  are 0.7782 and 2.4 respectively;  $T_A$  and  $T_B$  0.0648 and 0.3242 respectively. The site class is chosen ZC as a moderate class.

The analysis performed by SAP2000 computer software. The frame sections, as mentioned at previous parts, defined by the Autolist feature of the software.

As shown in Figure 5.5, the design R-value is taken as 4 and the overstrength factor is taken as 2.5 for normal ductility moment resisting frames. Additionally, frame type chosen as Ordinary Moment Frames (OMF) and the seismic code take into consideration.

Item	Value
1 Design Code	AISC 360-16
2 Multi-Response Case Design	Envelopes
3 Framing Type	OMF
4 Seismic Design Category	D
5 Importance Factor	1,
6 Design System Rho	1,
7 Design System Sds	0,5
8 Design System R	4,
9 Design System Omega0	2,5
10 Design System Cd	5,5
11 Design Provision	LRFD
12 Analysis Method	Direct Analysis
13 Second Order Method	General 2nd Order
14 Stiffness Reduction Method	Tau-b Fixed
15 Phi(Bending)	0,9
16 Phi(Compression)	0,9
17 Phi(Tension-Yielding)	0,9
18 Phi(Tension-Fracture)	0,75
19 Phi(Shear)	0,9
20 Phi(Shear-Short Webed Rolled I)	1,
21 Phi(Torsion)	0,9
22 Ignore Seismic Code?	No
23 Ignore Special Seismic Load?	No

Figure 5.5 Normal ductility level moment resisting frame design properties (SAP2000)

As shown in Figure 5.6, the design R-value is taken as 8 and the overstrength factor is taken as 3 for high ductility moment resisting frames. Additionally, frame type chosen as Special Moment Frames (SMF) and the seismic code take into consideration.

Item	Value
1 Design Code	AISC 360-16
2 Multi-Response Case Design	Envelopes
3 Framing Type	SMF
4 Seismic Design Category	D
5 Importance Factor	1,
6 Design System Rho	1,
7 Design System Sds	0,5
8 Design System R	8,
9 Design System Omega0	3,
10 Design System Cd	5,5
11 Design Provision	LRFD
12 Analysis Method	Direct Analysis
13 Second Order Method	General 2nd Order
14 Stiffness Reduction Method	Tau-b Fixed
15 Phi(Bending)	0,9
16 Phi(Compression)	0,9
17 Phi(Tension-Yielding)	0,9
18 Phi(Tension-Fracture)	0,75
19 Phi(Shear)	0,9
20 Phi(Shear-Short Webed Rolled I)	1
21 Phi(Torsion)	0,9
22 Ignore Seismic Code?	No
23 Ignore Special Seismic Load?	No

Figure 5.6 High ductility level moment resisting frame design properties (SAP2000)

The explanation of frame names that used in the analysis is shown at Table 5.3.

Table 5.3. Frame names and expressions

Name	R	Span	Story	Name	R	Span	Story
A33R4	4	3	3	A33R8	8	3	3
A36R4	4	3	6	A36R8	8	3	6
A39R4	4	3	9	A39R8	8	3	9
A43R4	4	4	3	A43R8	8	4	3
A46R4	4	4	6	A46R8	8	4	6
A49R4	4	4	9	A49R8	8	4	9
A53R4	4	5	3	A53R8	8	5	3
A56R4	4	5	6	A56R8	8	5	6
A59R4	4	5	9	A59R8	8	5	9
A63R4	4	6	3	A63R8	8	6	3
A66R4	4	6	6	A66R8	8	6	6
A69R4	4	6	9	A69R8	8	6	9
A73R4	4	7	3	A73R8	8	7	3
A76R4	4	7	6	A76R8	8	7	6
A79R4	4	7	9	A79R8	8	7	9
A83R4	4	8	3	A83R8	8	8	3
A86R4	4	8	6	A86R8	8	8	6
A89R4	4	8	9	A89R8	8	8	9

### 5.3 Nonlinear Static Analysis

The first step of the nonlinear analysis is defining plastic hinges. The plastic hinges defined by SAP2000 according to ASCE 41-13 [5] specification. As pointed at ASCE 41-13 Table 9-6 the beam hinges defined for the degree of freedom at flexure, M3, and column hinges defined for both the degree of freedom at axial load, P, and flexure, M3. Both column and beam hinges are deformation controlled. The followed figures show the automatically plastic hinge assigning at SAP2000. Figure 5.7 (hinge assigning) and Figure 5.8 (plastic hinge boundaries) deal with the beam hinges. Figure 5.9(hinge assigning) and Figure 5.10(interaction diagram) deal with the column hinges.

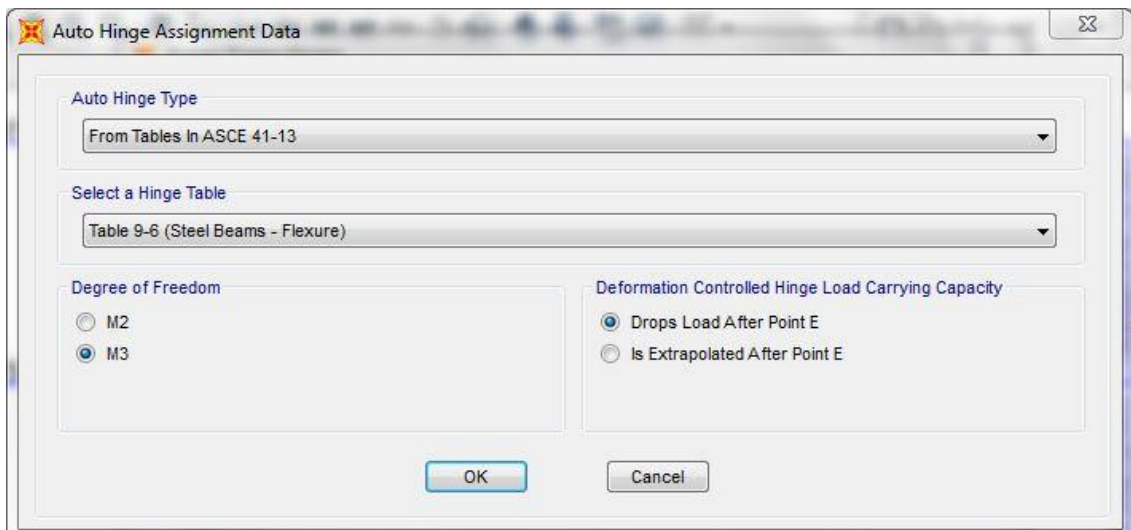


Figure 5.7 Auto plastic hinge defining properties for the beam (SAP2000)

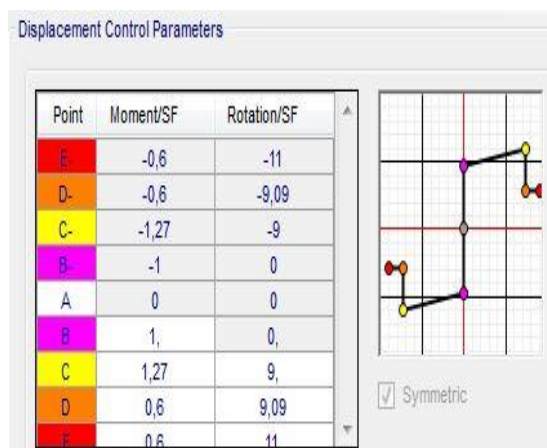


Figure 5.8 Defined plastic hinge boundaries for the beam (SAP2000)

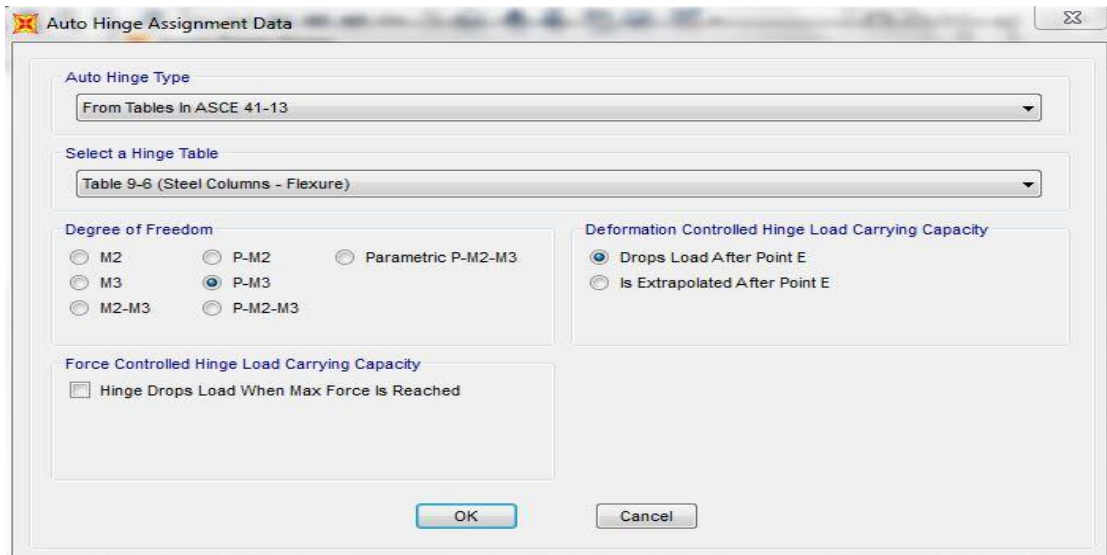


Figure 5.9 Auto plastic hinge defining properties for column (SAP2000)

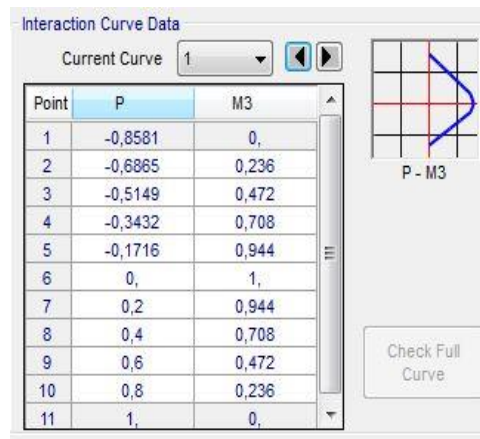


Figure 5.10 Interaction diagram properties for column (SAP2000)

## 5.4 Analysis Results

As mentioned before, the frame sections are assigned from a group of sections that defined as AutoList at SAP2000. Frame sections are firstly defined randomly than the system reanalyzed several times until fixing the frame sections. The frame sections are optimized at each step of the analysis. This cycle was continued until the frame sections were unchanged.

During the frame analysis process, plastic hinge formation locations were carefully followed. There is no need to satisfy the strong column-weak beam design criteria for OMRF, so the soft story formation can be occurred (Figure 5.11). But for SMRF, the presence of soft-story condition should be prevented and the strong column-

weak beam design criteria should be achieved. In this concept, firstly the plastic hinges was formed in beams. After plastic hinges formed in a majority of beams, the system reaches its global boundaries and the plastic hinges of lower columns are formed (Figure 5.12).

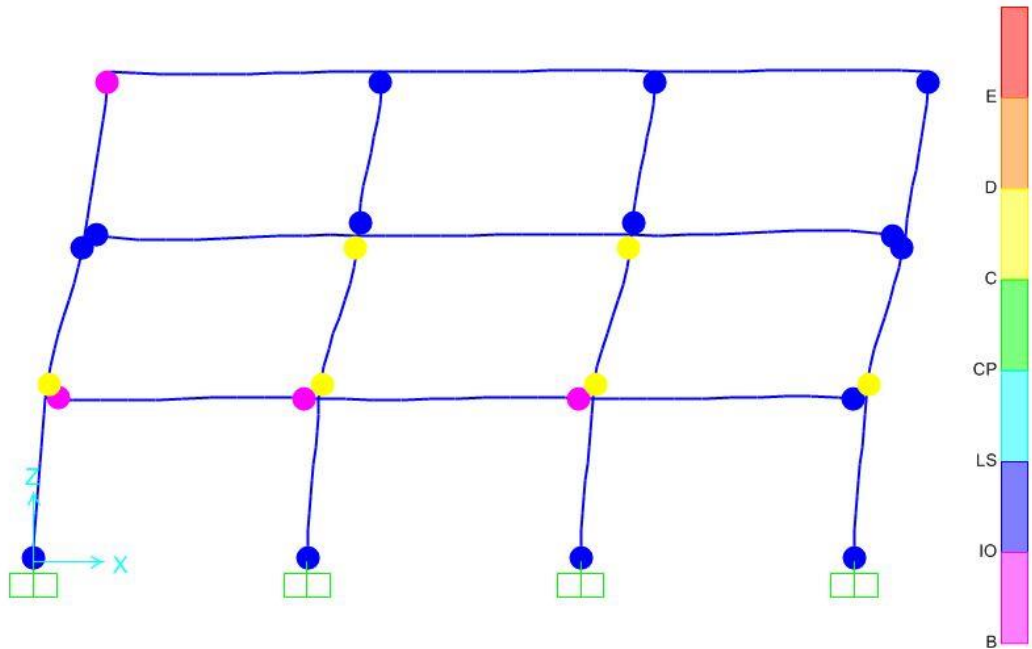


Figure 5.11 Plastic hinge formations for OMRF

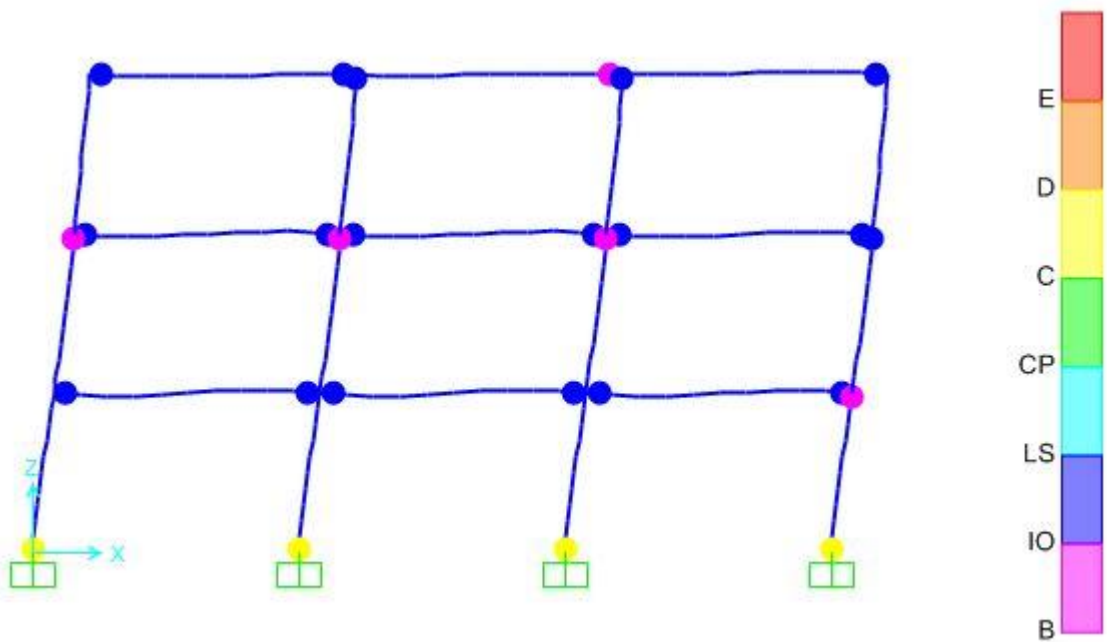
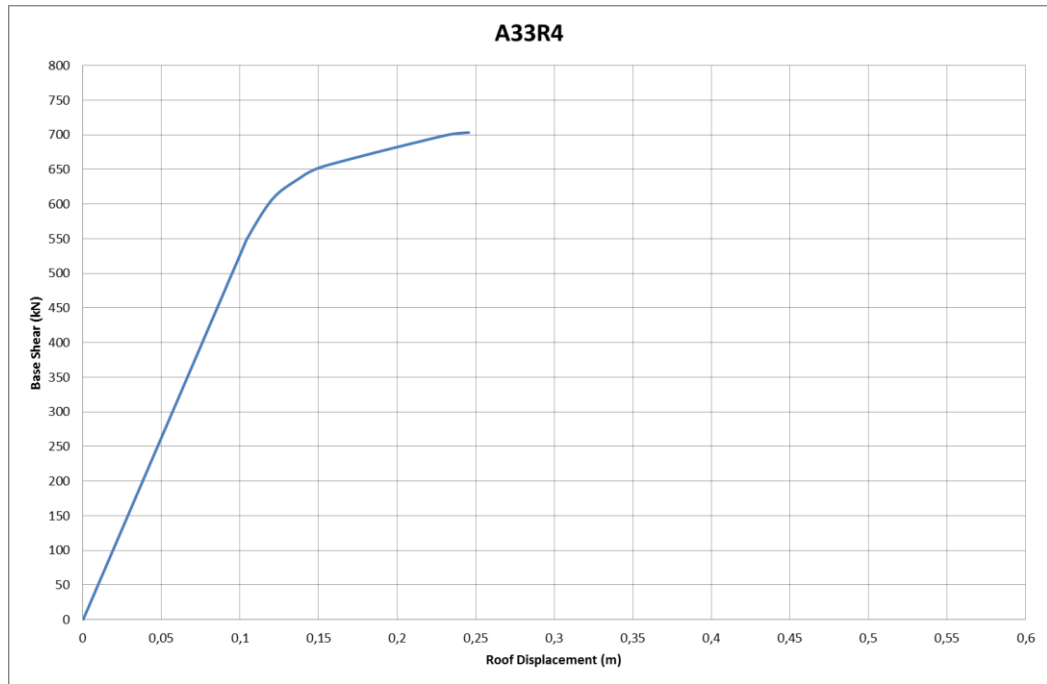


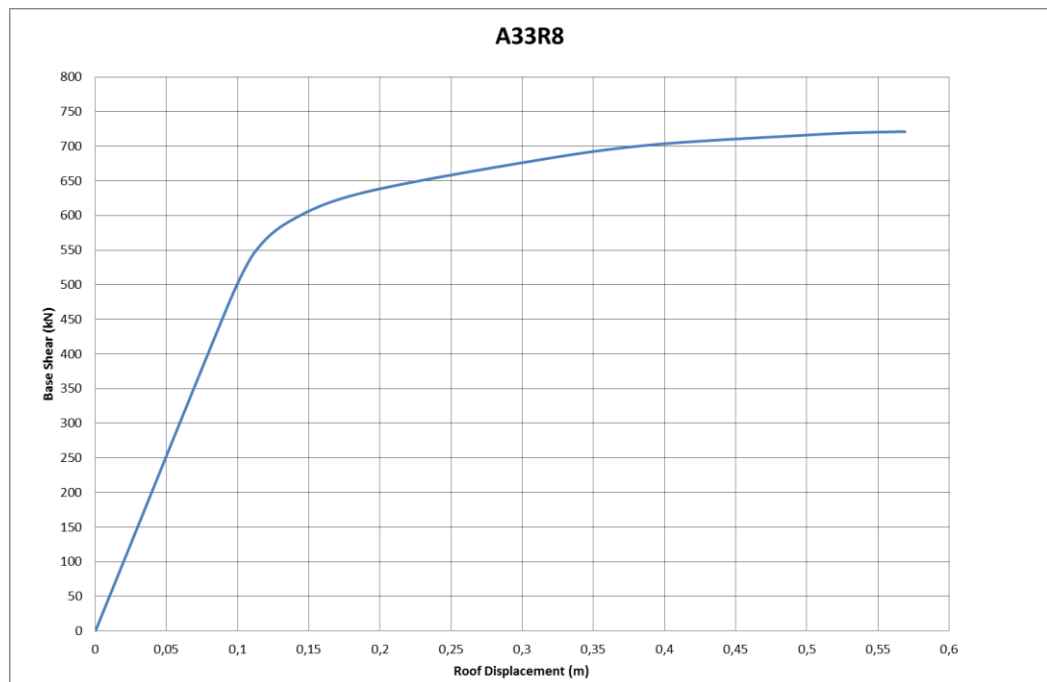
Figure 5.12 Plastic hinge formations for SMRF

### 5.4.1 Pushover Analysis

Pushover analysis results taken from SAP2000 computer software. Base shear versus roof displacement graph shown as in Figure 5.13.



a) A33R4



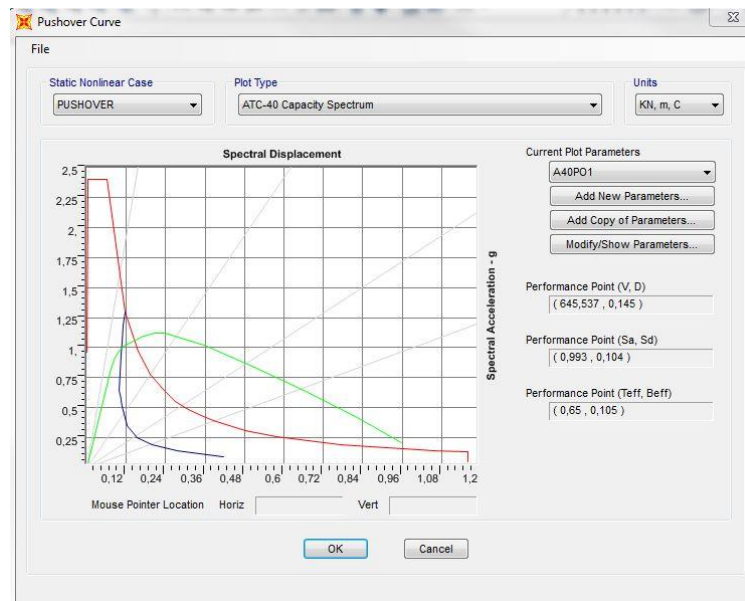
b) A33R8

Figure 5.13 Pushover curve for both normal (a) and high (b) ductility level 3x3 frames

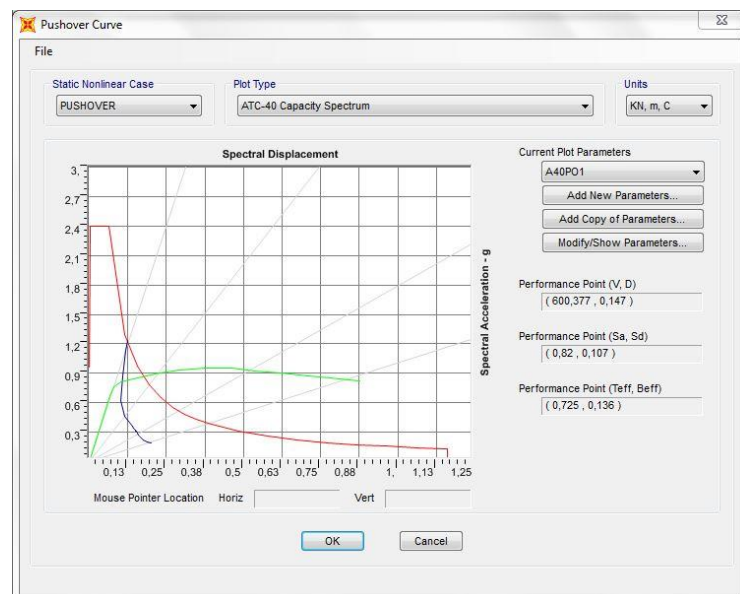
## 5.4.2 Capacity Spectrum

Procedure for obtaining ‘Modal Capacity Curve’ is explained in section 4.2 of this study. The base shear force values will be divided by the total effective mass to obtain the modal pseudo accelerations. Modal displacement values will be obtained by dividing the top displacements to modal participation factor and first mode amplitude.

The capacity curve also can be obtained from SAP2000 as shown in Figure 5.14:



a) Frame A33R4



b) Frame A33R8

Figure 5.14 Spectral capacity curve for both normal (a) and high (b) ductility level 3x3 frames (SAP2000)

The spectral capacity graph can be obtained as defined ATC-40 procedure (explained in Chapter 4). The information about the mass of the structure, modal participation mass ratio, modal participation mass factor and top displacement (amplitude) taken from SAP2000. After application ATC-40 procedure, the followed graphs are obtained (Figure 5.15):

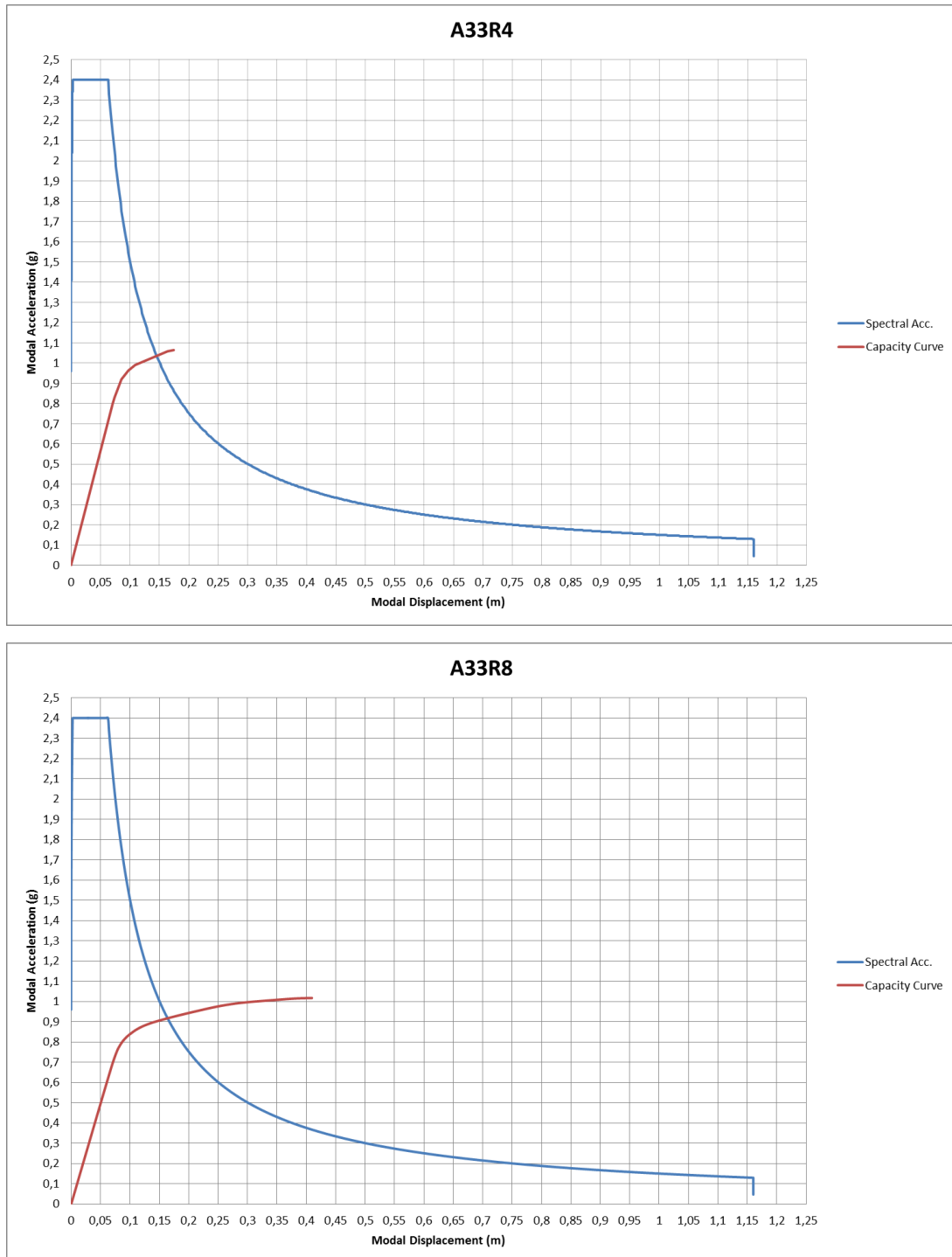


Figure 5.15 Spectral capacity curve for both normal (A33R4) and high (A33R8) ductility level 3x3 frames

### 5.4.3 The Idealization of Pushover Graph

The graph we need for defining R-value is the idealized pushover graph as a bilinear curve. The main reason for converting the pushover curve to a bilinear curve is to idealize the graph. Thus a clearer yield point is determined. In almost all R factor calculations, the global yield point of the system has great importance. The logic in this conversation is to keep the area under both graphs equal.

The bilinear curve consists of three points that are the initial point of the first line, the intersection of the first and second line and end point of the second line. The started point (0,0) and endpoint (collapse point- last step of a pushover) in the main pushover chart are clear. Then a yield point is assumed and linear lines are drawn from the starting point to assumed yield point and from the assumed yield point to the endpoint. Then the yield point idealized until reaching the equal area under the bilinear curve to main pushover curve. The idealization of area equality is performed with solver property of MS Excel. The converted pushover curves to bilinear curves of A33R4 and A33R8 frames are shown in Figure 5.16 and Figure 5.17.

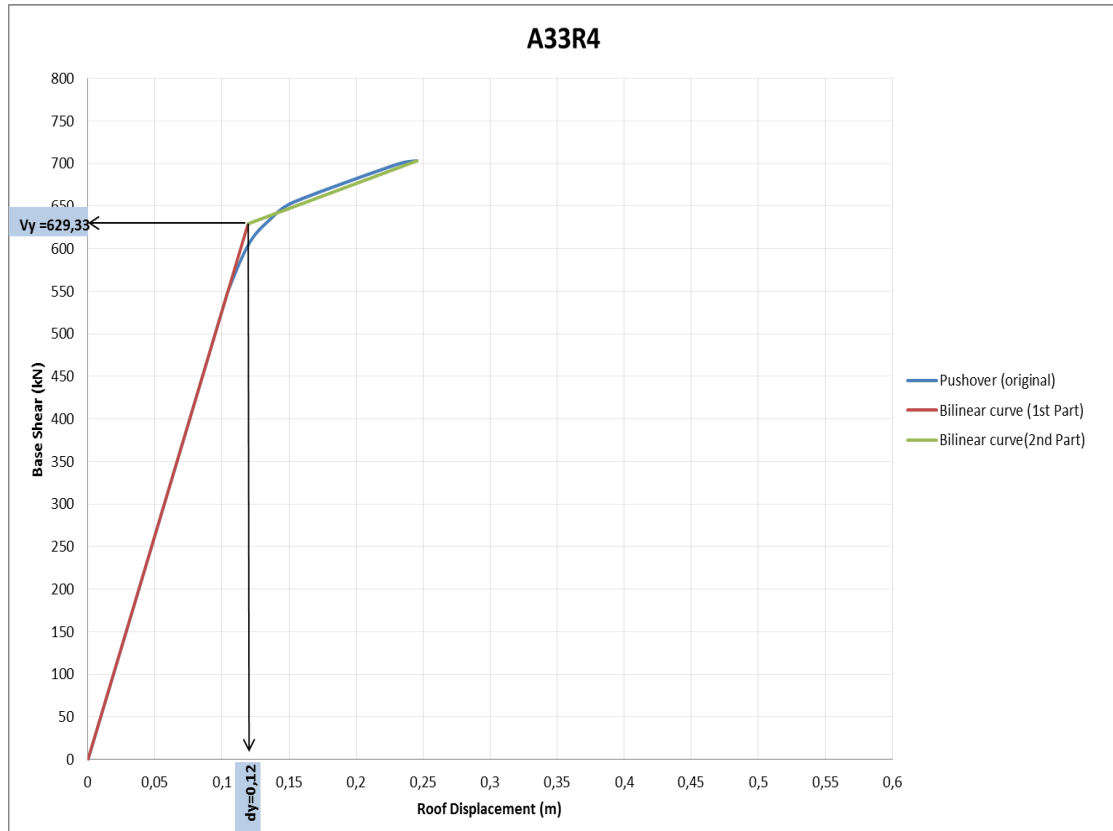


Figure 5.16 Idealized pushover curve for normal (A33R4) ductility level 3x3 frame

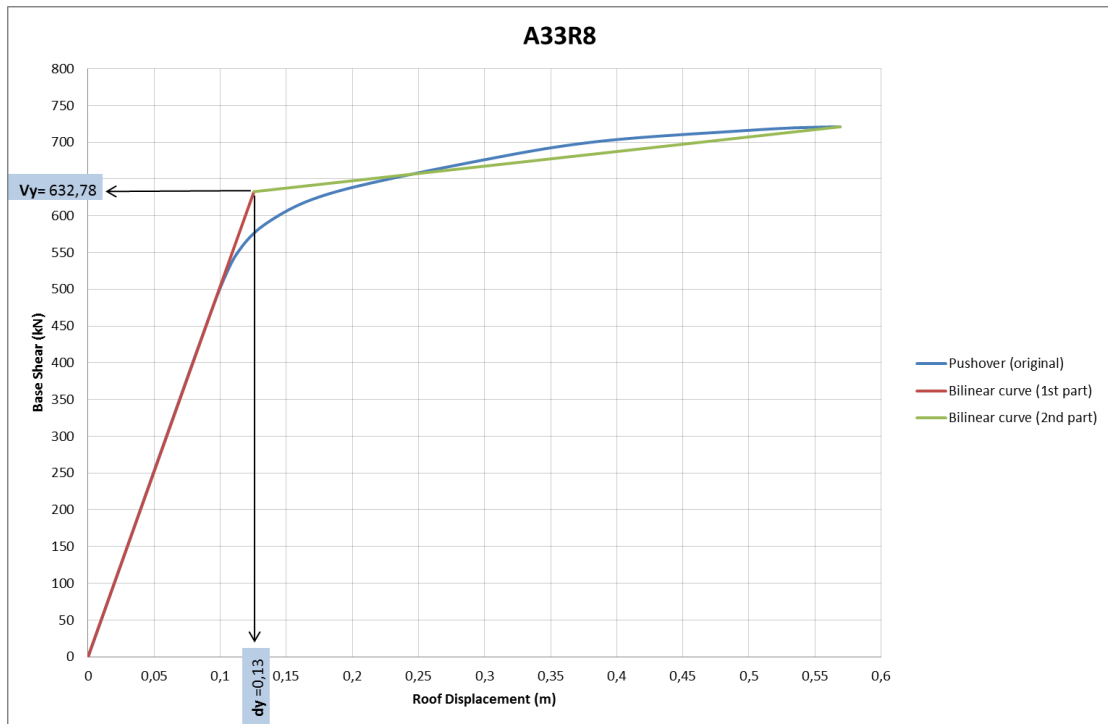


Figure 5.17 Idealized pushover curve for high (A33R8) ductility level 3x3 frame

The intersection point of the first line and second line of bilinear graph refers to the yielding point of the system. The yield force ( $V_y$ ) and yield displacement ( $d_y$ ) determined.

#### 5.4.4 Evaluation of R Factors

The evaluation of R factor is presented in this part.

Table 5.4 and Table 5.5 represents the R factor and its components that evaluation of study case frames.

The design force ( $V_d$ ) that specified by TBEC-2018 code and determined with equation (5.9). The larger value of  $V_{te1}$  and  $V_{te2}$  used as a design force ( $V_d$ ).

$$V_{TE} = m_t \cdot S_{aR} (T_p^{(x)}) \geq 0.04 \cdot m_t \cdot I \cdot S_{DS} \cdot g \quad (5.9)$$

Table 5.4. Design force  $V_{te}$

Frame	R	T(sec)	mt(ton)	Sae(T)	Sar(Tp)	Vte1(kN)	Vte2(kN)
A33	4	0,61	87,97	1,27	0,32	274,46	82,85
	8	0,64	88,21	1,22	0,15	132,08	83,07

Table 5.5. R factor and its parameters

Pushover Step	A33-R4		A33-R8	
	Disp (m)	Base F. (kN)	Disp (m)	Base F. (kN)
1	0,00	0,00	0,00	0,00
2	0,10	527,28	0,09	476,96
3	0,10	549,08	0,11	546,04
4	0,12	606,41	0,14	593,54
5	0,14	635,90	0,19	632,73
6	0,15	654,26	0,30	677,48
7	0,23	699,07	0,39	701,68
8	0,25	703,32	0,50	715,90
9			0,53	719,28
10			0,56	720,83
11			0,57	721,02
12				
13				
14				
15				
16				
17				
18				
19				
20				
Vd	274,46		132,08	
V1y	527,28		476,96	
Vy	629,33		632,78	
Ve	1097,82		1056,63	
dy	0,12		0,13	
du	0,25		0,57	
R $\Omega$	1,92		3,61	
R $\rho$	1,19		1,33	
$\mu$	2,06		4,53	
R $\mu$	2,06		4,53	
<b>R</b>	<b>4,71</b>		<b>21,71</b>	

In this study, the response modification factor evaluated as components of three factors which are overstrength factor, redundancy factor, and ductility reduction factor.

$V_{1y}$  is the first yield point value that first step of pushover analysis. Elastic base shear force ( $V_e$ ) basically can be defined as  $R \cdot V_d$ , for detail explanation the intersection point of the period and spectral ground motion curve on the capacity curve (initial point of performance point line) can be considered.

The ultimate displacement point ( $d_u$ ) of the system is the last step displacement of pushover curve, after this point the base shear goes down.

The overstrength factor ( $R_\Omega$ ) is the ratio of first yield force ( $V_{1y}$ ) to design force ( $V_d$ ). The redundancy factor ( $R_\rho$ ) is the ratio of yield force ( $V_y$ ) to first yield force ( $V_{1y}$ ).

**For OMRF (R=4)****For SMRF (R=8)**

$$R_{\Omega} = \frac{V_{1y}}{V_d} = \frac{527,28}{274,46} = 1,92$$

$$R_{\Omega} = \frac{V_{1y}}{V_d} = \frac{476,96}{132,08} = 3,61$$

$$R_{\rho} = \frac{V_y}{V_{1y}} = \frac{629,33}{527,28} = 1,19$$

$$R_{\rho} = \frac{V_y}{V_{1y}} = \frac{632,78}{476,96} = 1,33$$

The ductility reduction factor ( $R_{\mu}$ ) is a function of the ductility factor ( $\mu$ ) that displacement base. The ductility factor ( $\mu$ ) is the ratio of ultimate displacement ( $d_u$ ) to yield displacement ( $d_y$ ).  $R_{\mu} = \mu$  equation used for ductility reduction factor as pointed Equation 3.4a (  $T > T_B$  ).  $T_B=0,324$  and all frame periods larger than this value so followed condition valid for all frames:  $R_{\mu} = \mu$

$$\mu = \frac{du}{dy} = \frac{0,25}{0,12} = 2,06$$

$$\mu = \frac{du}{dy} = \frac{0,57}{0,13} = 4,53$$

$$R_{\mu} = \mu = 2,06$$

$$R_{\mu} = \mu = 4,53$$

$$R = R_{\mu} \cdot R_{\rho} \cdot R_{\Omega} = 1,92 \cdot 1,19 \cdot 2,06 = 4,71$$

$$R = R_{\mu} \cdot R_{\rho} \cdot R_{\Omega} = 3,61 \cdot 1,33 \cdot 4,53 = 21,71$$

The parameters of R factor components (overstrength factor, redundancy factor, and ductility factors) for A33R4 frame and A33R8 frame are shown in Figure 5.18 and Figure 5.19, respectively.

That should be noted that the overstrength factor defined at TBEC 2018 [4] (also given at Equation 3.3) is signed with letter D and the value is explained as the ratio of  $V_y$  (yield shear force) to  $V_d$  (design base shear). Redundancy factor is required to be included in this study so the overstrength factor is divided into two separate components that are overstrength and redundancy factors. As can be seen from the results of the R factor obtained below, the resulting value will be the same and only the intermediate step  $V_{1y}$  (first yield force) will be added.

According to a formulation that defined at informative attachment 4A part of TBEC 2018, which also defined at Equation 3.1 of this study, the R factor can be evaluated as:

$$R = D \cdot R_y(\mu, T)$$

$$D = \frac{V_y}{V_d} = \frac{629,33}{274,46} = 2,29$$

$$D = \frac{632,78}{132,08} = 4,79$$

$$R_y(\mu, T) = \mu$$

$$\mu = \frac{u_{max}}{u_y} = \frac{0,25}{0,12} = 2,06$$

$$\mu = \frac{0,57}{0,13} = 4,53$$

$$R = 2,29 * 2,06 = 4,71$$

$$R = 4,79 * 4,53 = 21,71$$

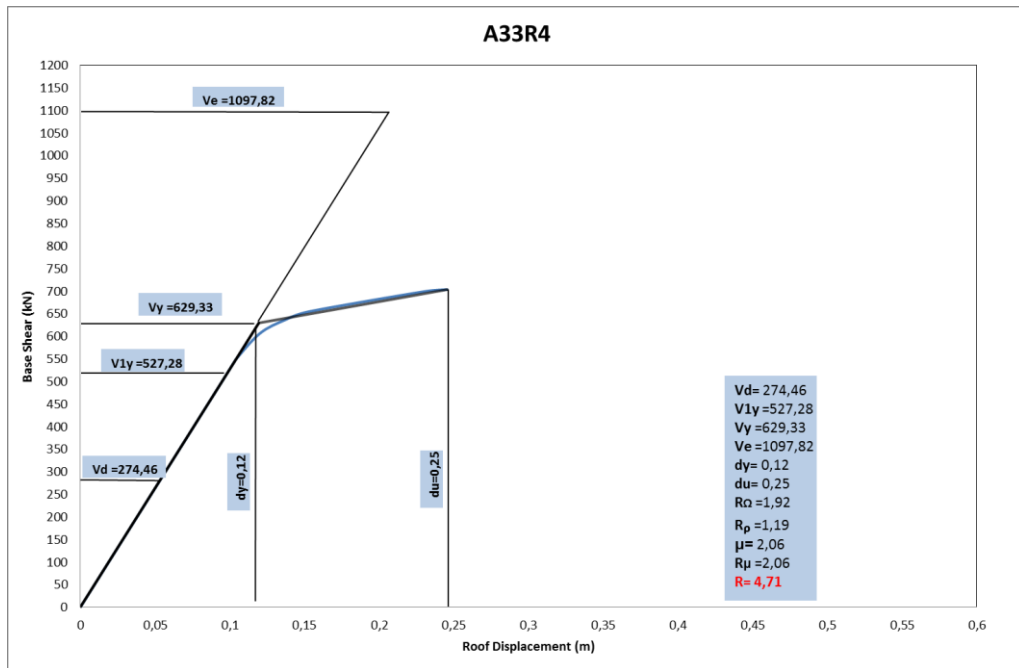


Figure 5.18 Representation of R value component's parameters for A33R4 frame

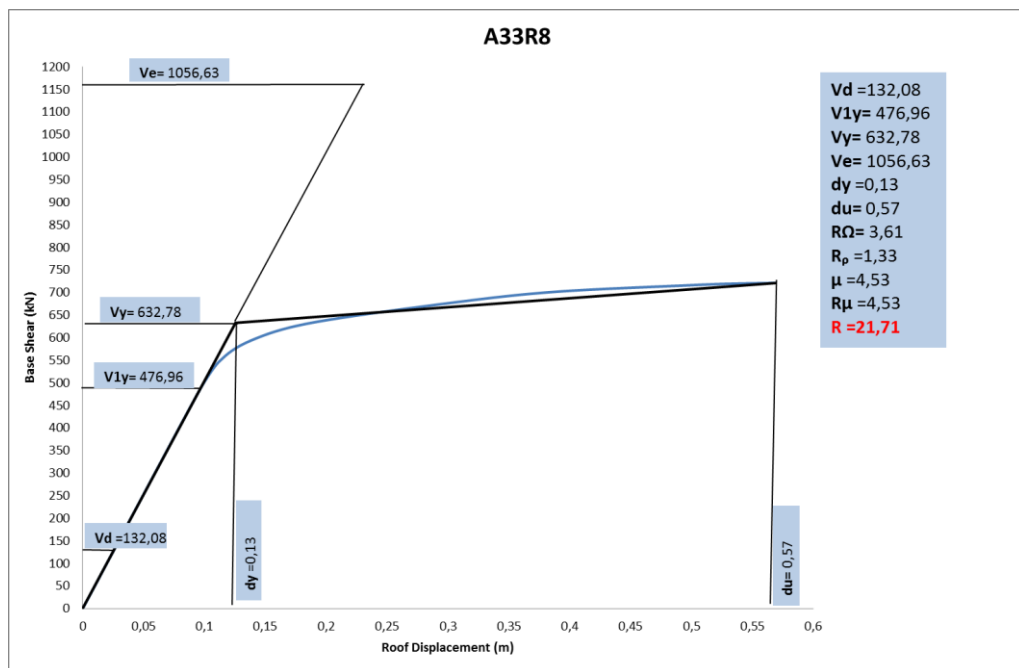


Figure 5.19 Representation of R value component's parameters for A33R8 frame

## CHAPTER 6

### RESULTS OF ANALYSIS AND FURTHER REMARKS

In this chapter, all frame analysis results as a result of pushover are presented in accordance with the process explained the previous case study to obtain R-value. The results are listed for both normal and high ductility level frames. The used frame sections are presented in Appendix A. The R values obtained as a result of the analysis are listed in Table 6.1.

Table 6.1. Calculated R factors

Frame	R	T(sec)	R $\Omega$	R $\rho$	R $\mu$	R
A33	4	0,61	1,92	1,19	2,06	4,71
	8	0,64	3,61	1,33	4,53	21,71
A36	4	1,04	2,12	1,16	2,64	6,47
	8	1,18	2,91	1,28	4,12	15,34
A39	4	1,36	1,91	1,25	3,15	7,56
	8	1,59	1,89	1,32	3,92	9,75
A43	4	0,64	1,94	1,17	2,63	5,98
	8	0,63	3,66	1,28	4,77	22,40
A46	4	1,03	1,99	1,25	2,94	7,28
	8	1,16	2,74	1,29	4,15	14,73
A49	4	1,35	1,92	1,21	2,82	6,55
	8	1,58	1,88	1,37	4,34	11,20
A53	4	0,61	1,98	1,16	2,23	5,09
	8	0,61	3,42	1,35	4,95	22,91
A56	4	1,04	2,04	1,17	2,53	6,04
	8	1,15	2,76	1,29	4,16	14,85
A59	4	1,37	1,87	1,22	2,63	6,02
	8	1,59	1,81	1,35	3,73	9,13
A63	4	0,61	1,96	1,09	2,08	4,44
	8	0,62	3,52	1,31	4,94	22,77
A66	4	1,04	1,96	1,23	2,56	6,17
	8	1,16	2,67	1,32	4,14	14,62
A69	4	1,36	1,96	1,18	2,70	6,22
	8	1,55	1,86	1,42	4,37	11,53
A73	4	0,62	1,89	1,19	2,47	5,56
	8	0,60	3,49	1,34	4,90	22,90
A76	4	1,03	1,92	1,24	2,13	5,06
	8	1,16	2,63	1,33	4,02	14,07
A79	4	1,36	1,87	1,22	2,53	5,78
	8	1,54	1,93	1,33	3,89	9,97
A83	4	0,62	1,86	1,16	2,14	4,64
	8	0,60	3,40	1,38	4,98	23,38
A86	4	1,04	2,00	1,20	2,55	6,14
	8	1,16	2,65	1,33	4,07	14,32
A89	4	1,36	1,86	1,20	2,19	4,89
	8	1,55	1,87	1,38	4,11	10,61

The results of the analysis were evaluated to obtain Table 6.1. As described in the case study (Chapter 5), the same steps are made for all frames. The graphs obtained as a result of pushover analysis for each frame are presented in Appendix B. In addition to pushover analysis, in order to show the performance of the frame in comparison to spectral ground acceleration, capacity spectrum graphs are given in Appendix B. These graphs are shown for both Ordinary Moment Resisting Frames (OMRF) and Special Moment Resisting Frames (SMRF), including the pushover curve and spectral capacity curve for each frame.

The classification of R values for both OMRF (normal ductility frames) and SMRF (high ductility frames) are listed in Table 6.2.

Table 6.2. R values for both OMRF and SMRF

Frame	R VALUES	
	OMRF	SMRF
A33	4,71	21,71
A36	6,47	15,34
A39	7,56	9,75
A43	5,98	22,40
A46	7,28	14,73
A49	6,55	11,20
A53	5,09	22,91
A56	6,04	14,85
A59	6,02	9,13
A63	4,44	22,77
A66	6,17	14,62
A69	6,22	11,53
A73	5,56	22,90
A76	5,06	14,07
A79	5,78	9,97
A83	4,64	23,38
A86	6,14	14,32
A89	4,89	10,61

The graphical comparison of calculated R values with design R value for Ordinary Moment Resisting Frames (R=4) shown in Figure 6.1 and for Special Moment Resisting Frames (R=8) shown in Figure 6.2. The black horizontal straight line on the graphs refers to the R value used in design.

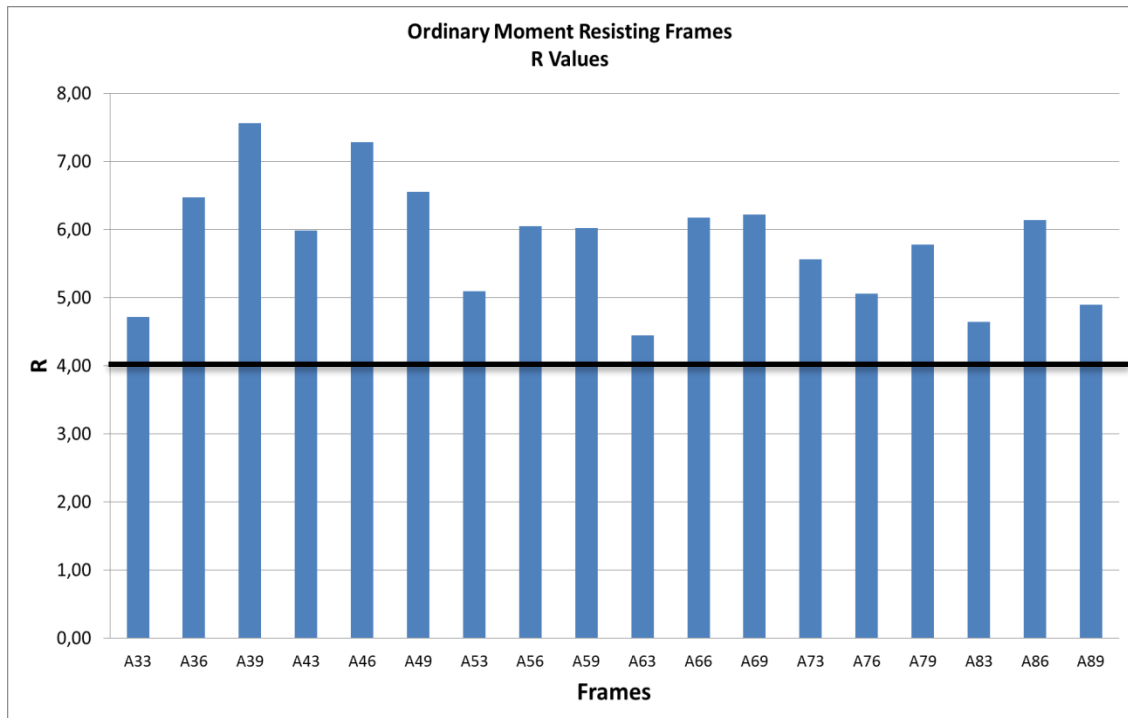


Figure 6.1 R Values for Ordinary Moment Resisting Frames

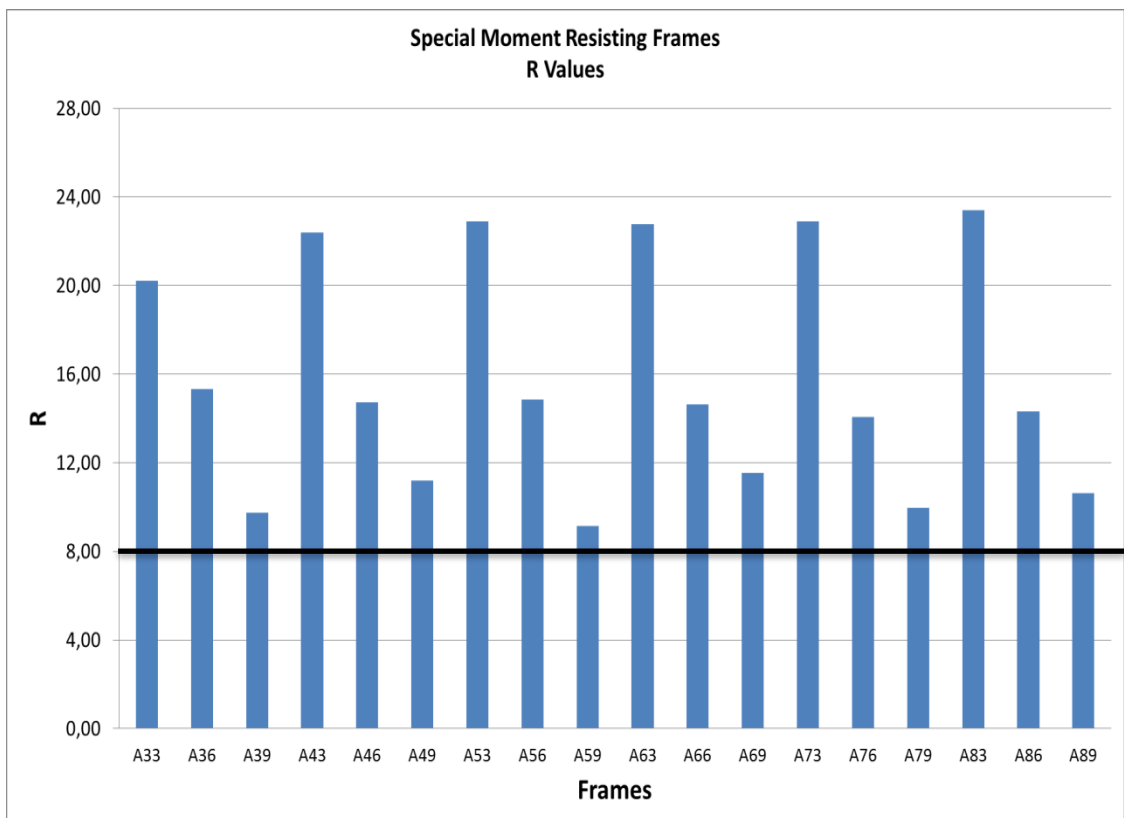


Figure 6.2 R Values for Special Moment Resisting Frames

The graphical comparison of R values for Ordinary Moment Resisting Frames (OMRF) is shown in Figure 6.3 for each story, and in Figure 6.4 for each bay. The details of each component of the R factors and pushover graphs of each frame are presented in section Appendix B.

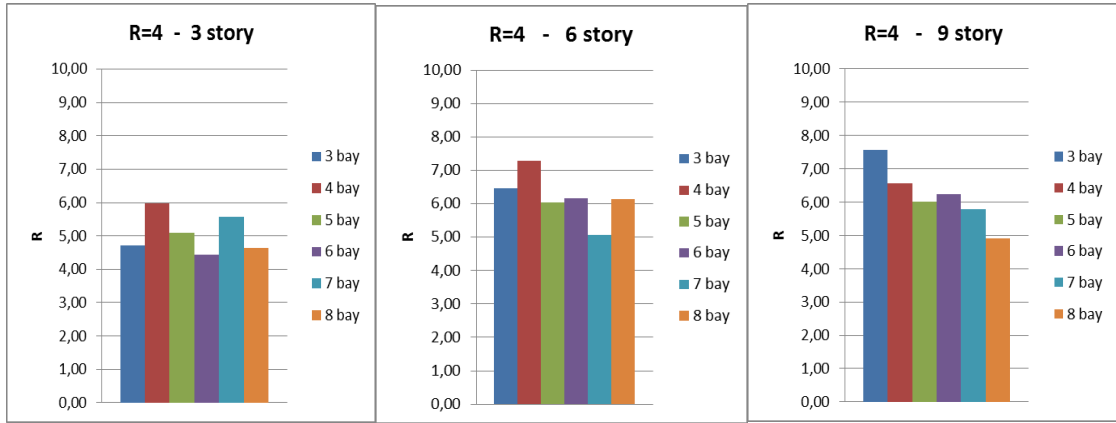


Figure 6.3 Response Modification Factor (R) for each story (3-6-9) vs. bays (3-4-5-6-7-8) ( $R_{design} = 4$ )

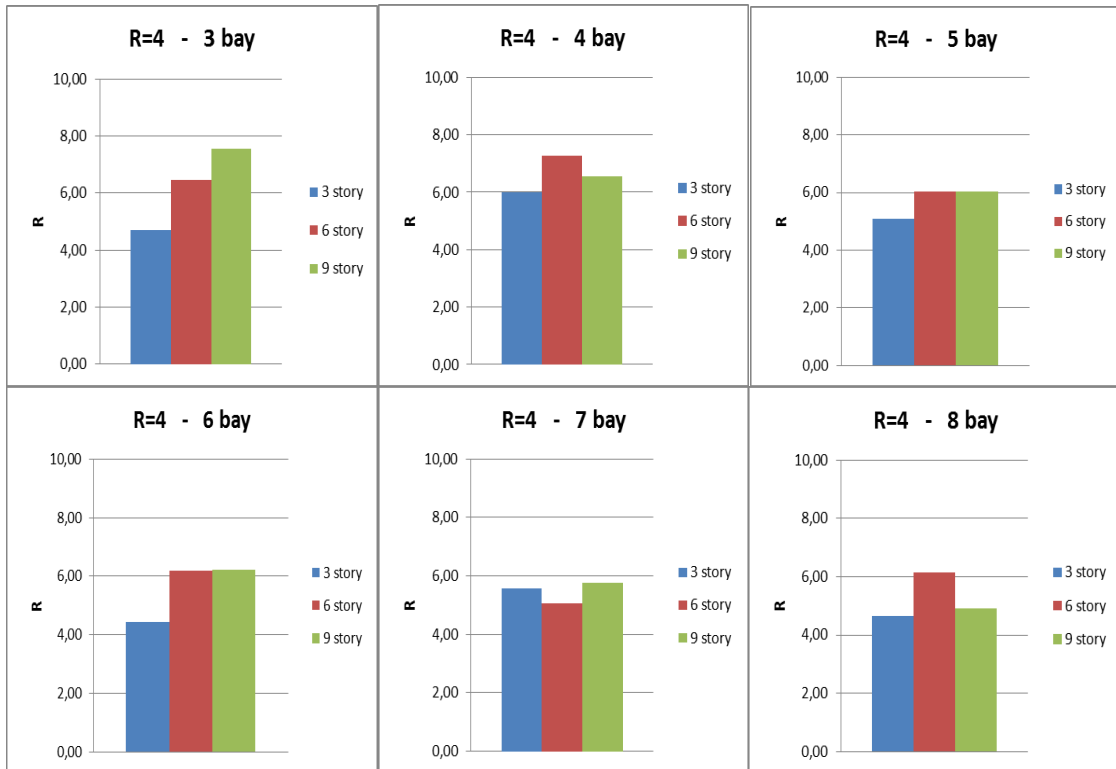


Figure 6.4 Response Modification Factor (R) for each bay (3-4-5-6-7-8) vs. stories (3-6-9) ( $R_{design} = 4$ )

The graphical comparison of the R values for the Special Moment Resisting Frames (SMRF) is shown in Figure 6.5 for each story, and in Figure 6.6 for each bay. The details of each component of the R factors and pushover graphs of each frame are presented in section Appendix B.

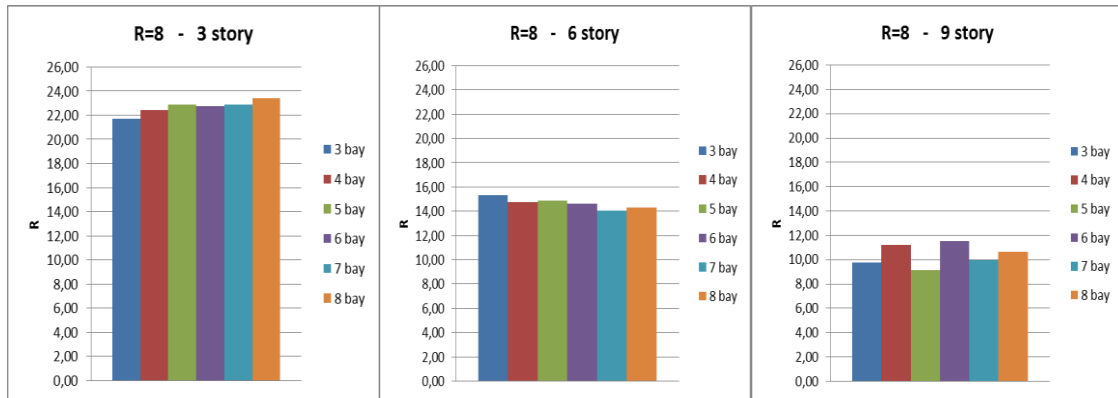


Figure 6.5 Response Modification Factor (R) for each story (3-6-9) vs. bays (3-4-5-6-7-8) ( $R_{design} = 8$ )

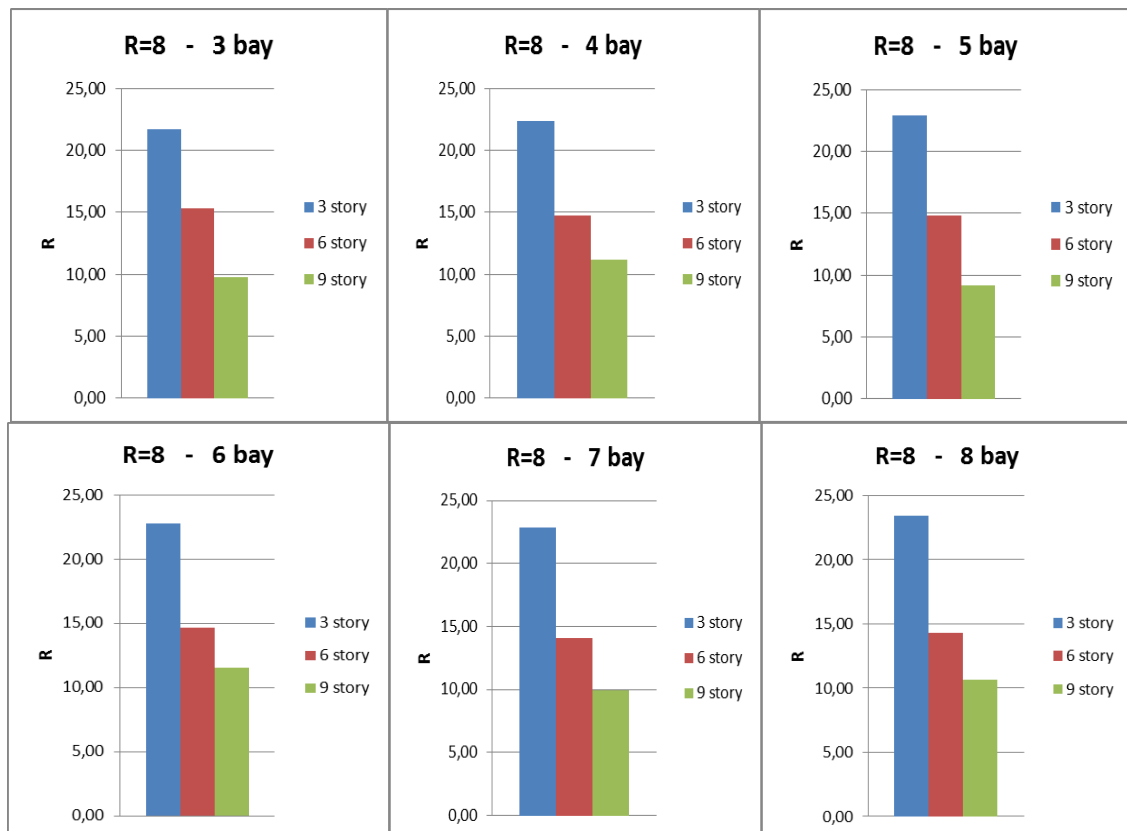


Figure 6.6 Response Modification Factor (R) for each bay (3-4-5-6-7-8) vs. stories (3-6-9) ( $R_{design} = 8$ )

The pushover curves and capacity curves are presented as following figures (Figure 6.7 and Figure 6.8). The pushover curves and capacity curves are shown in the same graph to better evaluate the behaviour of Special Moment Resisting Frames (SMRF) and Ordinary Moment Resisting Frames (OMRF).

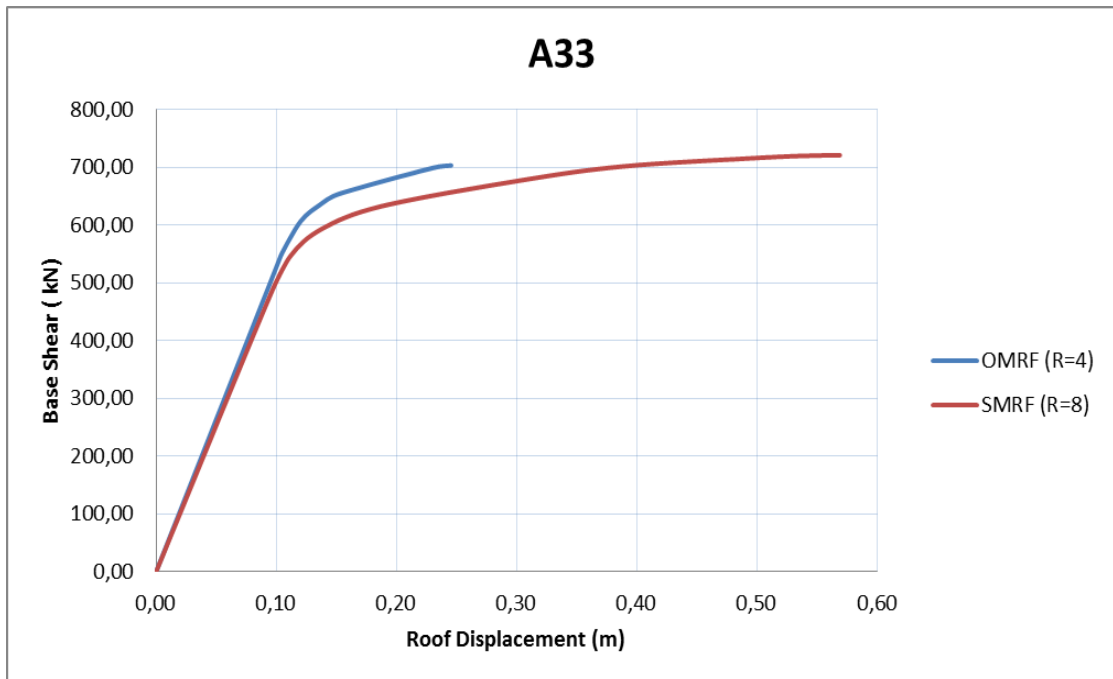


Figure 6.7 Superimposing pushover curve of OMRF and SMRF

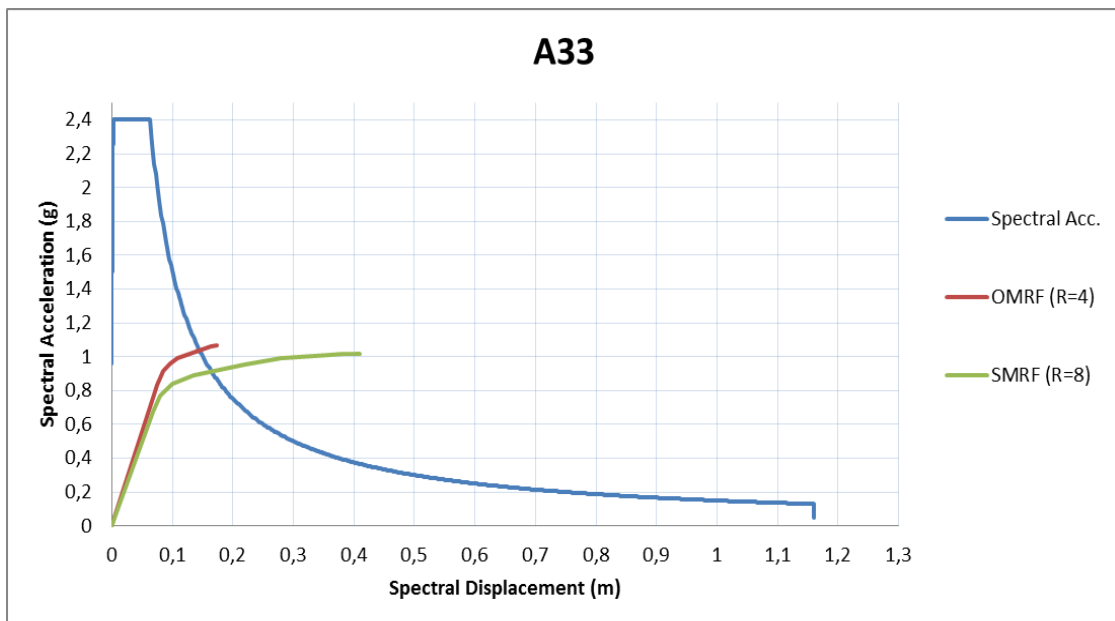


Figure 6.8 Superimposing capacity curve of OMRF and SMRF

## CHAPTER 7

### SUMMARY OF RESULTS AND CONCLUSIONS

#### 7.1 SUMMARY OF RESULTS

In this section, the results of the analysis expressed by the graphs and tables will be evaluated and interpreted. A total of 36 analyses were performed; half of them had a high ductility level and the other half had normal ductility level frames.

As shown in Table 6.1, the period of all frames are larger than the second corner period of the spectral acceleration graph ( $T_B = 0,324$ ) so the ductility factor can be used as the ratio of maximum displacement ( $d_u$ ) to yield displacement ( $d_y$ ). (TBEC-2018 [4])

Figure 6.1 shows the distribution of R values for each frame are designed as processing normal ductility. The design R coefficient was taken as 4, (as stated in Figure 5.5) Figure 6.1 showed that the obtained R values were close to this value for all related frames. Figure 6.2 shows the distribution of R values for each frame which was designed as possessing high ductility. Although the design R coefficient was taken as 8, (as stated in Figure 5.6) Figure 6.2 showed that the R values obtained were greater than 8 for the all related frames.

As seen in the graphs of Figure 6.3 and Figure 6.4, for  $R=4$ , there is no significant change in the R factor as the span changes at a constant story. When a constant span is taken into consideration, the R-values do not show uniform distribution as the number of stories increases.

As seen in the graphs of Figure 6.5 and Figure 6.6, for  $R=8$ , there is no significant change in the R factor as the span changes at a constant story. However, as the story number increases the R factor decreases. The average value of R factors is 22.68, 14.66, 10.37 for three, six and nine story numbers respectively. When a constant span is taken into consideration, the R-value decreases significantly as the number of stories increases.

As seen in the graph of Figure 6.7, although the OMRF performed less displacement beyond elastic limit, the displacement capacity of the SMRF is

remarkable. As shown in the Figure 6.8, although both frame system meet the demand, the OMRF remains minimal in terms of elasto-plastic behaviour. On the other hand, both graph reflect that, the elastic capacity of OMRF is seems to be better than SMRF.

Although the obtained R values for OMRF are close to code value, the obtained R values for SMRF are considerably higher than the code value. The difference between codes and analysis results originally comes from a high ductility frames tendencies. This difference is mostly affected by the strong column-weak beam procedure for frames that are designed for high ductility. Therefore, as a result of this procedure, when the columns have a larger plastic capacity than the beams, this situation results in a considerable unused capacity for lateral loads.

As seen in Table 6.2, the obtained R values for SMRFs are very different and higher than those defined in code. This situation causes an extreme design and deviation from the optimum design. Over-designed frames can withstand greater capacity levels than the prescribed values.

Additionally, according to the spectral capacity curves in Appendix B, all frames provide the demand. No frame remained below the spectral acceleration graph that represented the demand. It should be also noted that all the frames have passed their plastic limit, which indicates that the performance beyond elasticity. As seen in Appedix C, OMRFs showed higher elastic performance, whereas SMRFs showed higher elasto-plastic (ductility) performance.

## **7.2 CONCLUSIONS**

The results obtained from this study are evaluated in this section. All the studies on seismic design aim to ensure safety against earthquakes at a reasonable cost. The prominent subject of recent analytical and experimental studies on seismic design has been the reliability of the modern buildings in terms of the performance (response) of these structures against seismic activities. As the knowledge and experience gained through all the studies and practice improved, it would be expected to estimate the behavior against the seismic actions better and better. This would probably be reflected in more economical designs without jeopardizing the safety of public.

In this study, the modification factors used in seismic design codes are investigated to seek if some suggestions can be made to better represent and take

advantage of inelastic behaviour's energy dissipation potential against seismic activity. The engineering community seems to accept that the concept of displacement based design would allow more rational and economical designs against probable earthquake demands. The results of the analysis in this study, although limited in number, provide some insight on not fully utilizing the advantage of the inelastic behavior of the structures studied. When a general response modification factor  $R$  accounting for the expected behavior type of the structure is used without considering parameters, such as height of the building some of the deformation capacity is underutilized in design. More specifically, the results for special moment resisting frames presumed response modification factor equal to 8, shows the evaluated response factor is much higher for the low number stories compared to high number of stories. The results also suggest that ordinary moment resisting frames provides more comparable results at number of story changes.

So it is believed that there is room for improvement in prescribing the response modification factor,  $R$  to be used in design codes. In lieu of the results representing the response modification factor, it would be better to define  $R$  factor as a product of the overstrength factor ( $R_{\Omega}$ ), redundancy factor ( $R_{\rho}$ ) and ductility factor ( $R_{\mu}$ ). So, rather than aggregating the all these factor in a single value and prescribing it as a generic solution, one would allow to optimize designs without jeopardizing the safety.

### **7.3 SUGGESTIONS**

The response modification factor is incompatible with seismic design codes that give a single value for all buildings regardless of it's height. The result of analysis in this study although limited in number, show that the obtained  $R$  values are directly affected by story heights for Special Moment Resisting Frames (SMRF). According to the results (and assumptions) of this thesis, the  $R$  factors appear larger than designed and varying in a wide range. The  $R$  factor can be classified according to story heights for high ductility frame systems.

Pushover analysis and capacity spectrum method need to be more encouraged and recommended by codes to define the behaviour of structural system. Thanks to development in computer softwares and faster computer processors in recent years, this will not be very hard to do.

Although the Turkish Building Earthquake Code has been improved with last update, it is recommended to include the Redundancy Factor ( $R_p$ ) as a result of this study. Because the behaviour of the structure in the process from the first yield to global yield is also seen important.

In reality, it is believed that the use of higher material strengths than specified in the design, the fulfillment of minimum code requirements for detailing, the additional strength effect of non-structural components, and the oversizing of members all have an effect on the R factor.

## REFERENCES

- [1] T. V. Galambos, *Structural Engineering Report No. 88-06 : Reliability of Structural Steel Systems*. University of Minnesota, 1988.
- [2] UBC (Uniform Building Code), *Uniform Building Code: Volume 2*, vol. 2. 1997.
- [3] FEMA273 (Federal Emergency Management Agency), *NEHRP Guidelines for The Seismic Rehabilitation of Buildings*, no. October. 1997.
- [4] TSC-2018 (Türk Deprem Yönetmeliği), *Ek deprem etkisi altında binaların tasarımı için esaslar*. 2018.
- [5] ASCE/SEI 41-13 (American Society of Civil Engineers), *Seismic evaluation and retrofit of existing buildings*. 2013.
- [6] ATC-40 Applied Technology Council, *Seismic Evaluation and Retrofit of Concrete Buildings*. Redwood City, California, 1996.
- [7] R. O. Hamburger, “Facts for Steel Buildings Seismic Design - Earthquakes and Seismic Design,” *Am. Inst. Steel Constr.*, no. 3, 2009.
- [8] G. Victor and F. M. Mazzolani, *Seismic Design of Steel Structures*. 2014.
- [9] F. M. Mazzolani and V. Gioncu, *Seismic Resistant Steel Structures*. 2000.
- [10] İ. Köse, “Seismic Design Of Steel Structures,” *Boğaziçi Univ.*, 1996.
- [11] FEMA356 (Federal Emergency Management Agency), *Prestandard and Commentary for the Seismic Rehabilitation of Buildings*, no. 1. 2000.
- [12] Applied Technology Council (ATC), *Guidelines for Nonlinear Structural Analysis for Design of Buildings Part IIa – Steel Moment Frames*. 2017.
- [13] ANSI/AISC 341-16 (American Institute of Steel Construction), *Seismic Provisions for Structural Steel Buildings*. 2016.

- [14] ASCE/SEI 7-05 (American Society of Civil Engineers), *Minimum Design Loads for buildings and other Structures*. 2006.
- [15] NEHRP, “Recommended Provisions for Seismic Regulations for New Buildings and Other Structures,” *Fed. Emerg. Manag. Agency*, 2003.
- [16] FEMA-P695 (Federal Emergency Management Agency), *Quantification of Building Seismic Performance Factors*, no. June. 2009.
- [17] ATC 3-06 (Applied Technology Council), *Tentative Provisions for The Development of Seismic Regulations for Buildings For Use in Trial Designs*. 1982.
- [18] H. Chaulagain, H. Rodrigues, E. Spacone, R. Guragain, R. Mallik, and H. Varum, “Response reduction factor of irregular RC buildings in Kathmandu valley,” *Earthq. Eng. Eng. Vib.*, vol. 13, no. 3, pp. 455–470, 2014.
- [19] EUROCODE-8, *Design of structures for earthquake resistance Part 1: General rules, seismic actions and rules for buildings*, vol. 3. 2004.
- [20] SEAOC-Blue Book, *Recommended Lateral Force Requirements and Commentary*. 1999.
- [21] M. Ferraioli, A. Lavino, and A. Mandara, “Behaviour Factor for seismic design of moment-resisting steel frames,” *15th World Conf. Earthq. Eng. Lisbon, Port.*, pp. 1–10, 2012.
- [22] P. Fajfar and M.EERI, “A nonlinear analysis method for performance-based seismic design,” *Earthquake Spectra*, vol. 16, pp. 573–592, 2000.
- [23] A. Whittaker, G. Hart, C. Rojahn, Members, and ASCE, “Seismic Response Modification Factors,” *Struct. Eng.*, vol. 125, no. 1, pp. 438–444, 1999.
- [24] A. Demir, “Response Modification Factors for Moment Resisting and Eccentrically Braced Steel Frames,” *Boğaziçi Univesity*, 2006.
- [25] E. Miranda and V. V. Bertero, “Evaluation of Strength Reduction Factors for

- Earthquake-Resistant Design,” *Earthq. Spectra*, vol. 10, no. 2, pp. 357–379, 1994.
- [26] D. Vamvatsikos *et al.*, “A risk-consistent approach to determine behavior factors for innovative steel lateral load resisting systems,” *Ce/Papers*, vol. 1, no. 2–3, pp. 3434–3443, 2017.
- [27] S. Bakır, “Evaluation of Seismic Response Modification Factors for Steel Frames by Non-linear Analysis,” *Middle East Tech. Univ.*, no. Master Thesis, 2006.
- [28] B. Ö. Odabaşı, “Response Modification Factors for Concentrically Braced Steel Frames,” *Boğaziçi Univ.*, no. Master Thesis, 2006.
- [29] Eurocode3, *Design od steel structures Part 1-3: General rules - Supplementary rules for cold - formed members and sheeting*, vol. 3, no. 2006. 1996.
- [30] TSC-2007 (Türk Deprem Yönetmeliği), *Deprem Bölgelerinde Yapılacak Binalar Hakkında Yönetmelik*, vol. 1, no. 1. 2007.
- [31] C. M. Uang, “Establishing R (or  $R_w$ ) Cd Factors for Building Seismic Provisions,” *Struct. Eng.*, vol. 117, 1991.
- [32] ATC-19 (Applied Technology Council, *Structural Response Modification Factors*. 1995.
- [33] B. Patel and D. Shah, “Formulation of Response Reduction Factor for RCC Framed Staging of Elevated Water Tank using Static Pushover Analysis,” *Proc. World Congr. Eng.*, vol. III, no. June, 2010.
- [34] D. Yahmi, T. Branci, A. Bouchair, and E. Fournely, “Evaluation of behaviour factors of steel moment-resisting frames Evaluation of behaviour factors of steel moment-resisting frames using standard pushover method using standard pushover method,” *X Int. Conf. Struct. Dyn. EURODYN 2017*, vol. 00, pp. 397–403, 2017.
- [35] C. A. Castiglioni, A. Alavi, G. Brambilla, and A. Kanyılmaz, “A Procedure for the Assessment of the Behaviour Factor for Steel MRF Systems Based on Pushover Analysis,” *6th ECCOMAS Themat. Conf. Comput. Methods Struct. Dyn. Earthq. Eng.*, pp. 1636–1644, 2017.

- [36] Türk Çelik Yapılar Yönetmeliği (2016), *Çelik Yapıların Tasarım, Hesap ve Yapımına Dair Esaslar*. 2016.
- [37] J. D. Osteraas and H. Krawinkler, “Strength and Ductility Considerations in Seismic Design,” *Blume Earthq. Eng. Cent.*, 1990.
- [38] A. I. H. M. and A. S. A.-S. SAMAR A. BARAKAT, “A Step Towards Evaluation of the Seismic Response Reduction Factor in Multistorey Reinforced Concrete Frames,” *Nat. Hazards*, pp. 65–80, 1997.
- [39] A. S. Elnashai and A. M. Mwafy, “Overstrength and force reduction factors of multistorey reinforced-concrete buildings,” *Struct. Des. Tall Build.*, vol. 11, no. 5, pp. 329–351, Dec. 2002.
- [40] M. H. Arslan and İ. H. Erkan, “Betonarme Binaların Deprem Yüğü Azaltma Katsayısı Üzerine Yeni Bir Bakış,” *e- J. New World Sci. Acad.*, vol. 6, no. Engineering Sciences, 2011.
- [41] Z. X. Fang and H. T. Fan, “Redundancy of structural systems in the context of structural safety,” *Procedia Eng.*, vol. 14, pp. 2172–2178, 2011.
- [42] E. A. Godínez-Domínguez and A. Tena-Colunga, “Redundancy factors for the seismic design of ductile reinforced concrete chevron braced frames,” *Lat. Am. J. Solids Struct.*, vol. 13, no. 11, pp. 2088–2112, 2016.
- [43] H. Krawinkler and G. D. P. K. Seneviratna, “Pros and cons of a pushover analysis of seismic performance evaluation,” *Eng. Struct.*, vol. 20, pp. 452–464, 1998.
- [44] S. A. Freeman, “Review of The Development of The Capacity Spectrum Method,” *Earthq. Technol.*, vol. 41, no. 438, pp. 1–13, 2004.
- [45] Army - Navy and Airforce, *Technical manual seismic design guidelines for essential buildings*, no. February. 1986.
- [46] L. Sanchez-Ricart and A. Plumier, “Parametric study of ductile moment-resisting steel frames: A first step towards Eurocode 8 calibration,” *Earthq. Eng. Struct. Dyn.*, vol. 37, no. 7, pp. 1135–1155, 2008.

- [47] P. Fajfar, “A nonlinear analysis method for performance-based seismic design,” *Earthq. Spectra*, vol. 16, pp. 573–592, 2000.
- [48] P. Fajfar, “Capacity Spectrum Method Based on Inelastic Demand Spectra,” *Earthq. Eng. Struct. Dyn.*, pp. 979–993, 1999.
- [49] S. E. Dritsos, “Seismic Assessment and Retrofitting of Structures : Eurocode8 - Part3 and the Greek Code on Seismic Structural Interventions,” *IABSE*, no. Earthquake Resistant Structure, 2015.
- [50] ANSI/AISC 360-16 (American Institute of Steel Construction), *Specification for Structural Steel Buildings*. 2016.
- [51] TS 498, *Yapı Elemanlarının Boyutlandırılmasında Alınacak Yüklerin Hesap Değerleri*. Ankara, 1997.

# APPENDIX A

## FRAME SECTIONS

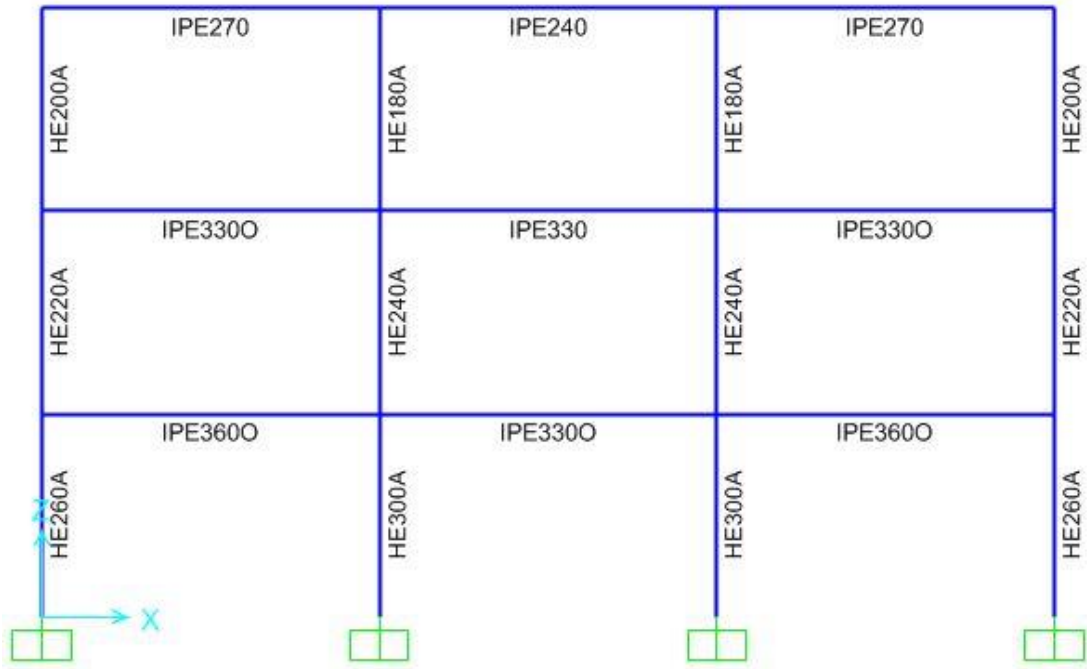


Figure A.1 Frame A33R4 member sections

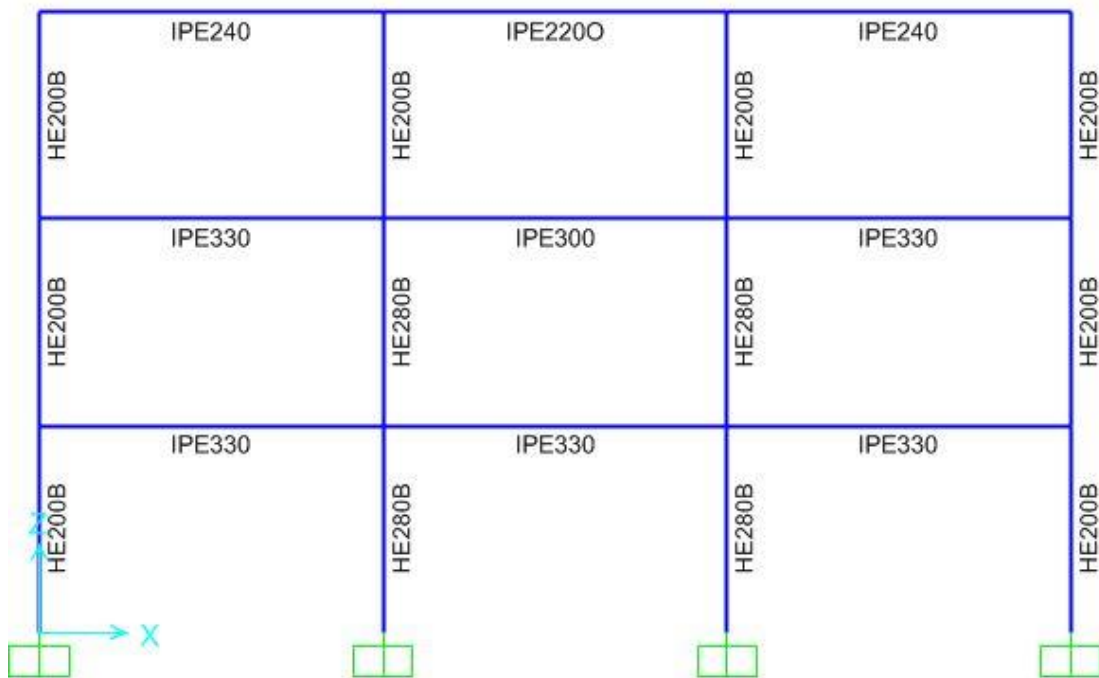


Figure A.2 Frame A33R8 member sections

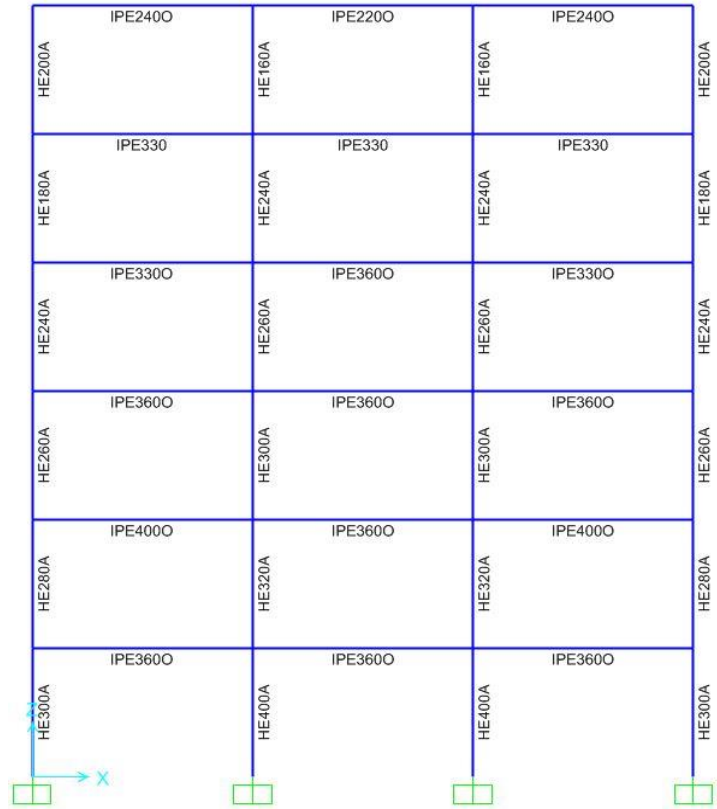


Figure A.3 Frame A36R4 member sections

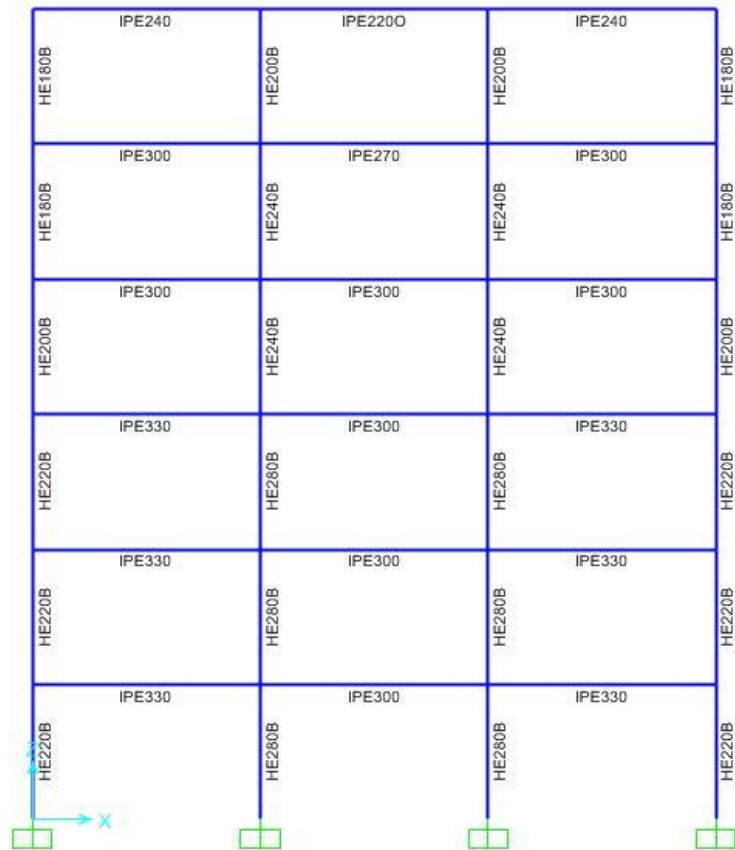


Figure A.4 Frame A36R8 member sections

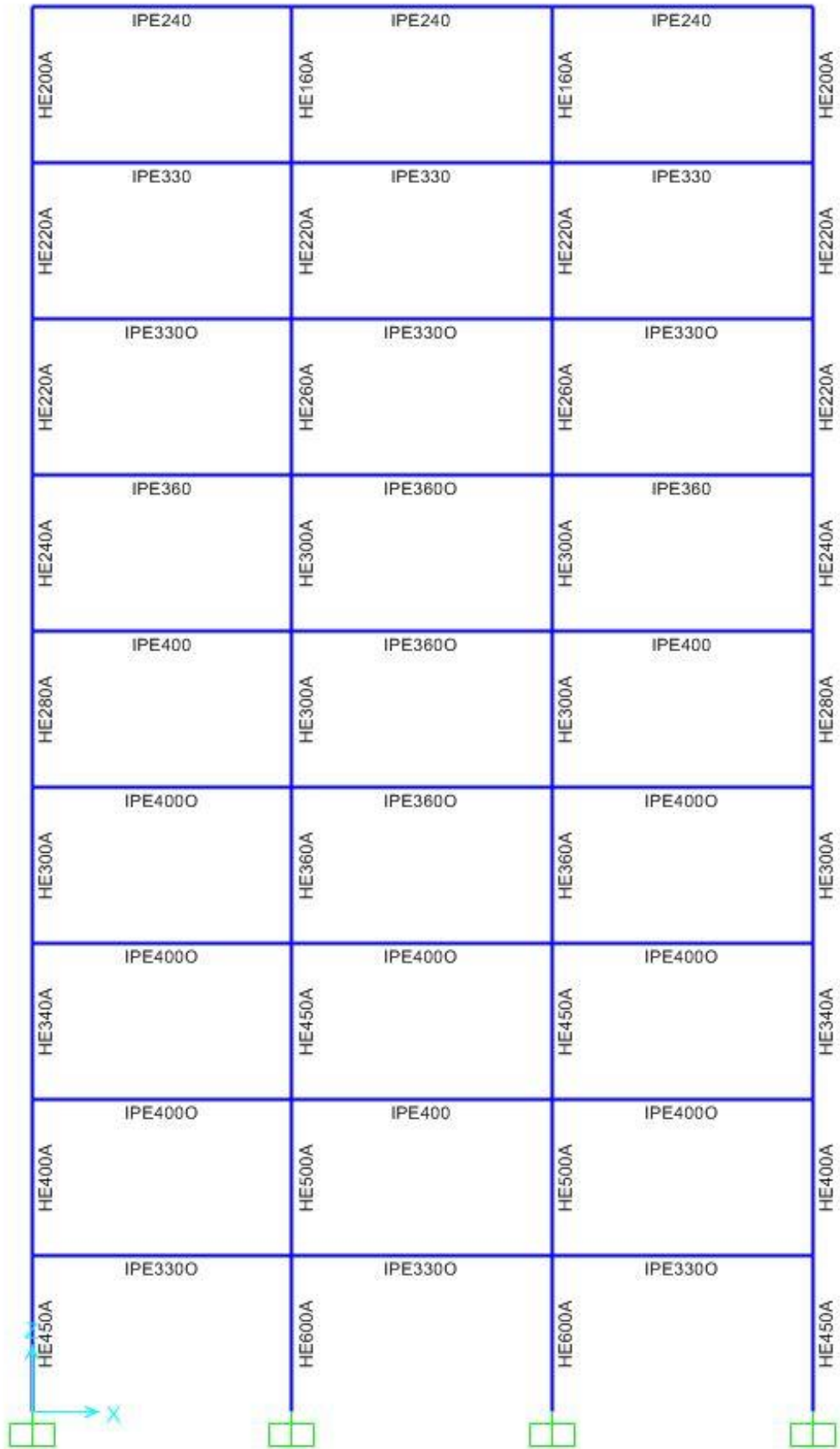


Figure A.5 Frame A39R4 member sections

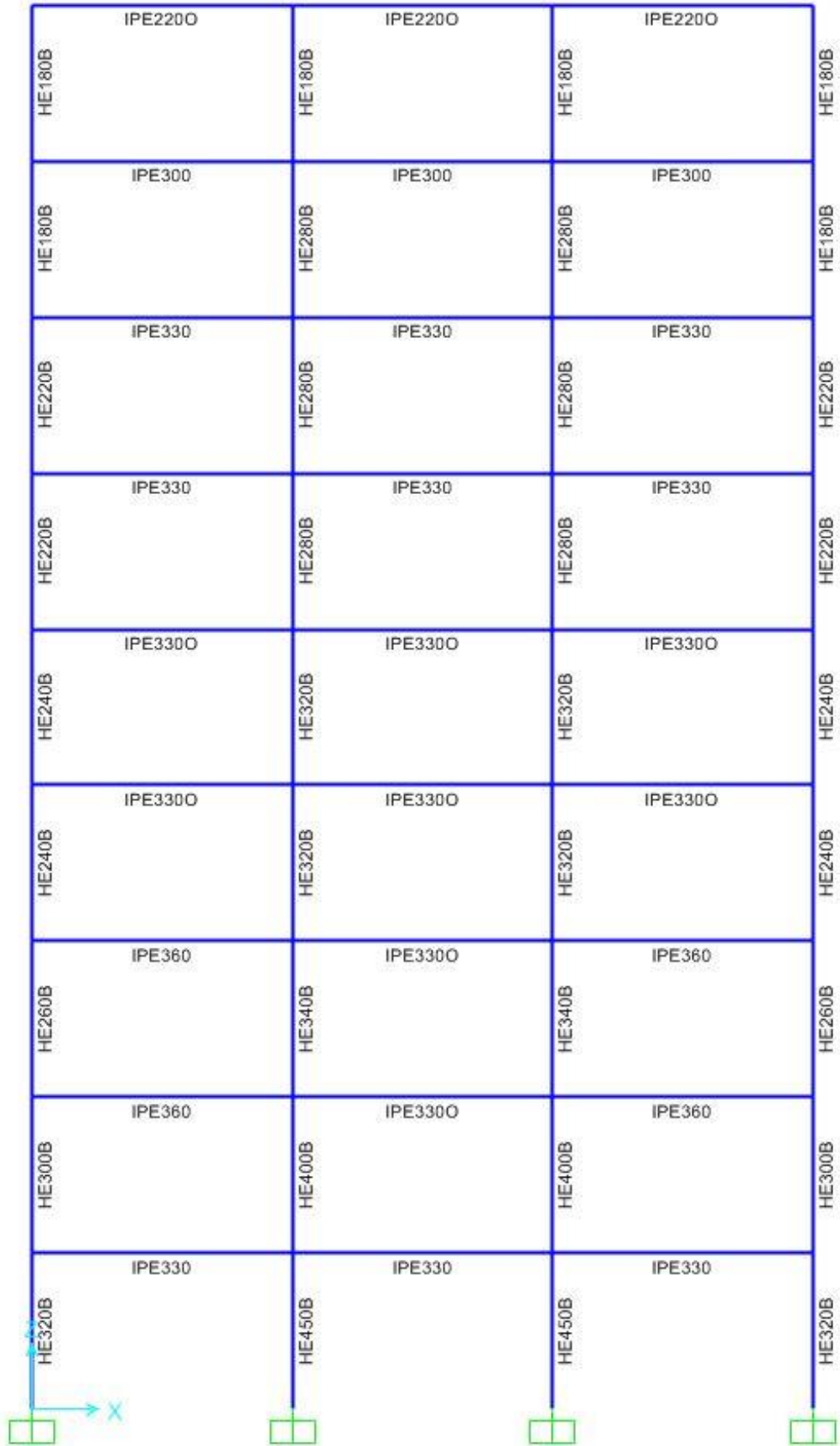


Figure A.6 Frame A39R8 member sections

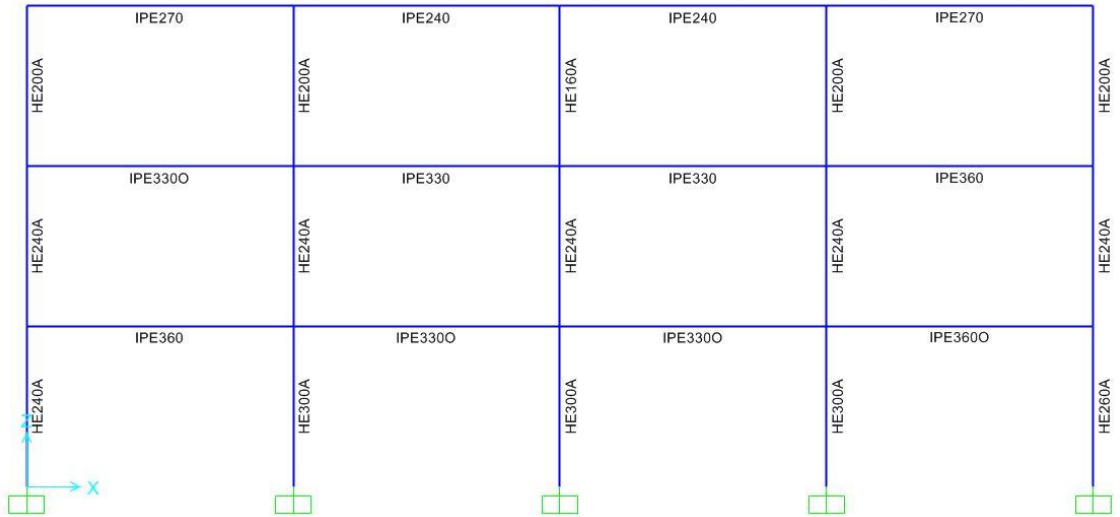


Figure A.7 Frame A43R4 member sections

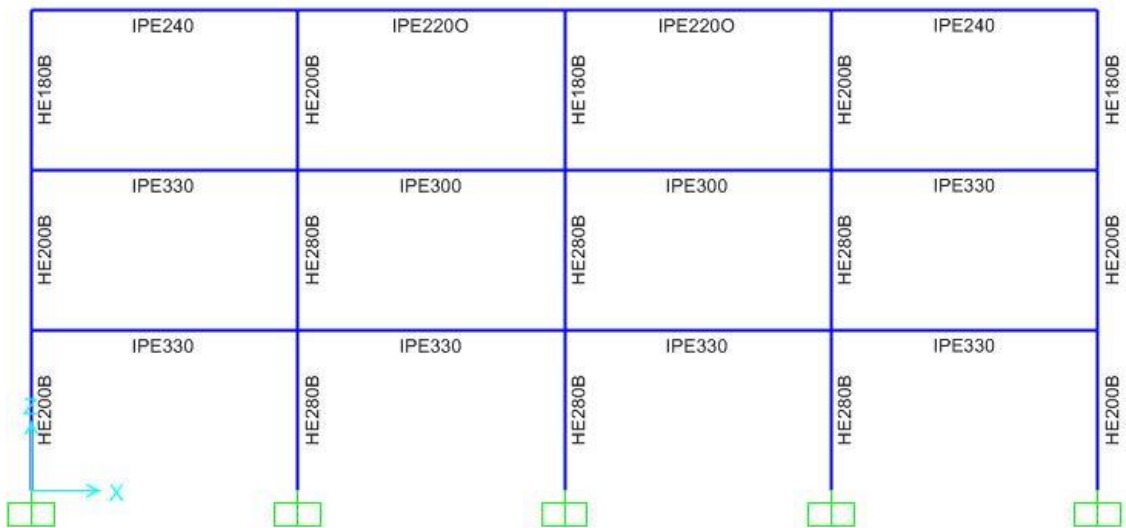


Figure A.8 Frame A43R8 member sections



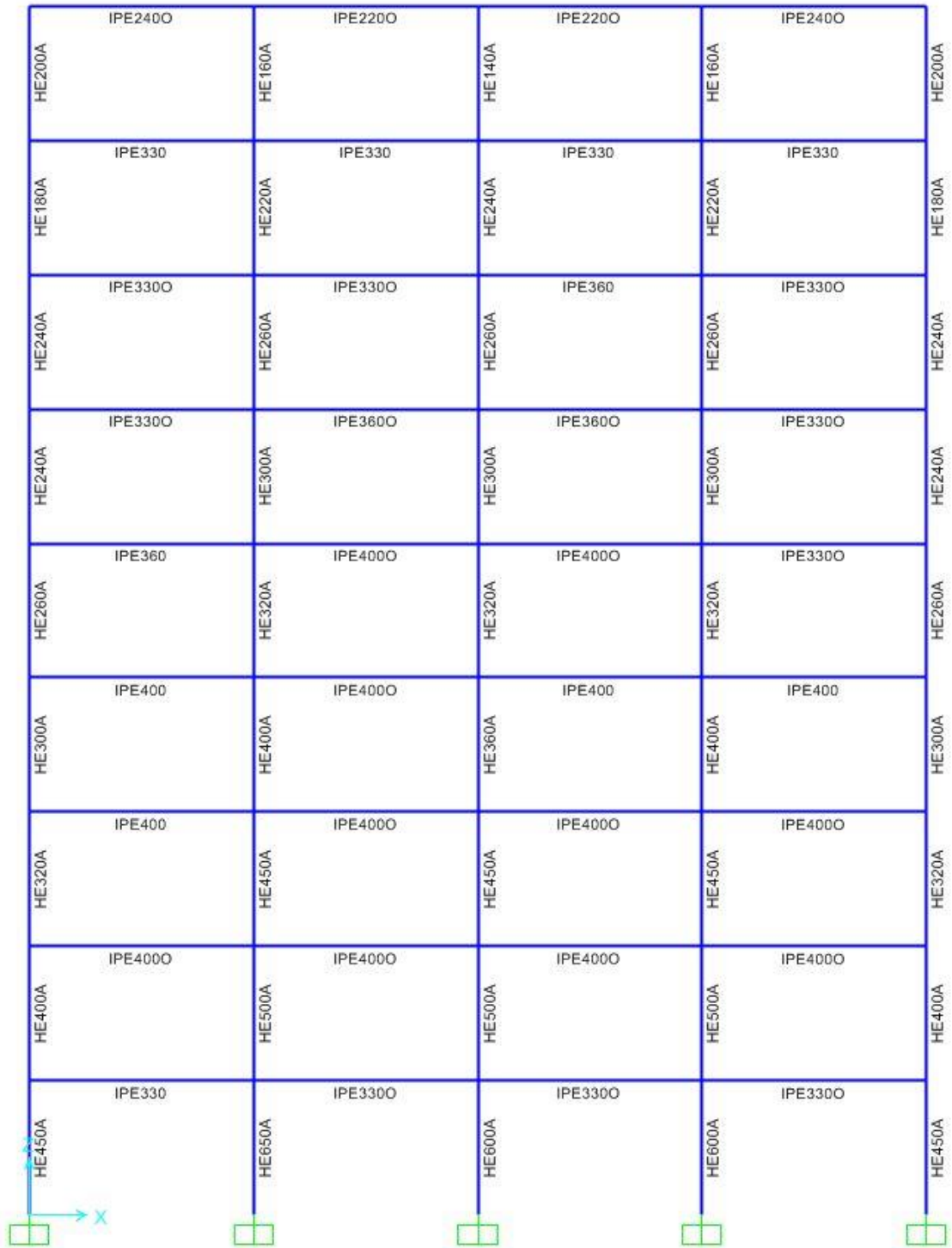


Figure A.11 Frame A49R4 member sections

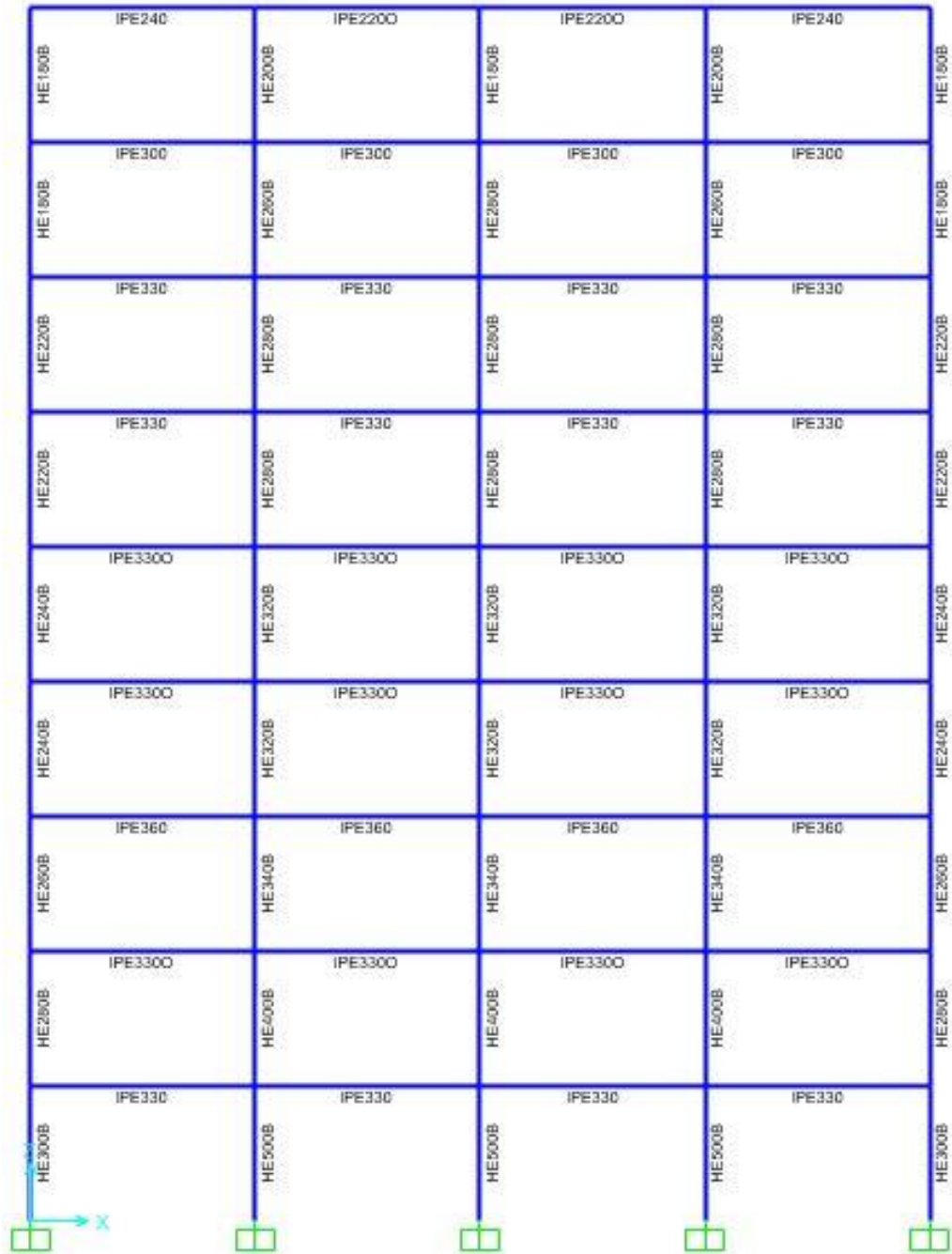


Figure A.12 Frame A49R8 member sections

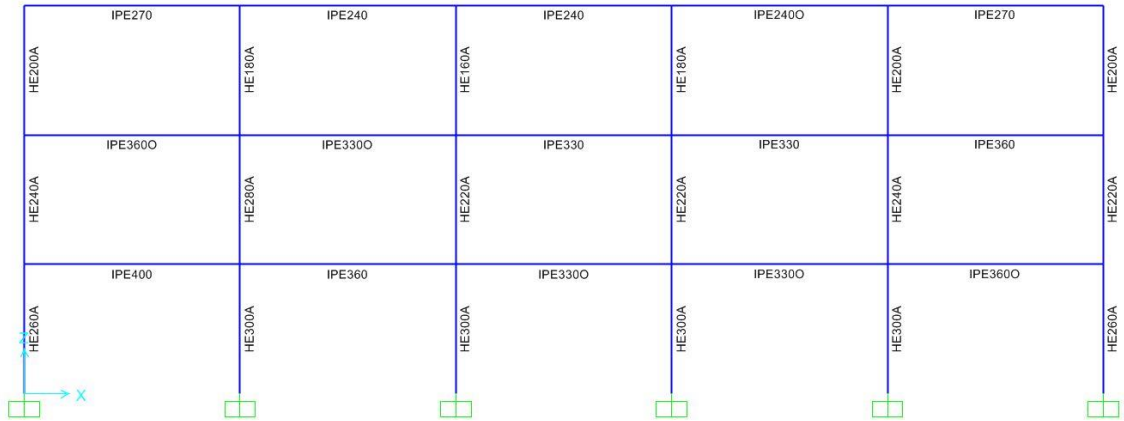


Figure A.13 Frame A53R4 member sections

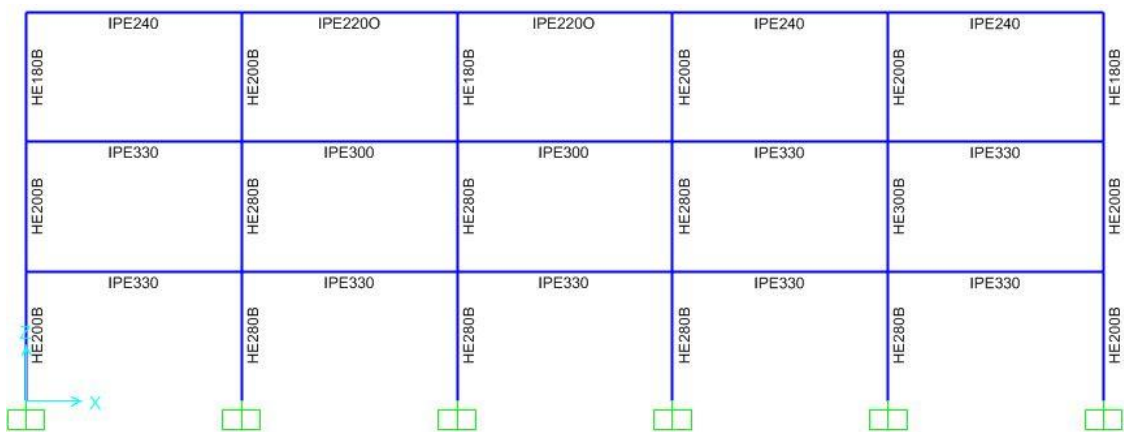


Figure A.14 Frame A53R8 member sections



Figure A.15 Frame A56R4 member sections

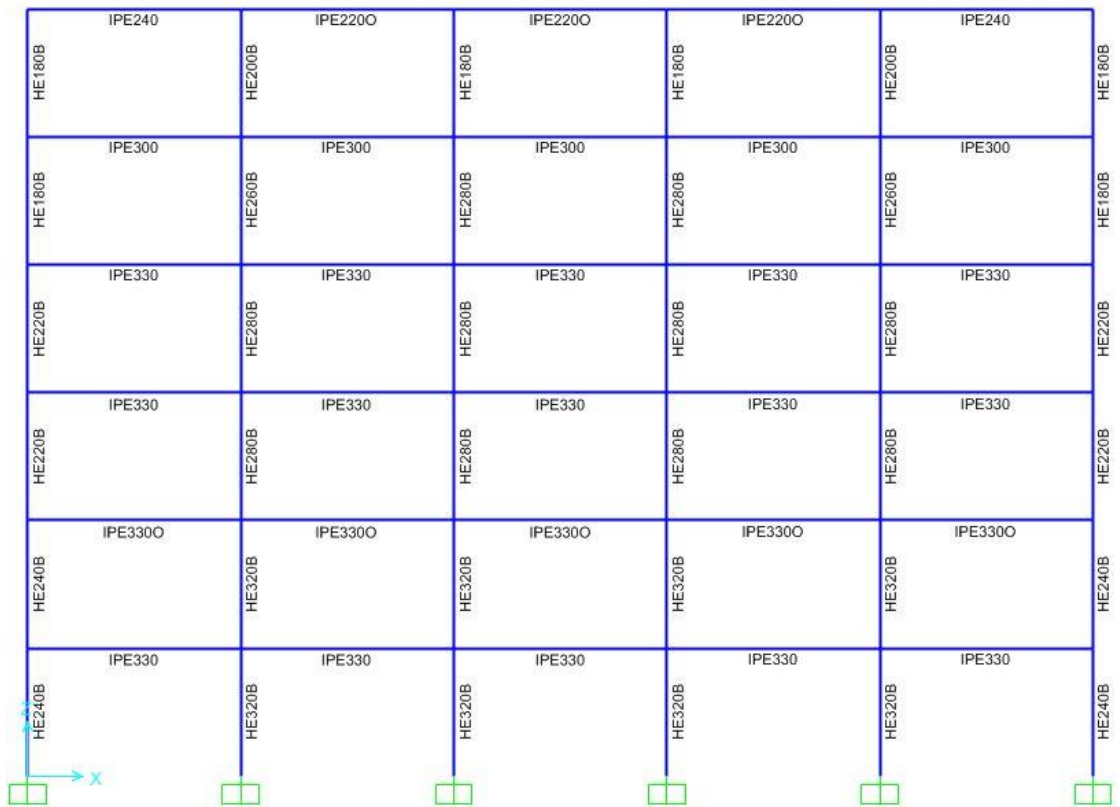


Figure A.16 Frame A56R8 member sections

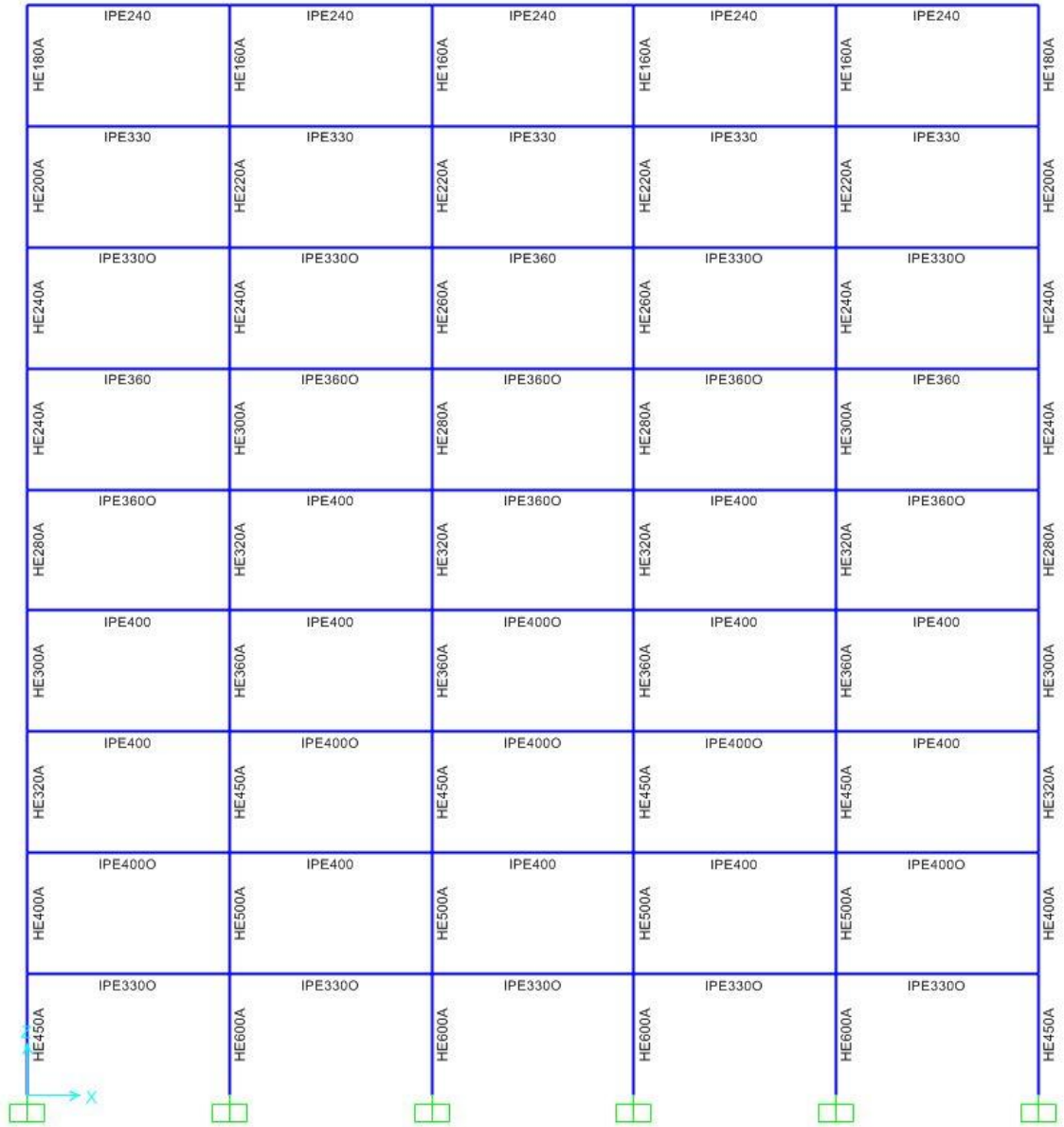


Figure A.17 Frame A59R4 member sections

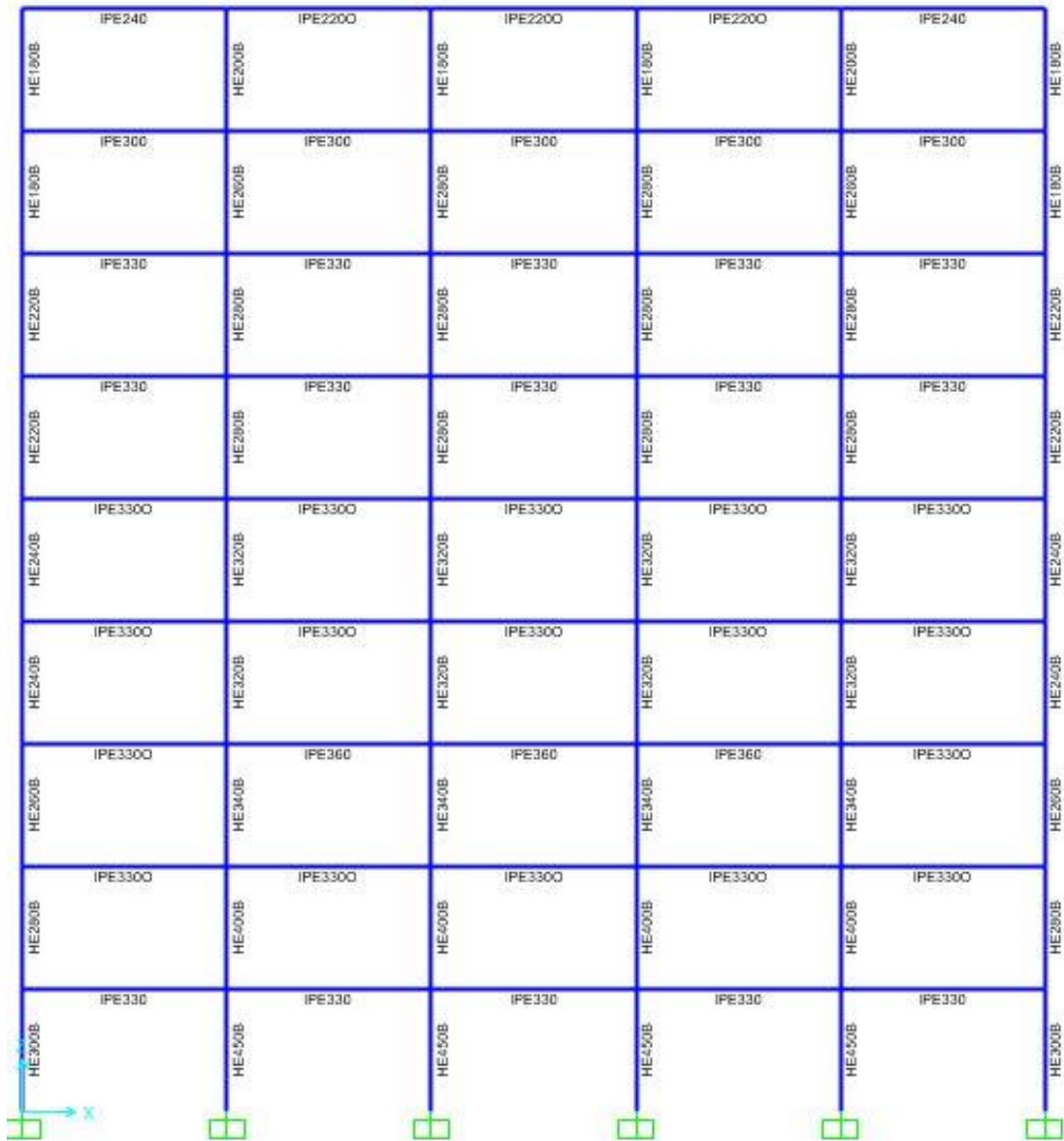


Figure A.18 Frame A59R8 member sections

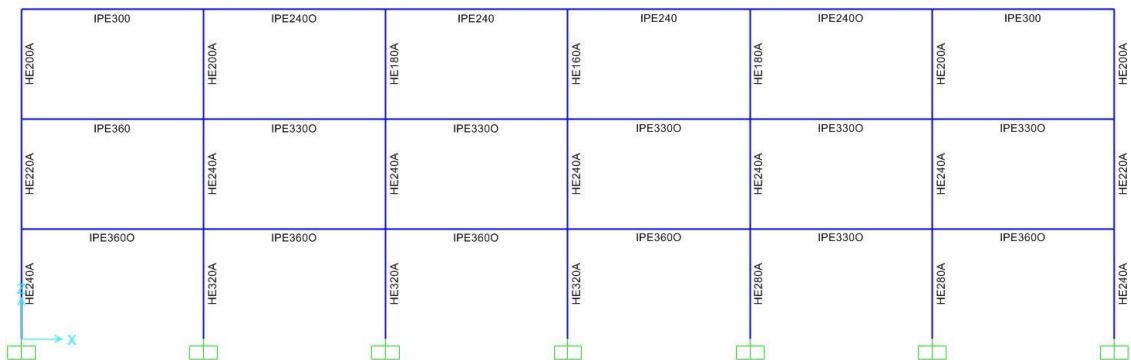


Figure A.19 Frame A63R4 member sections

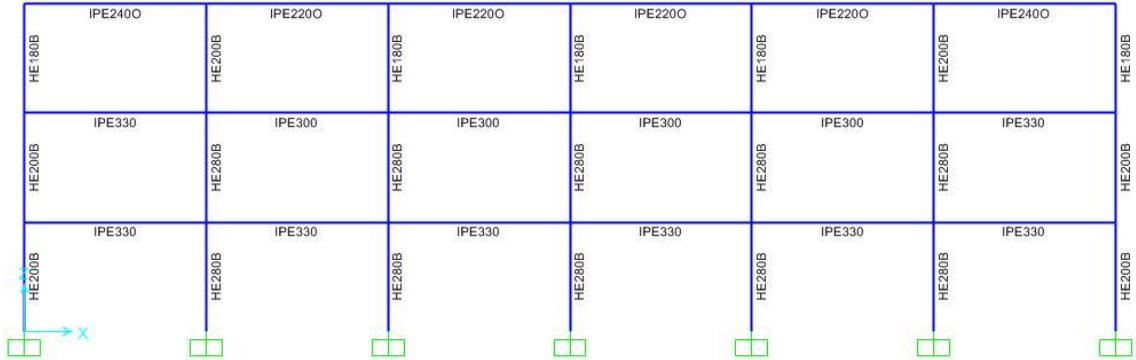


Figure A.20 Frame A63R8 member sections



Figure A.21 Frame A66R4 member sections

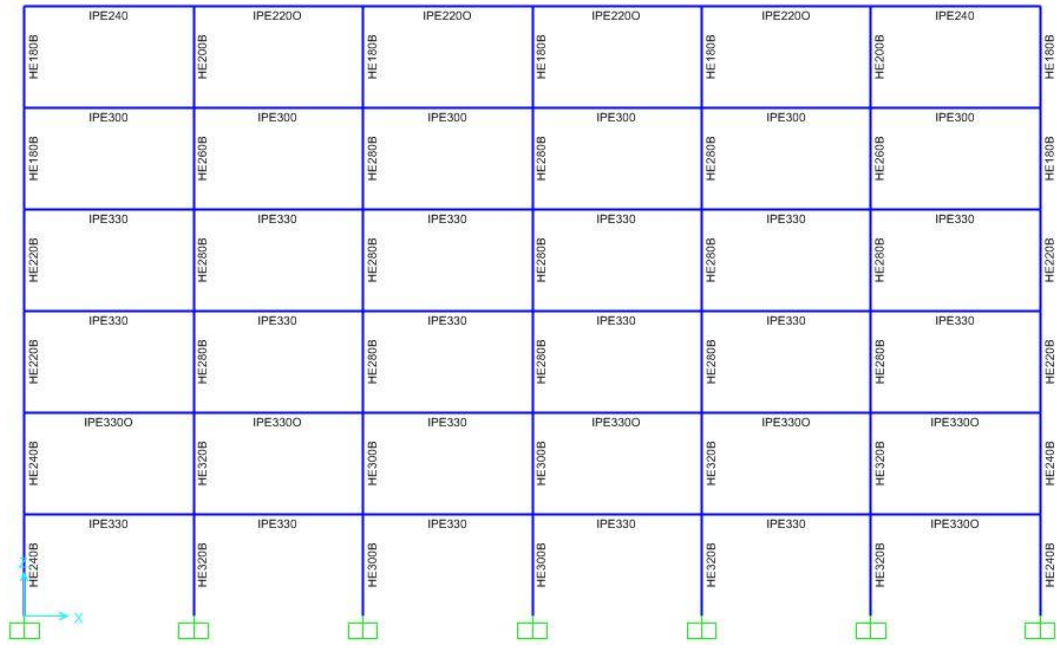


Figure A.22 Frame A66R8 member sections

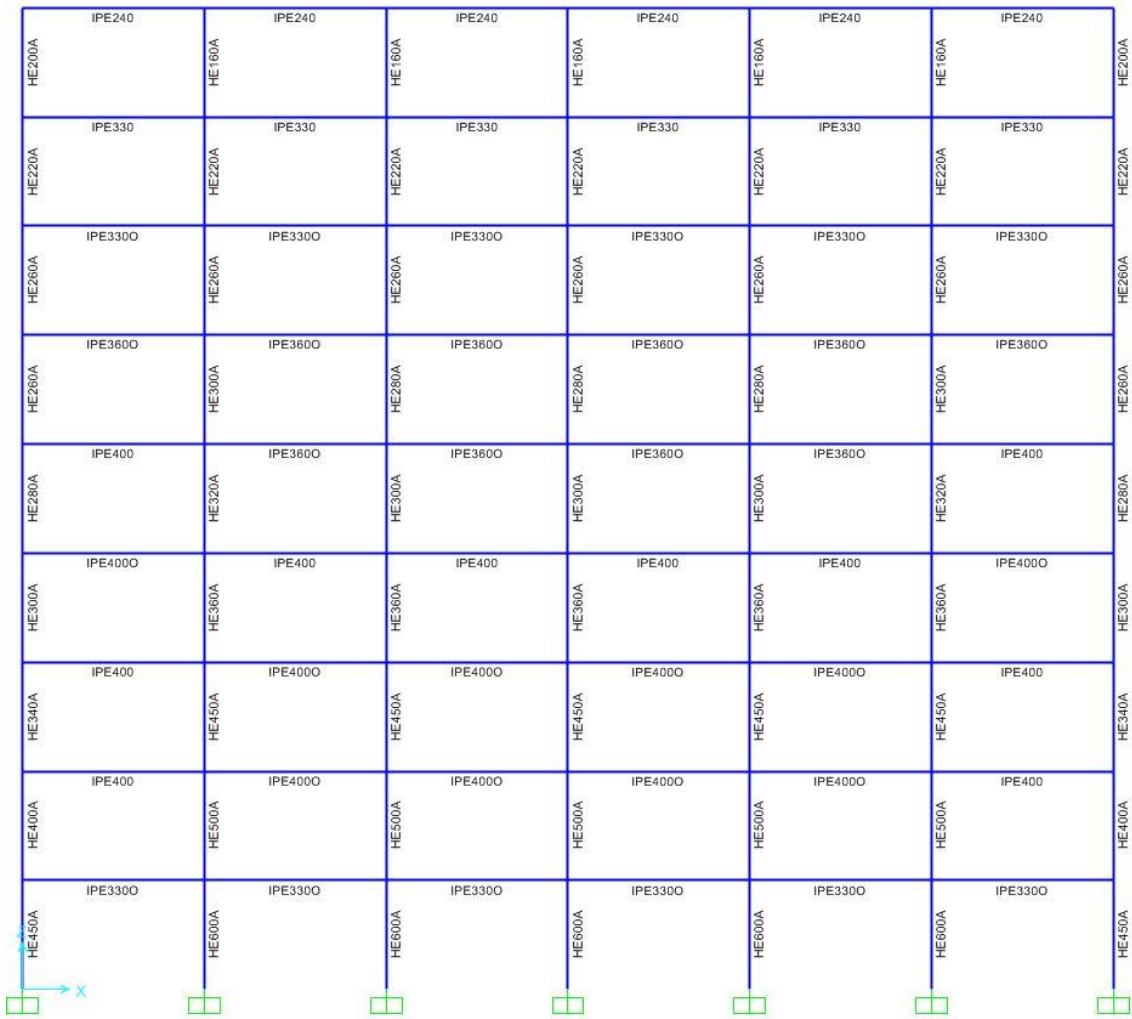


Figure A.23 Frame A69R4 member sections



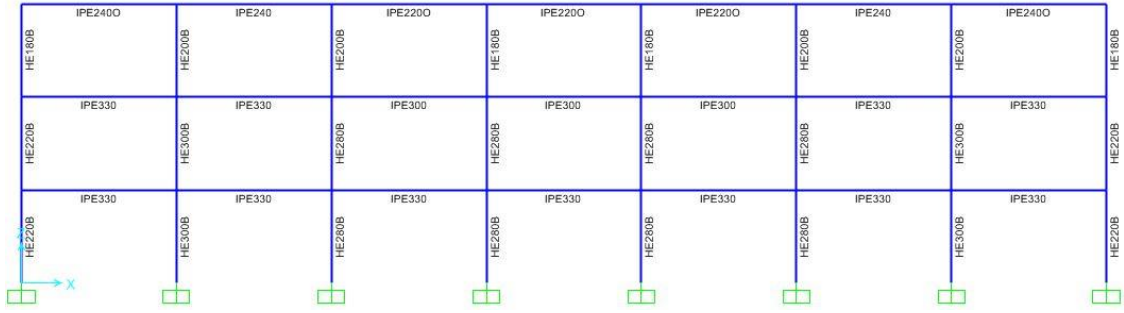


Figure A.26 Frame A73R8 member sections

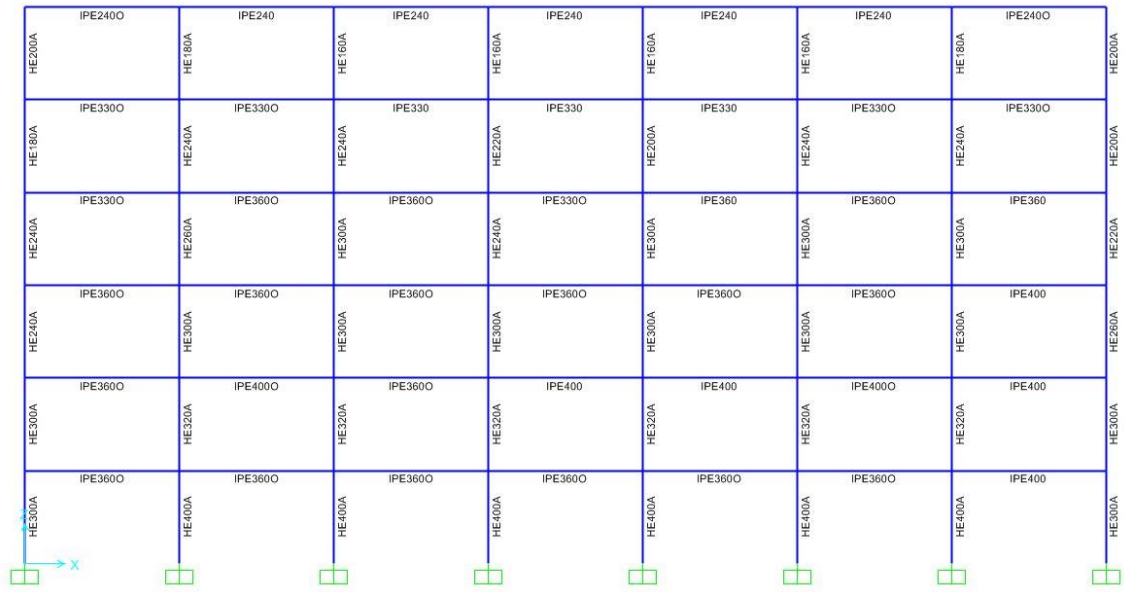


Figure A.27 Frame A76R4 member sections

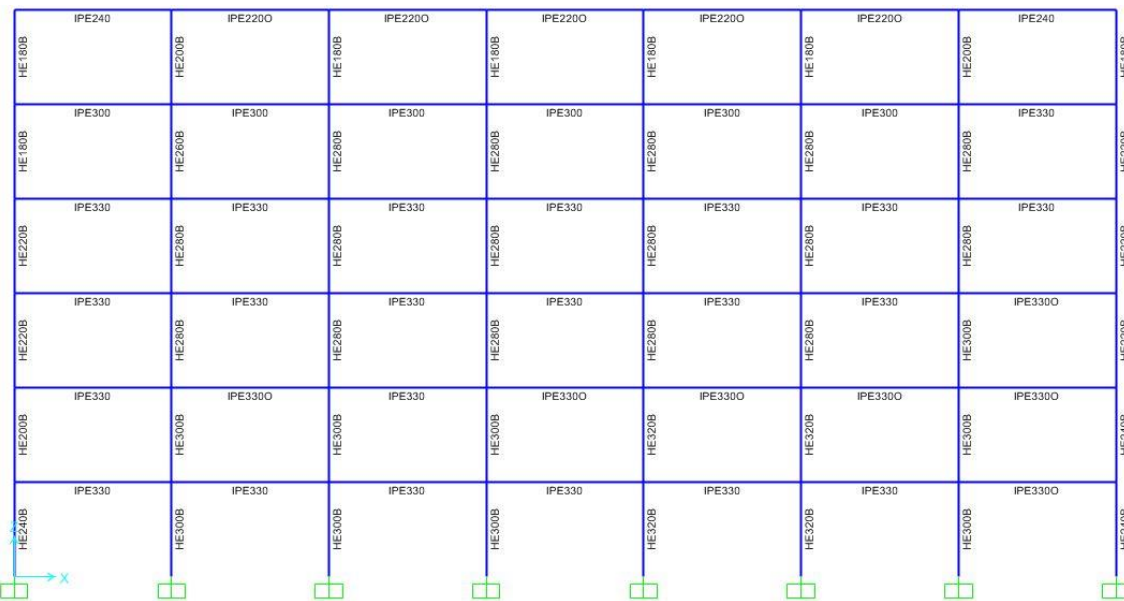


Figure A.28 Frame A76R8 member sections

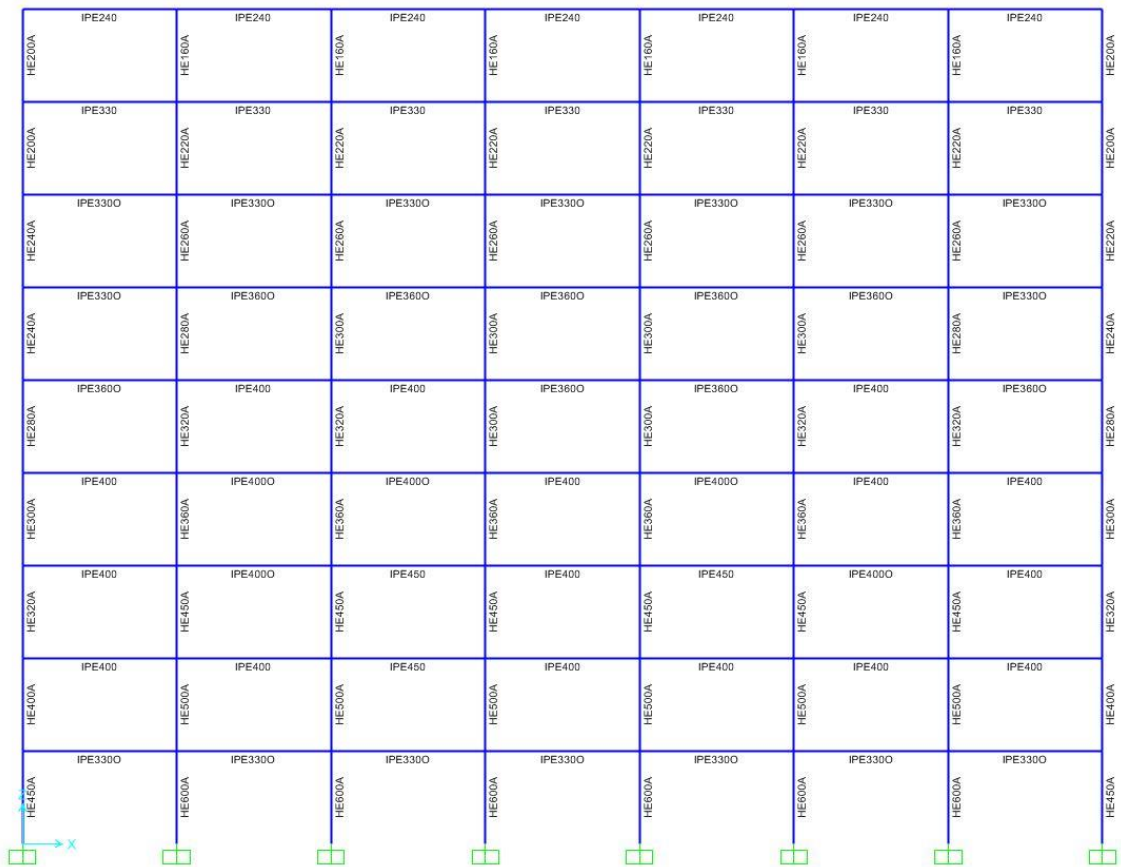


Figure A.29 Frame A79R4 member sections



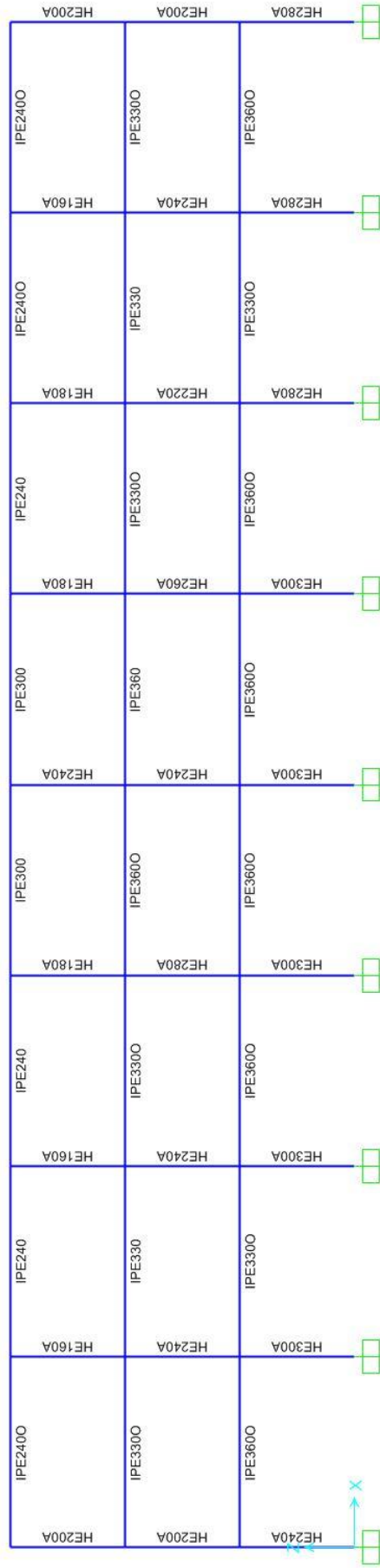


Figure A.31 Frame A83R4 member sections

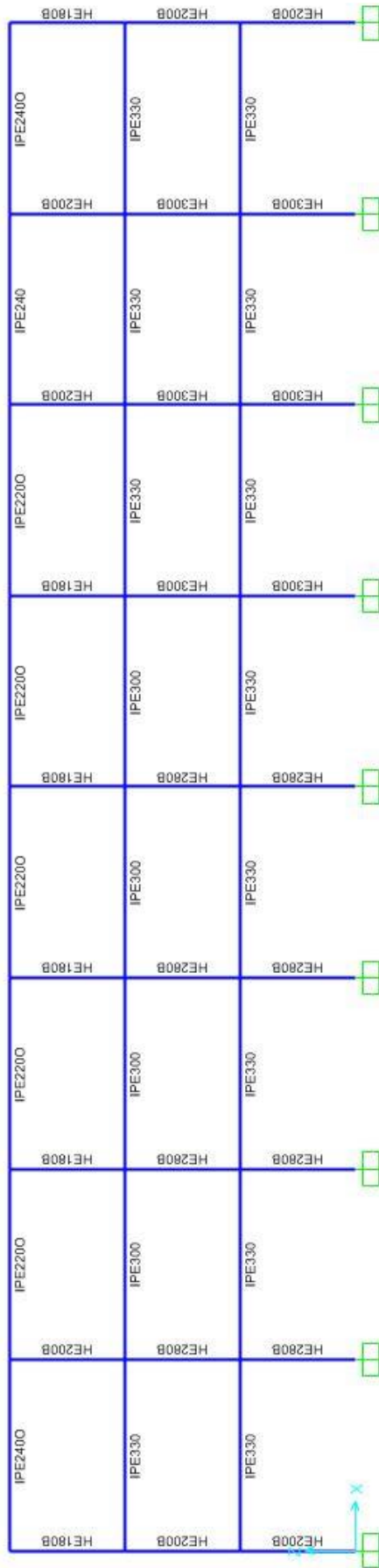


Figure A.32 Frame A83R8 member sections





Figure A.34 Frame A86R8 member sections





# APPENDIX B

## PUSHOVER AND SPECTRAL CAPACITY CURVES

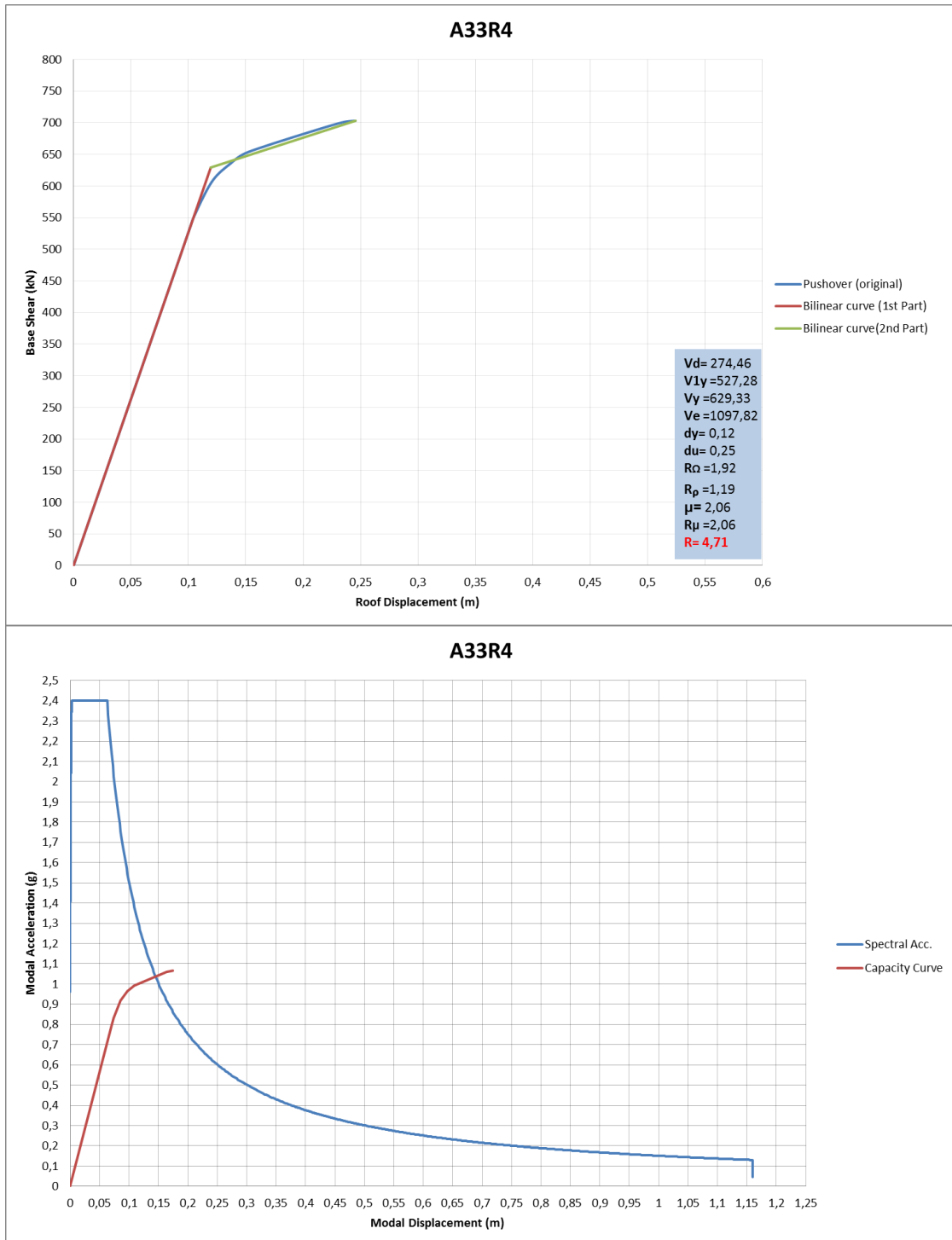


Figure B.1 Frame A33R4 Idealized pushover curve and spectral capacity curve

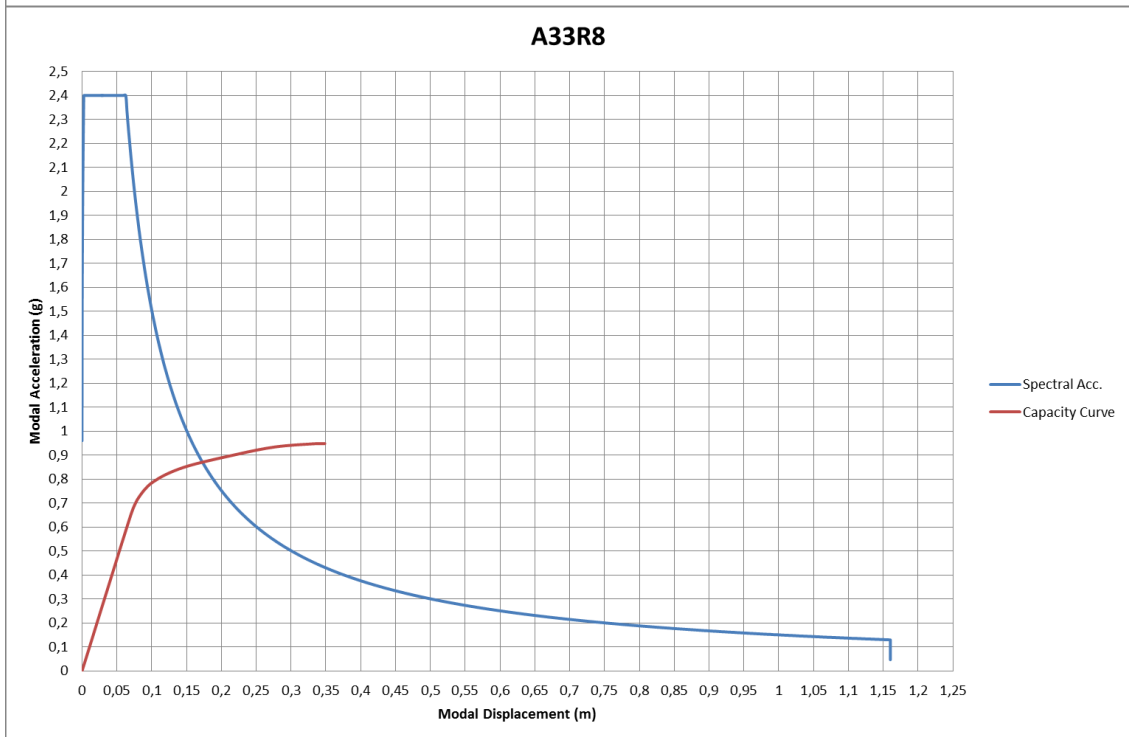
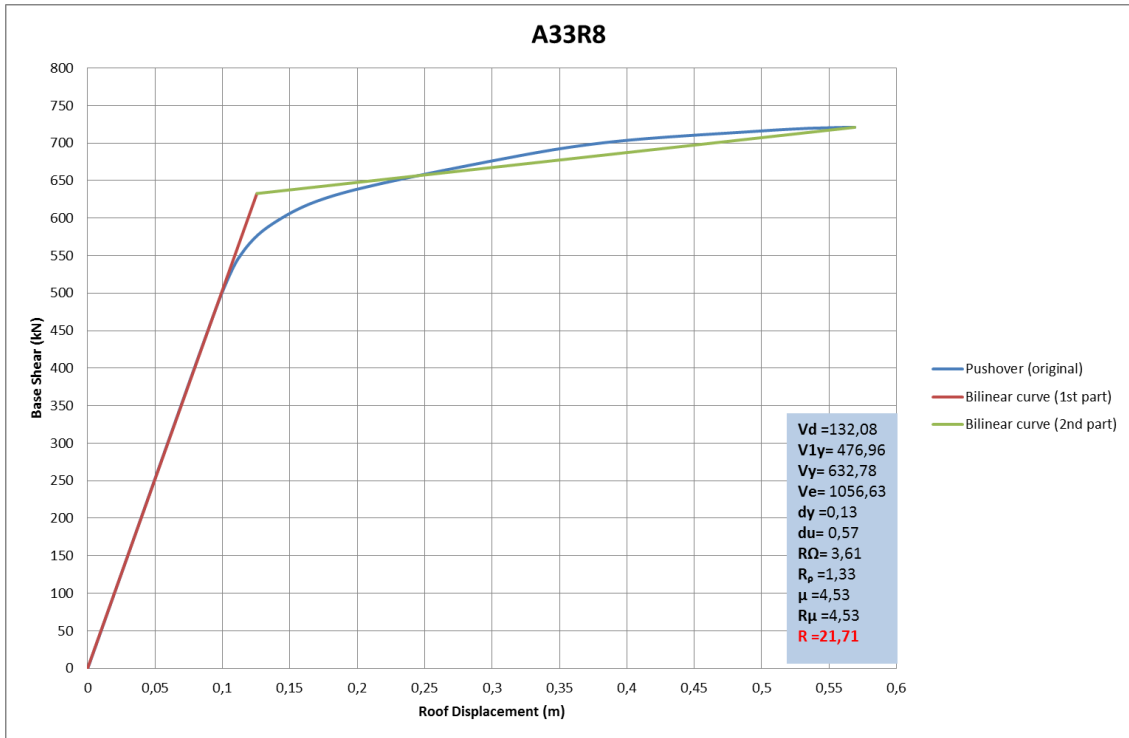


Figure B.2 Frame A33R8 Idealized pushover curve and spectral capacity curve

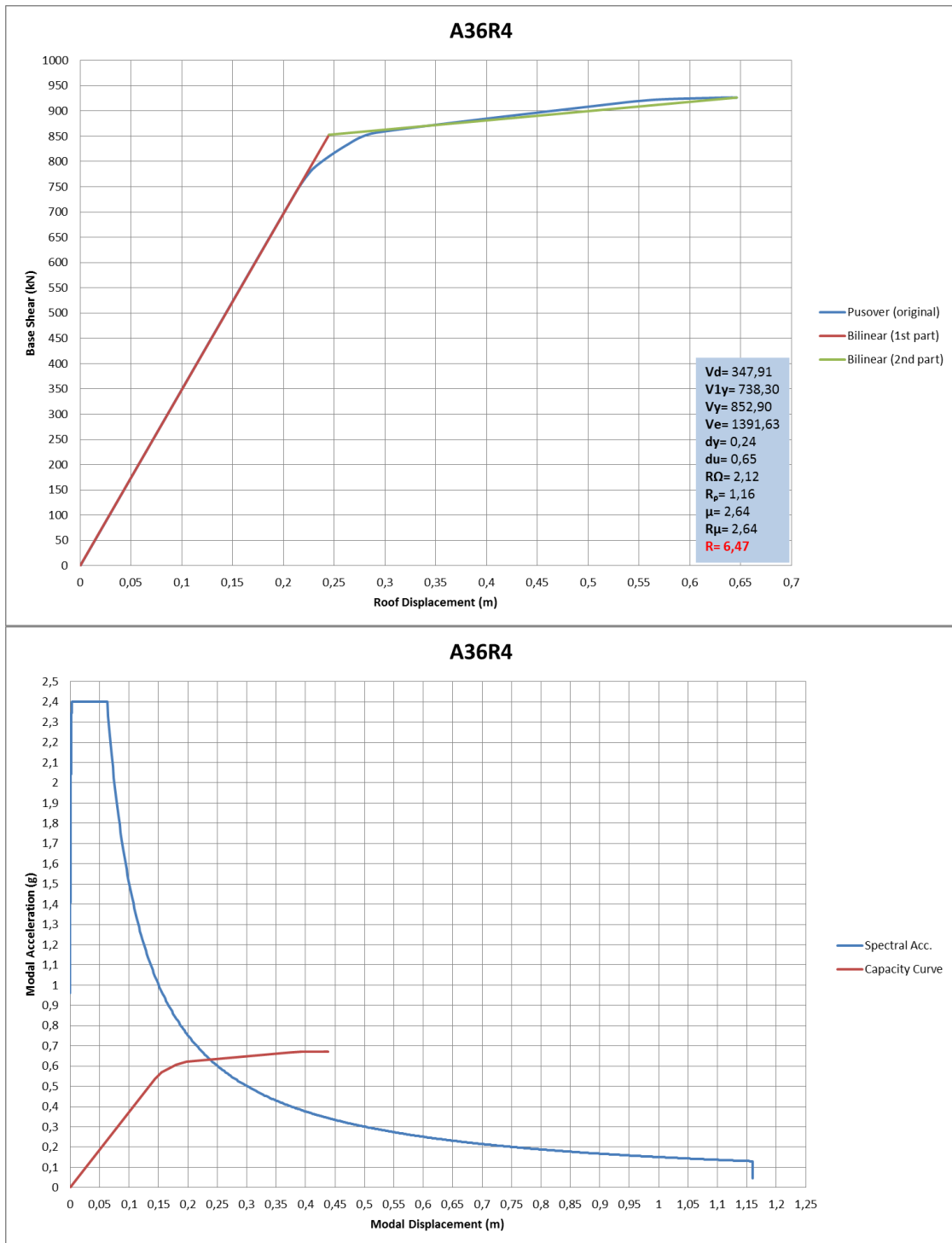


Figure B.3 Frame A36R4 Idealized pushover curve and spectral capacity curve

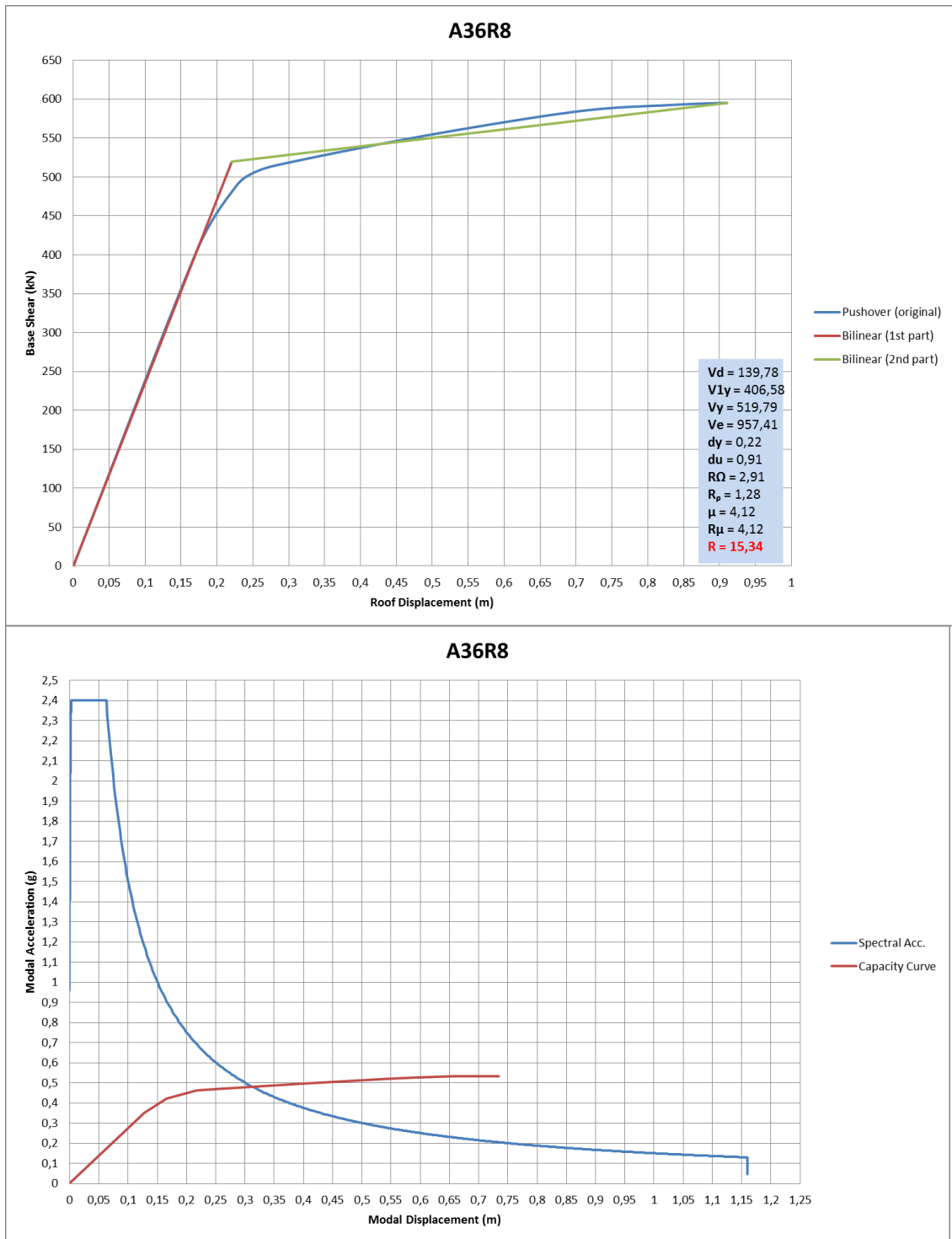


Figure B.4 Frame A36R8 Idealized pushover curve and spectral capacity curve

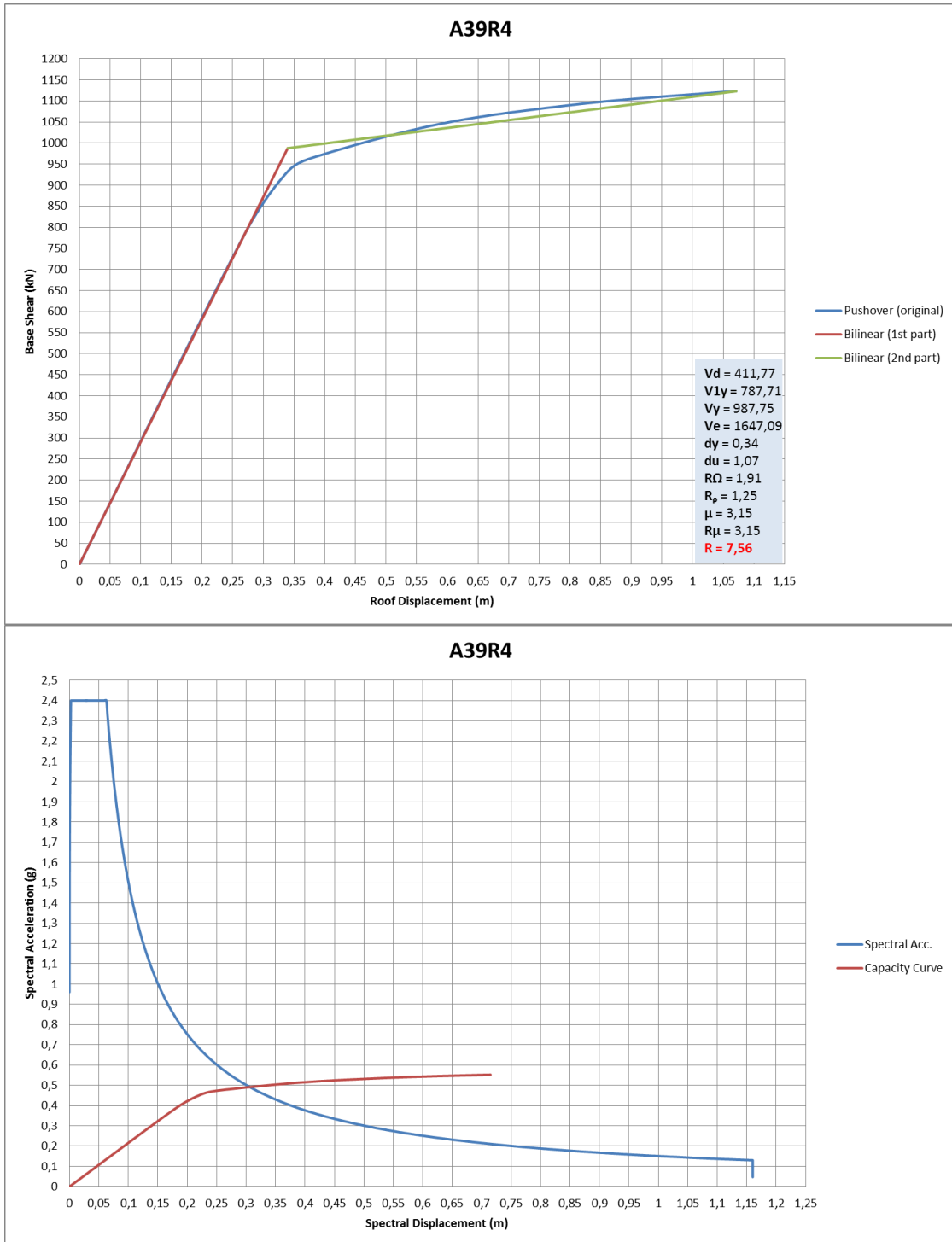


Figure B.5 Frame A39R4 Idealized pushover and spectral capacity curve

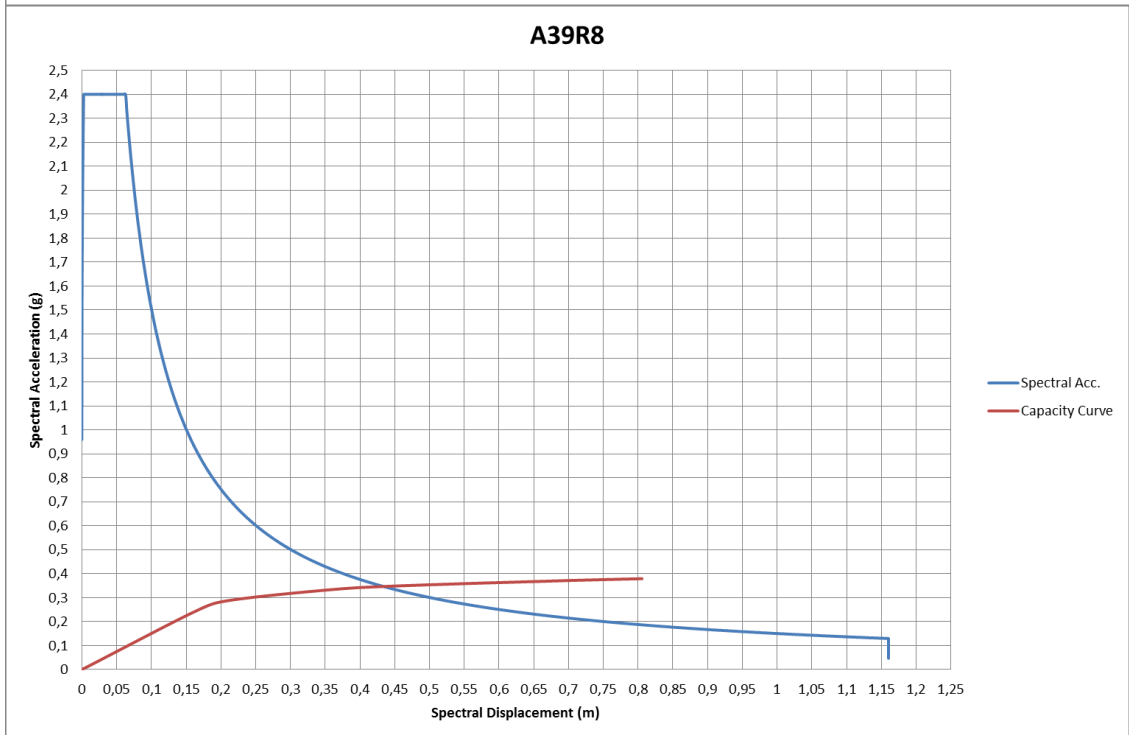
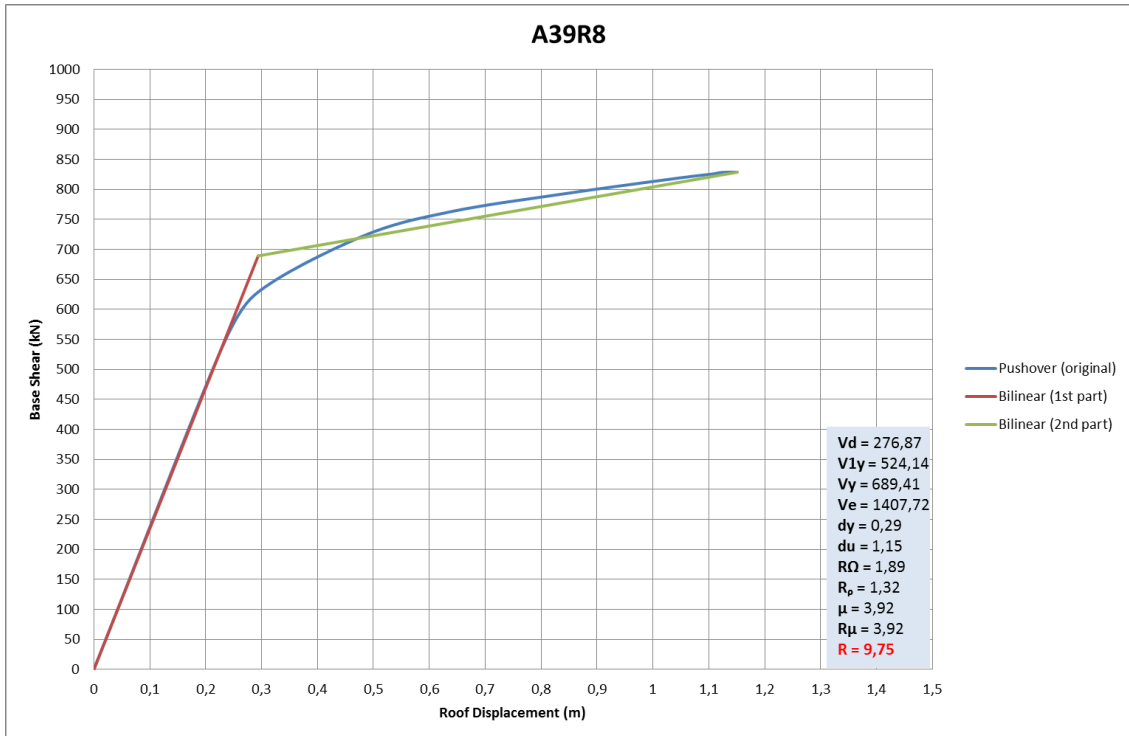


Figure B.6 Frame A39R8 Idealized pushover curve and spectral capacity curve

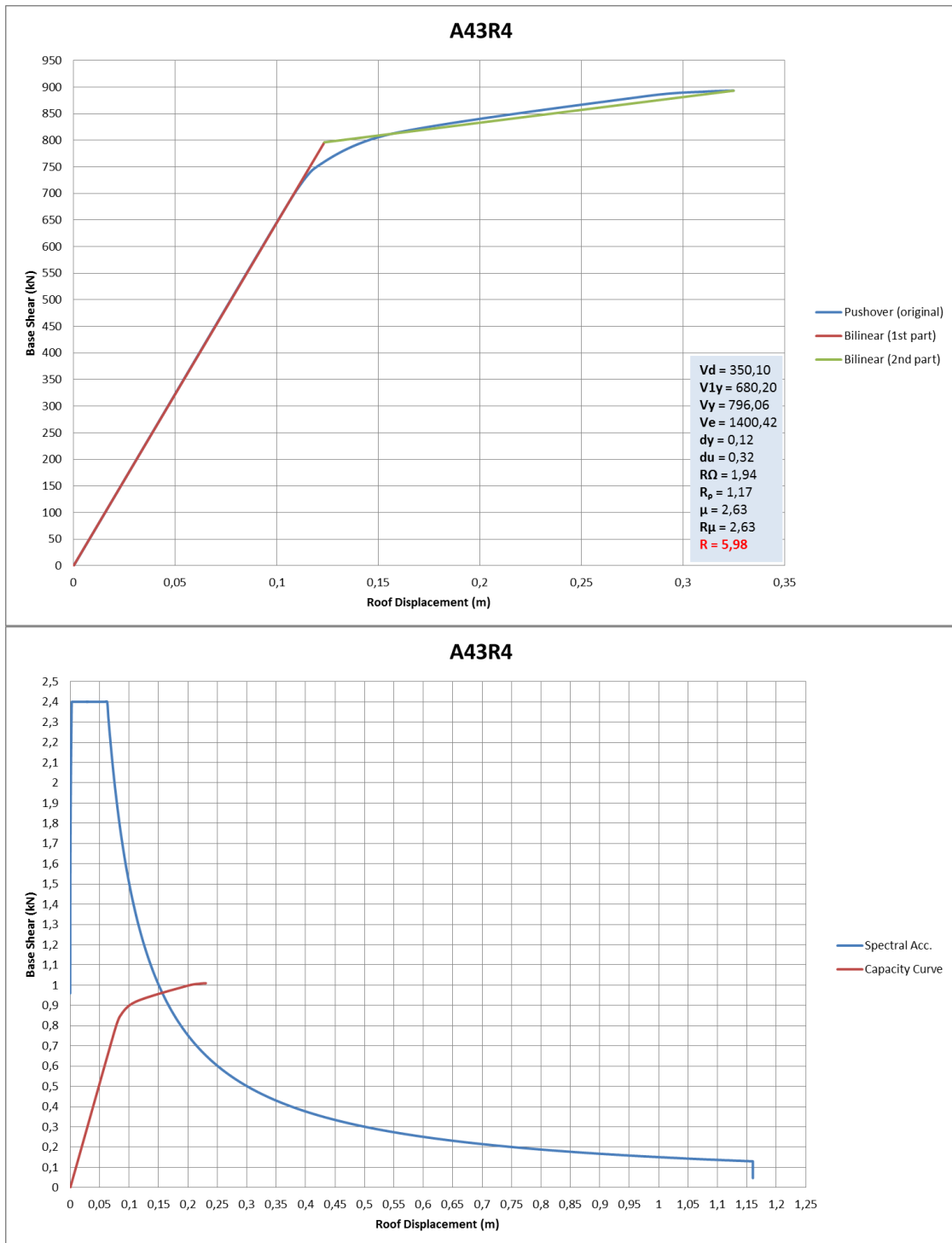


Figure B.7 Frame A43R4 Idealized pushover curve and spectral capacity curve

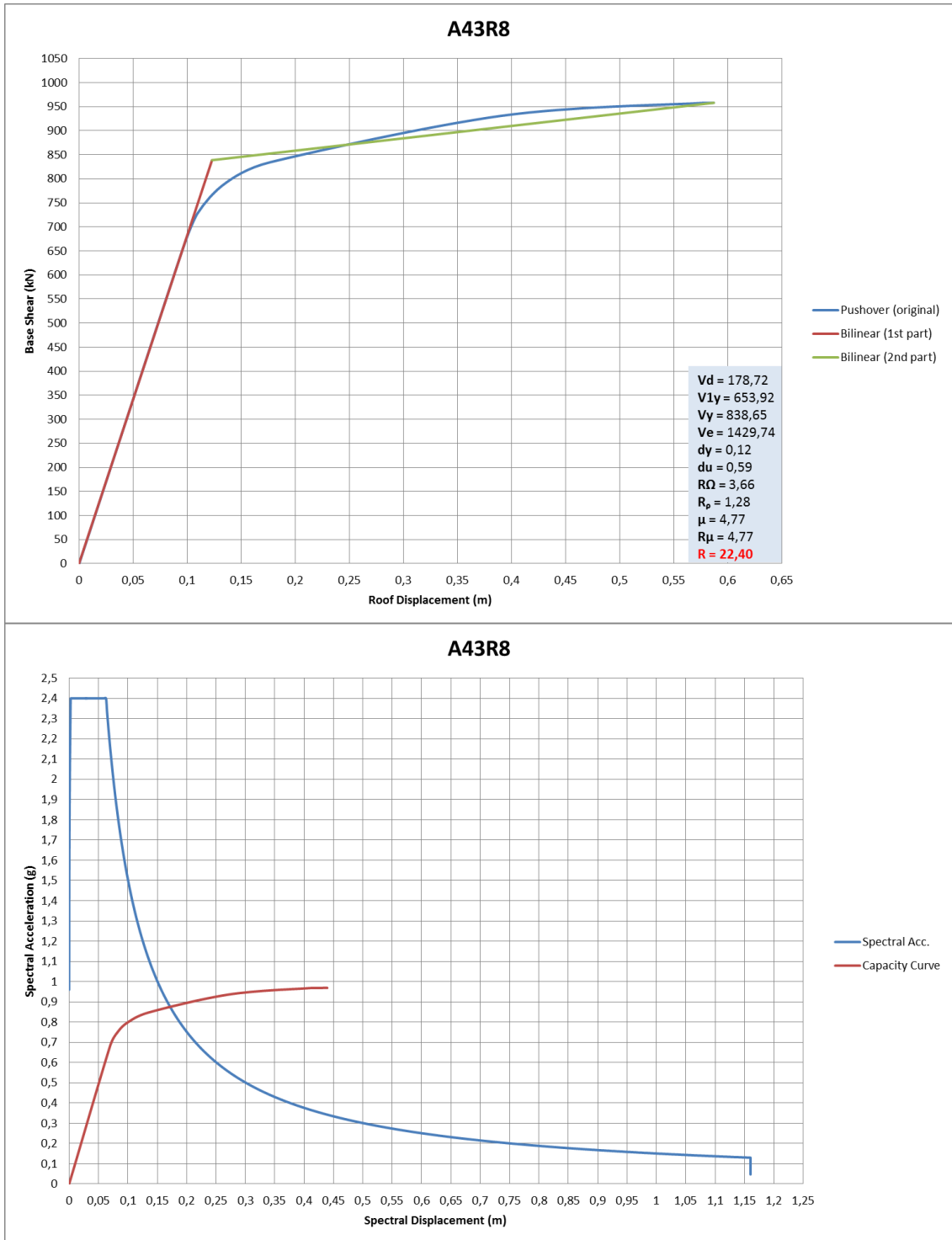


Figure B.8 Frame A43R8 Idealized pushover curve and spectral capacity curve

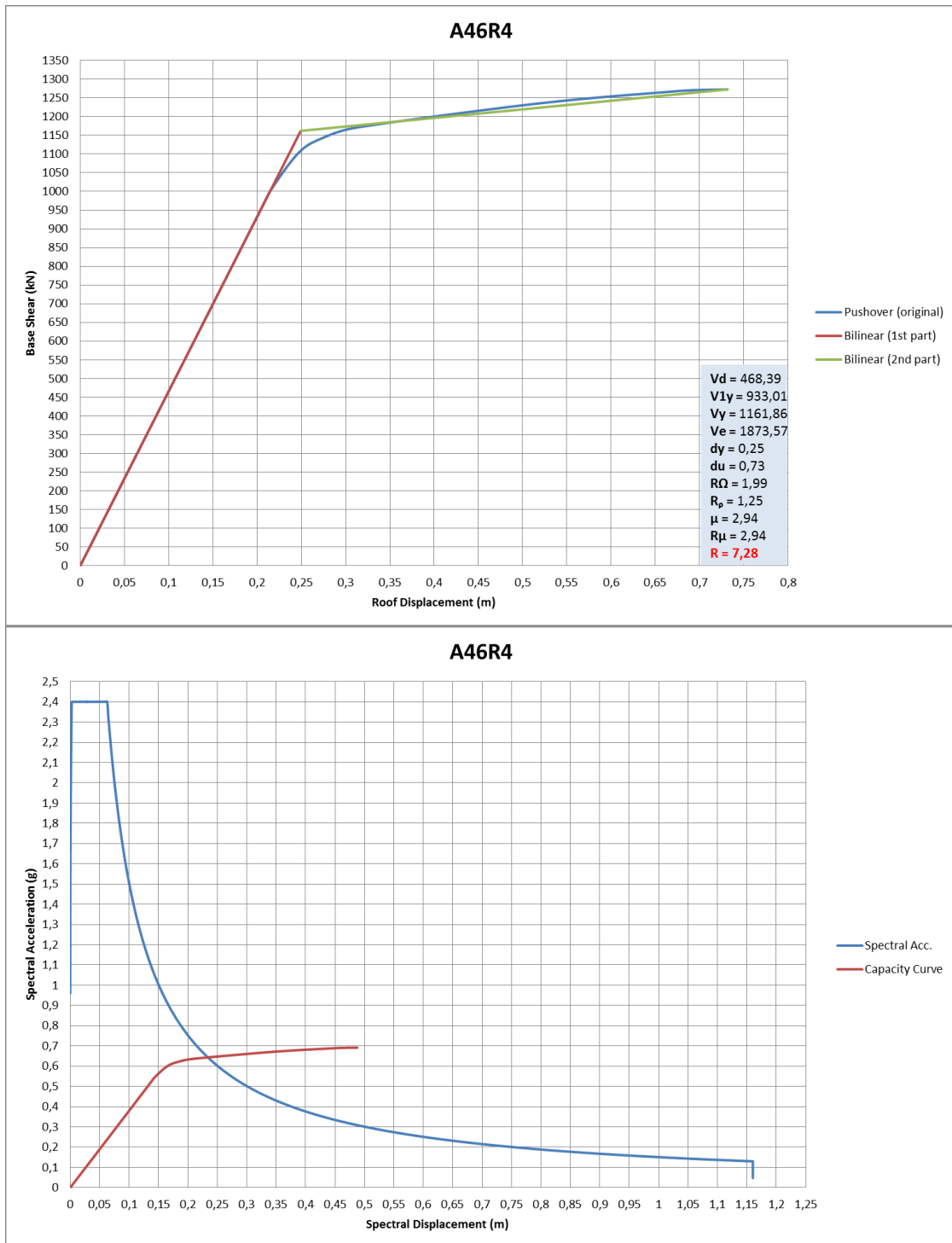


Figure B.9 Frame A46R4 Idealized pushover curve and spectral capacity curve

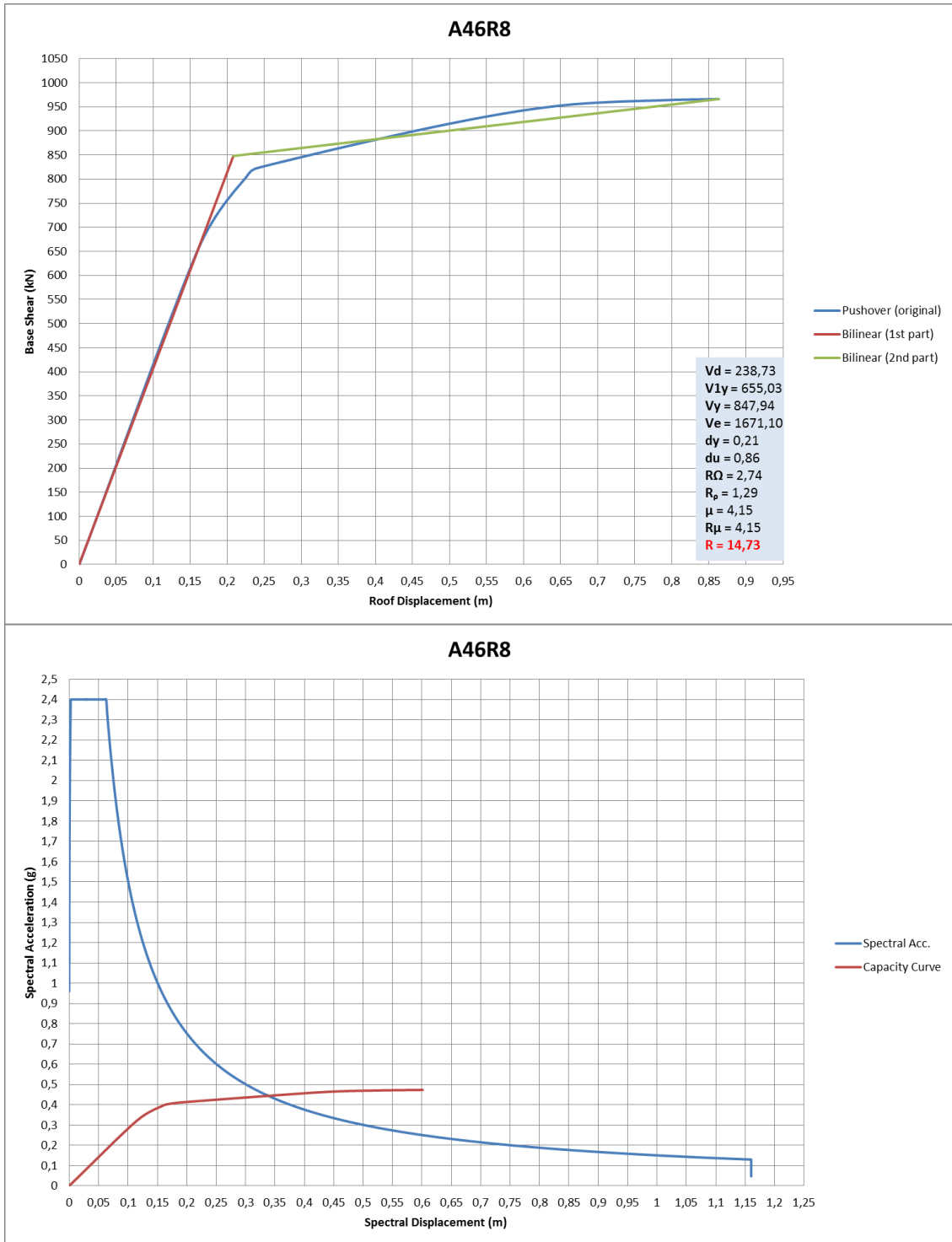


Figure B.10 Frame A46R8 Idealized pushover curve and spectral capacity curve

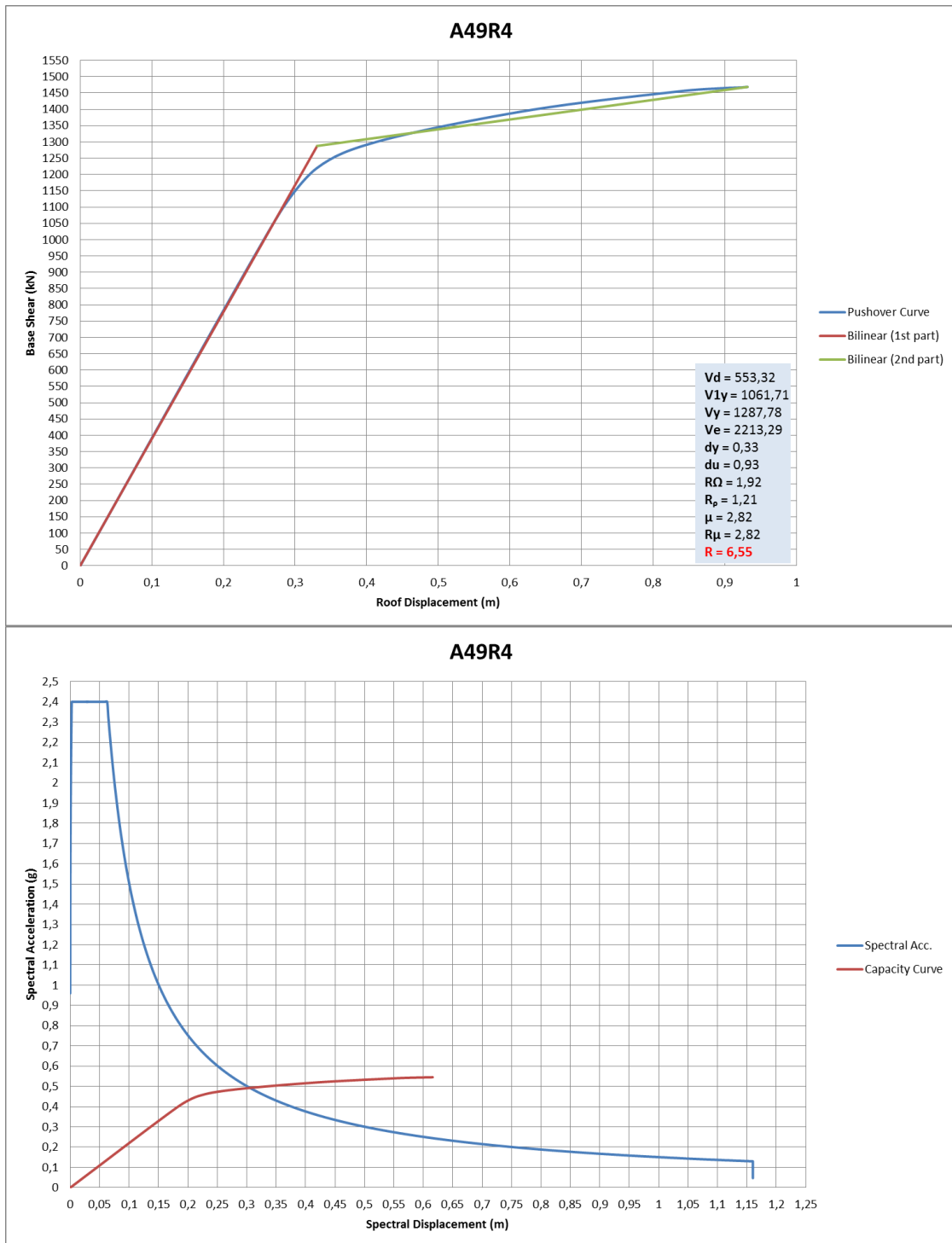


Figure B.11 Frame A49R4 Idealized pushover curve and spectral capacity curve

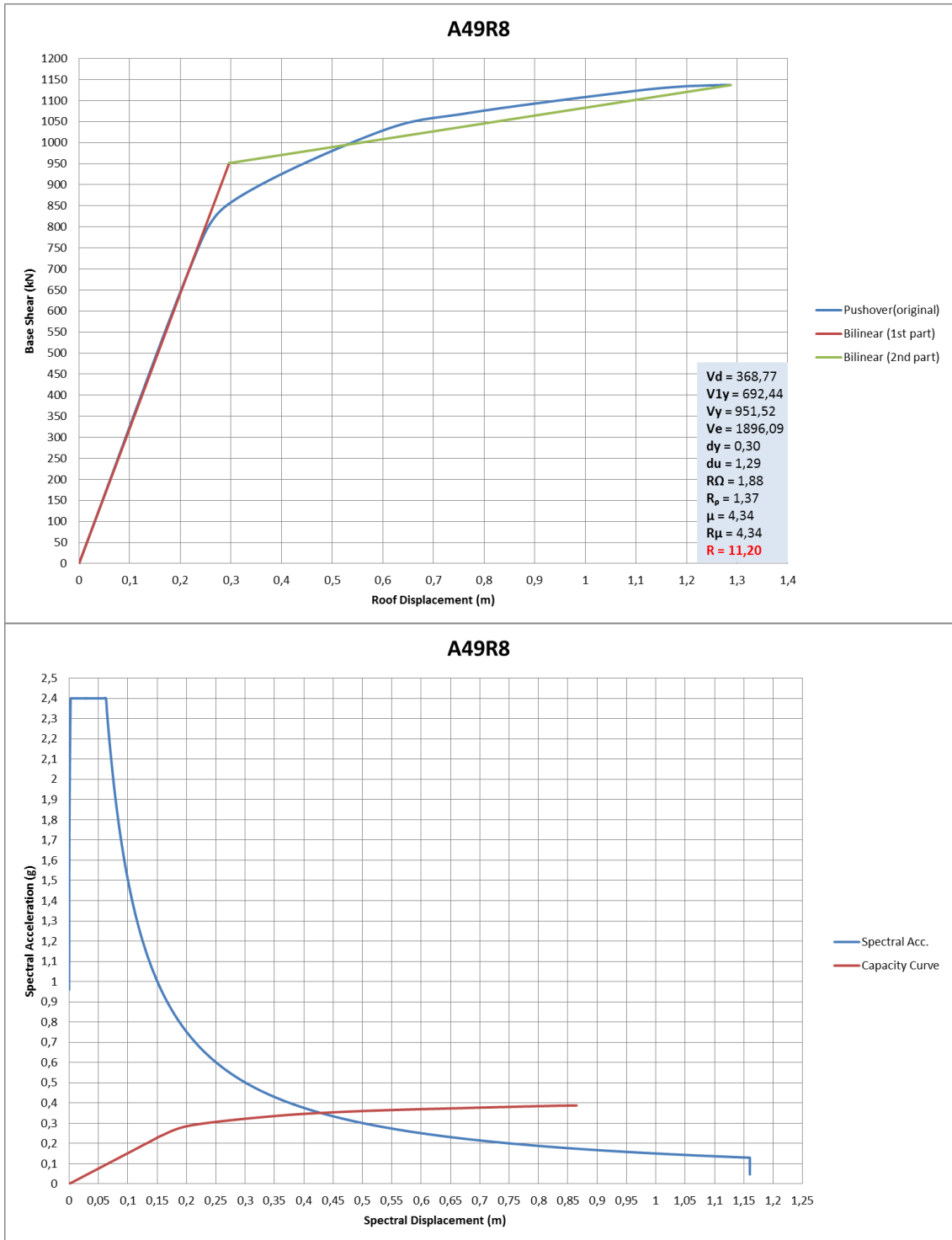


Figure B.12 Frame A49R8 Idealized pushover curve and spectral capacity curve

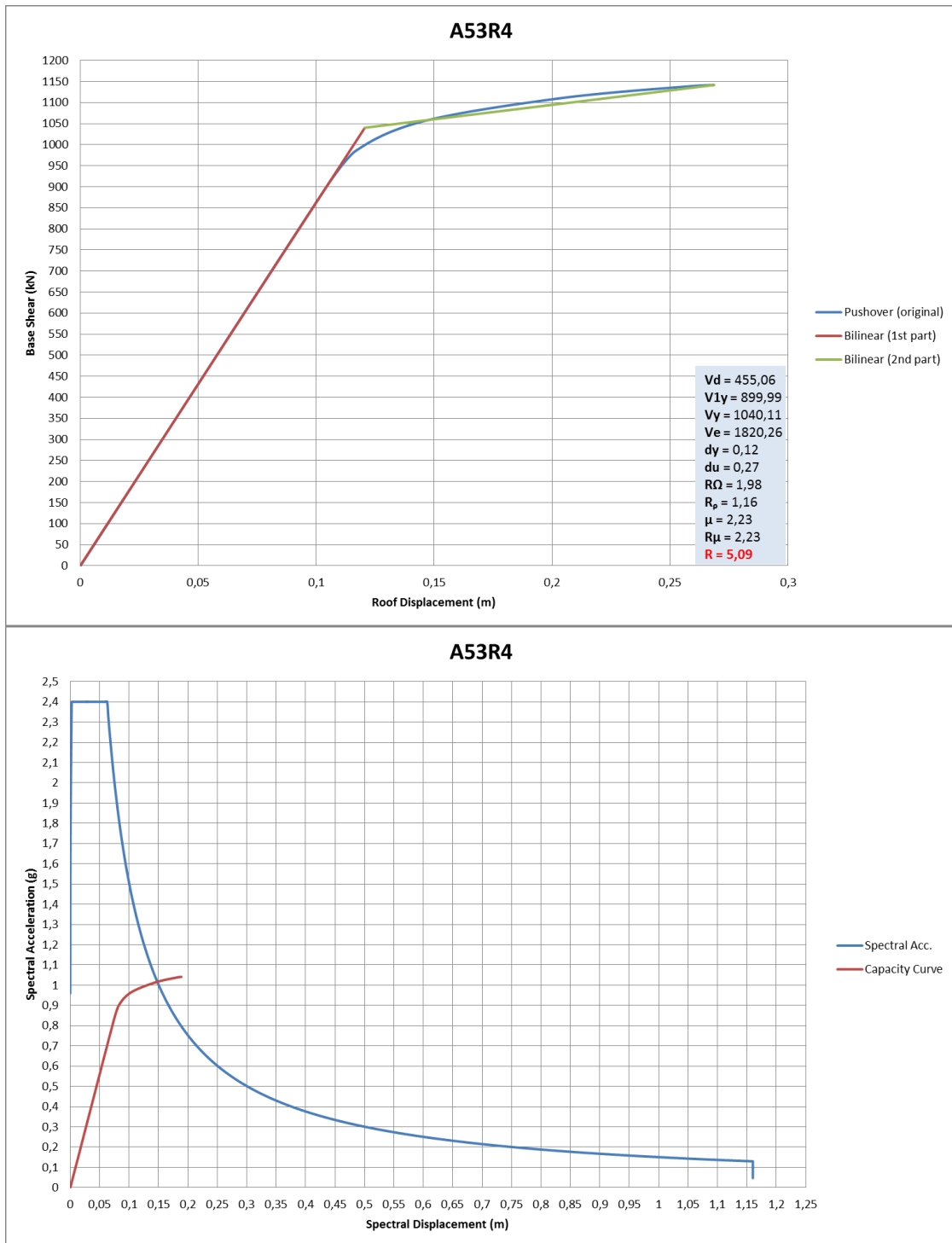


Figure B.13 Frame A53R4 Idealized pushover curve and spectral capacity curve

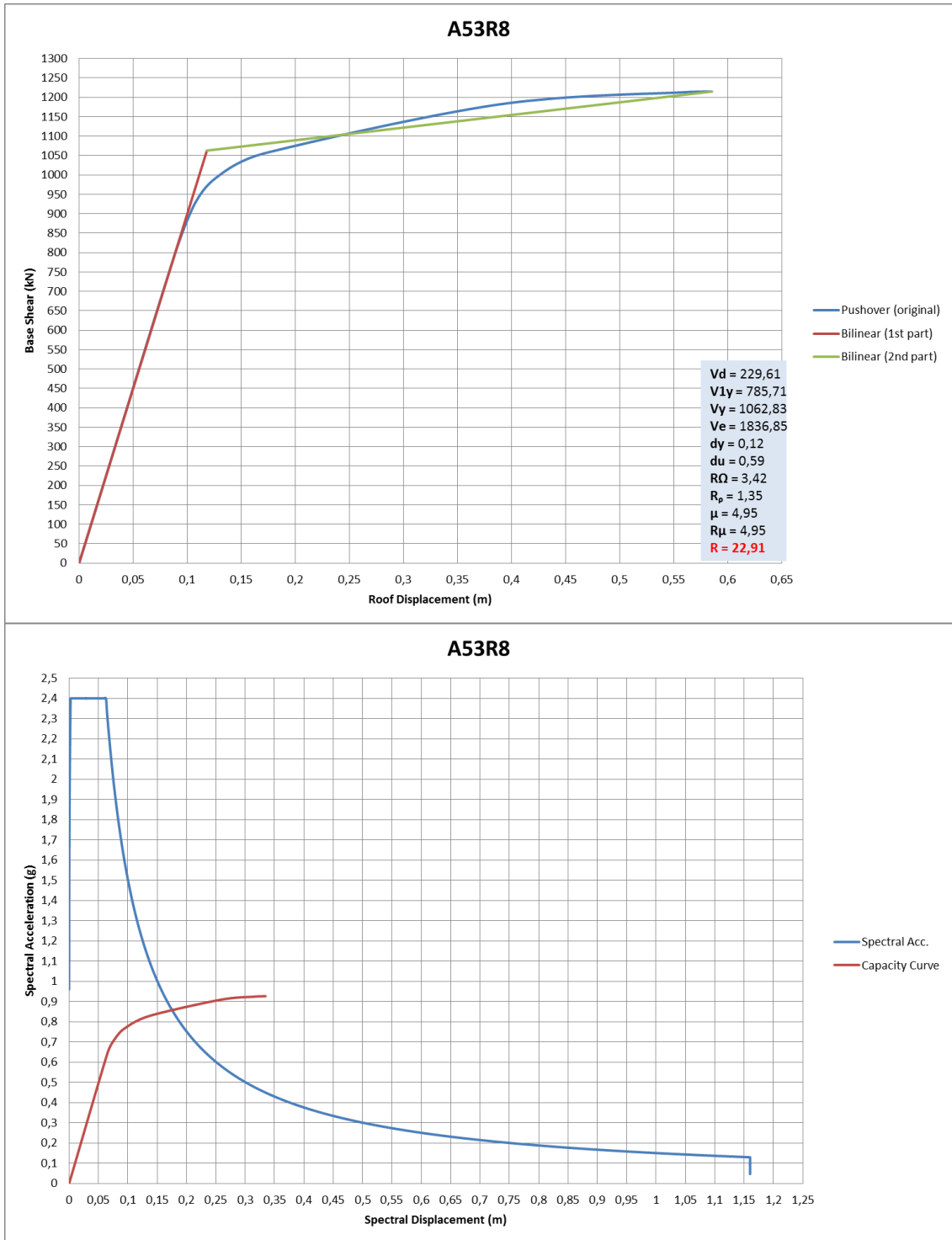


Figure B.14 Frame A53R8 Idealized pushover curve and spectral capacity curve

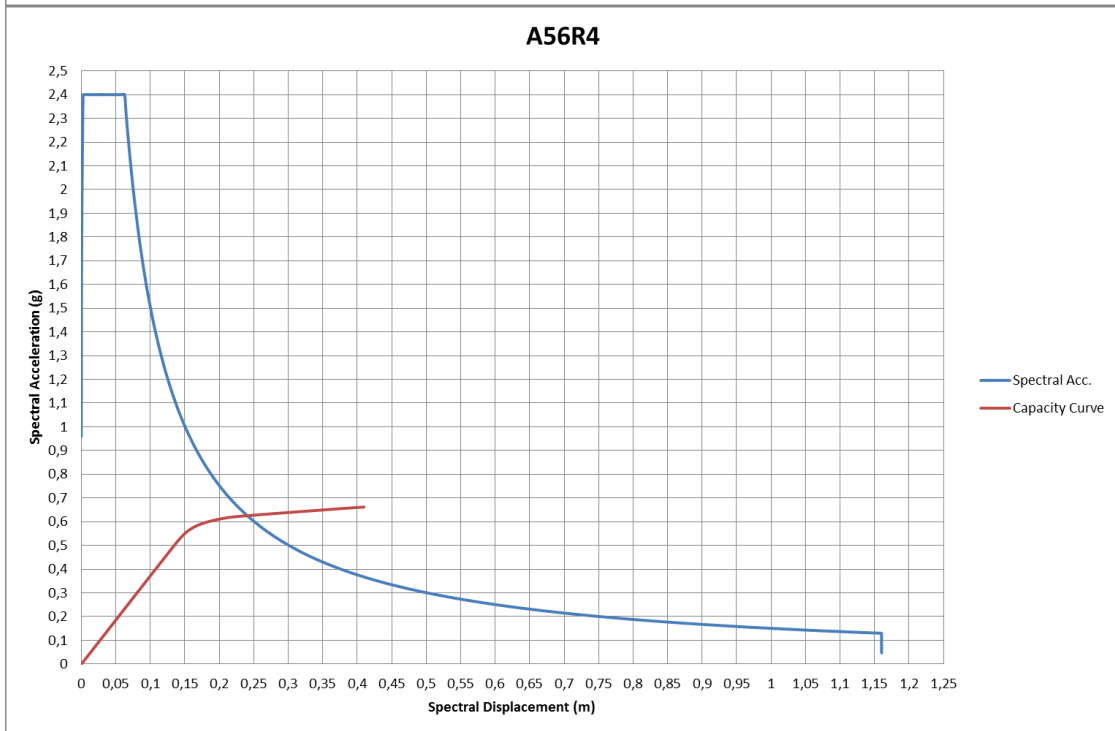
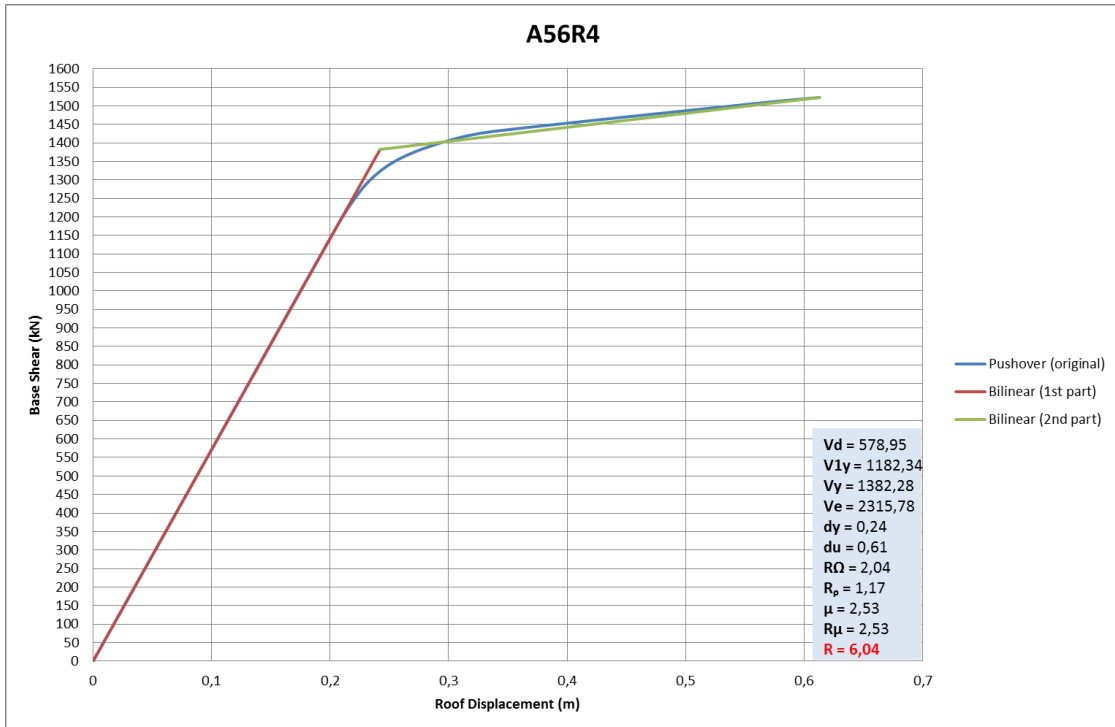


Figure B.15 Frame A56R4 Idealized pushover curve and spectral capacity curve

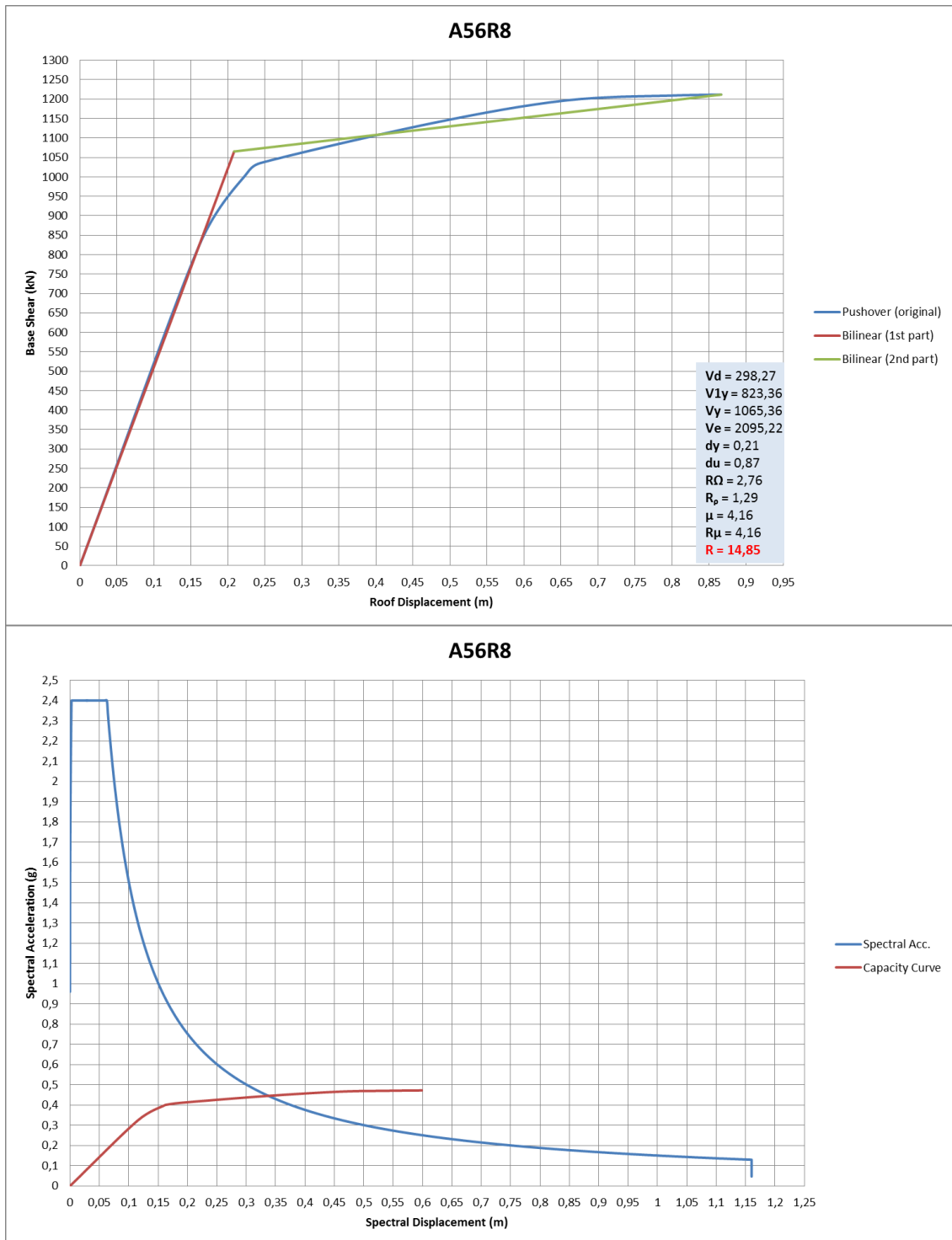


Figure B.16 Frame A56R8 Idealized pushover curve and spectral capacity curve

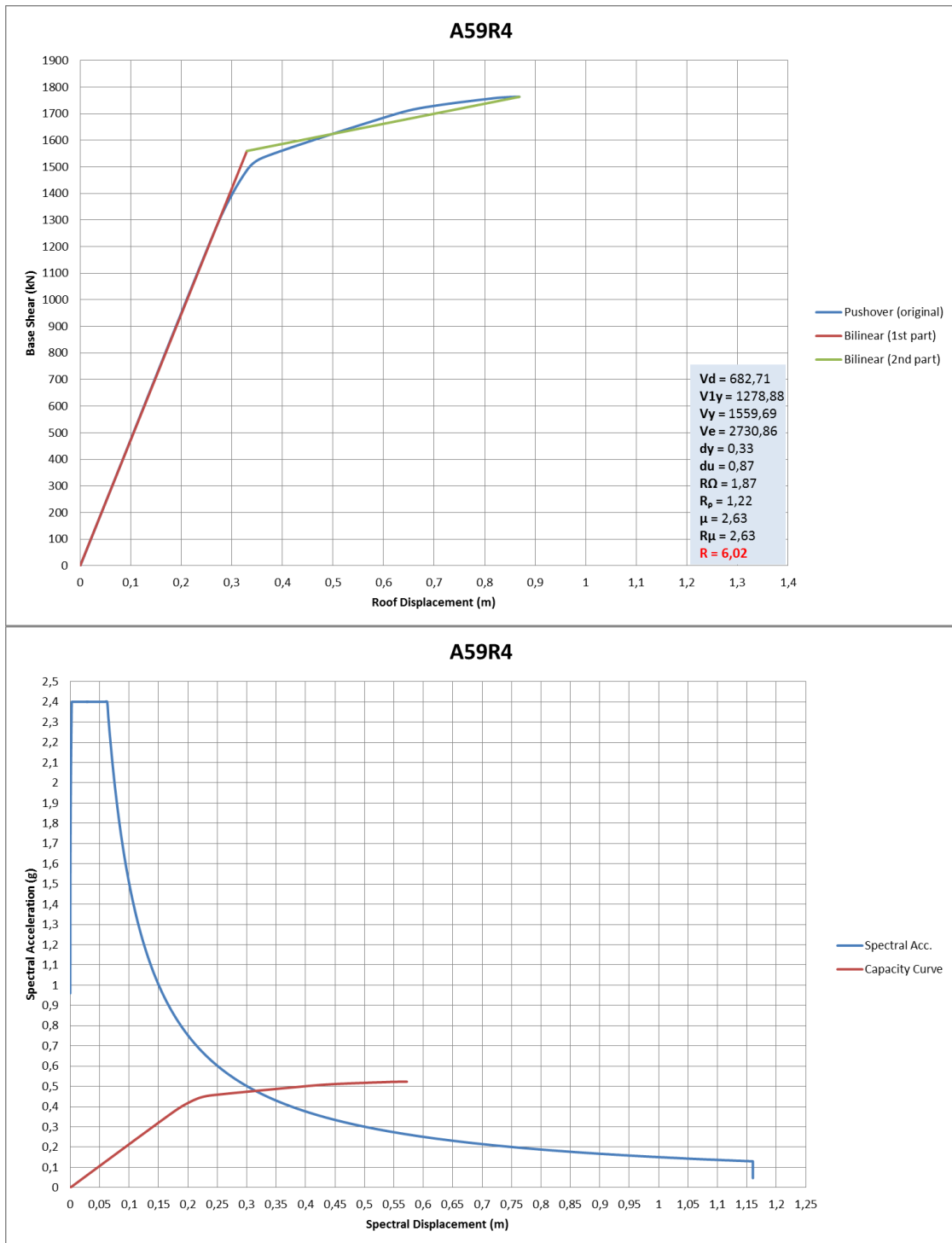


Figure B.17 Frame A59R4 Idealized pushover curve and spectral capacity curve

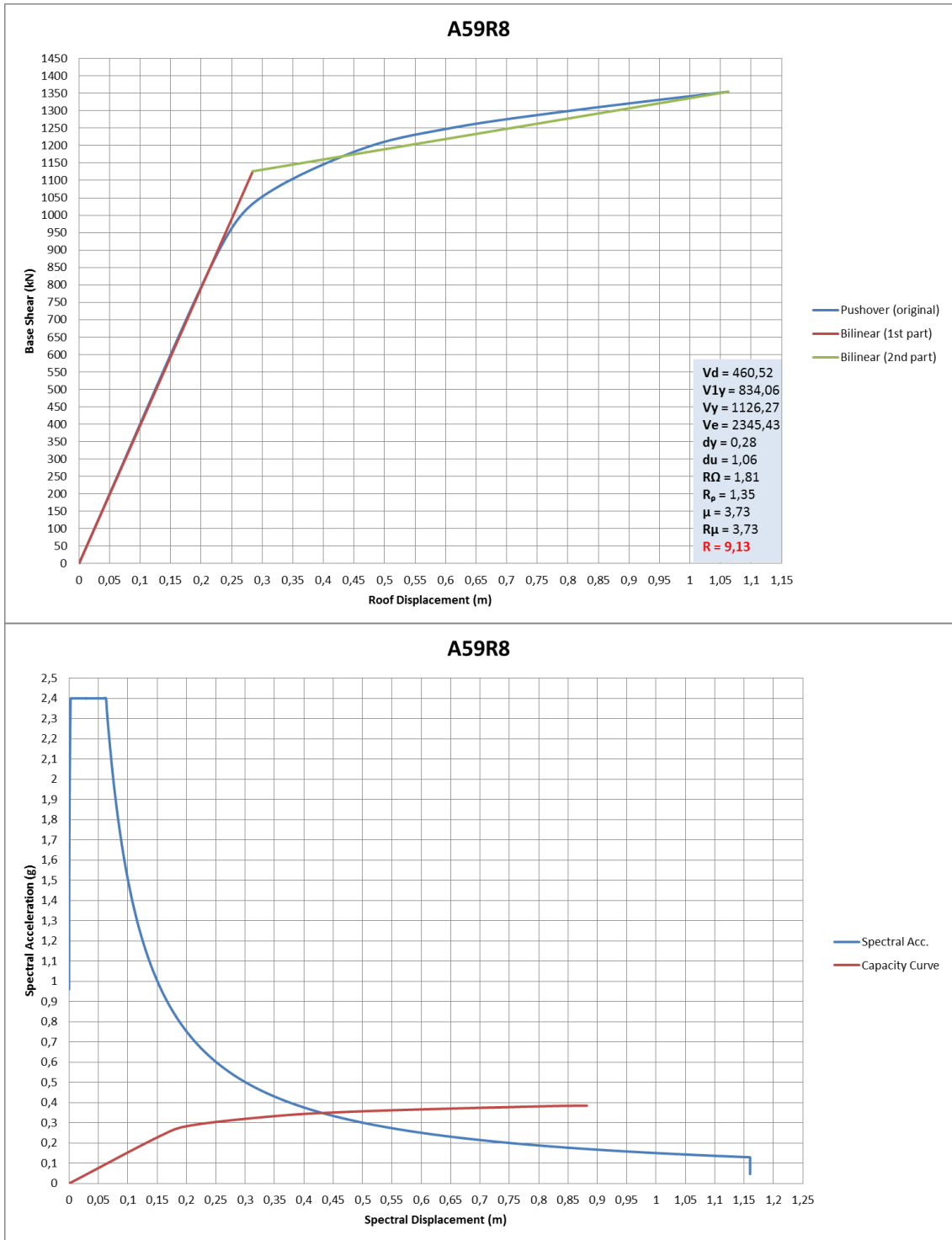


Figure B.18 Frame A59R8 Idealized pushover curve and spectral capacity curve

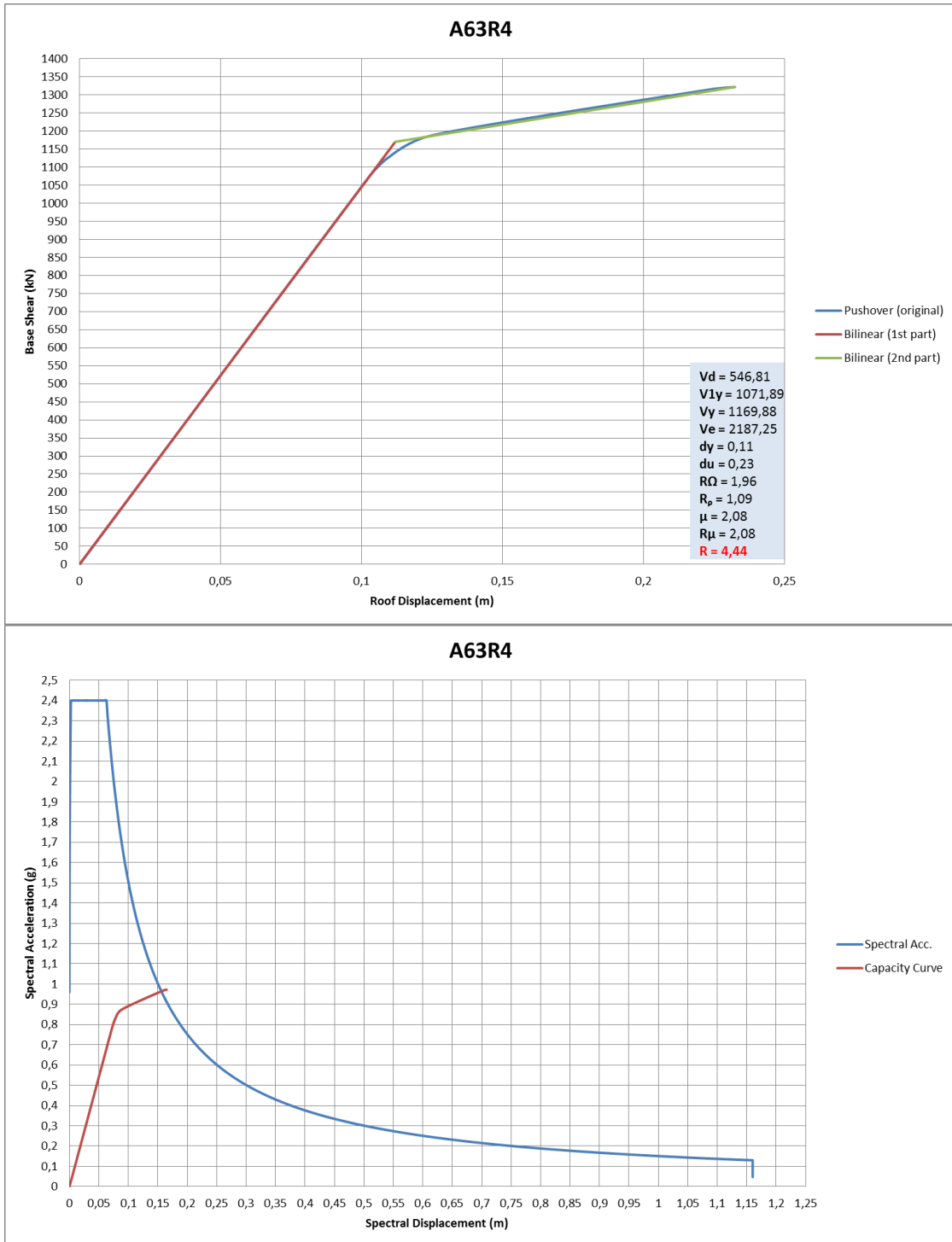


Figure B.19 Frame A63R4 Idealized pushover curve and spectral capacity curve

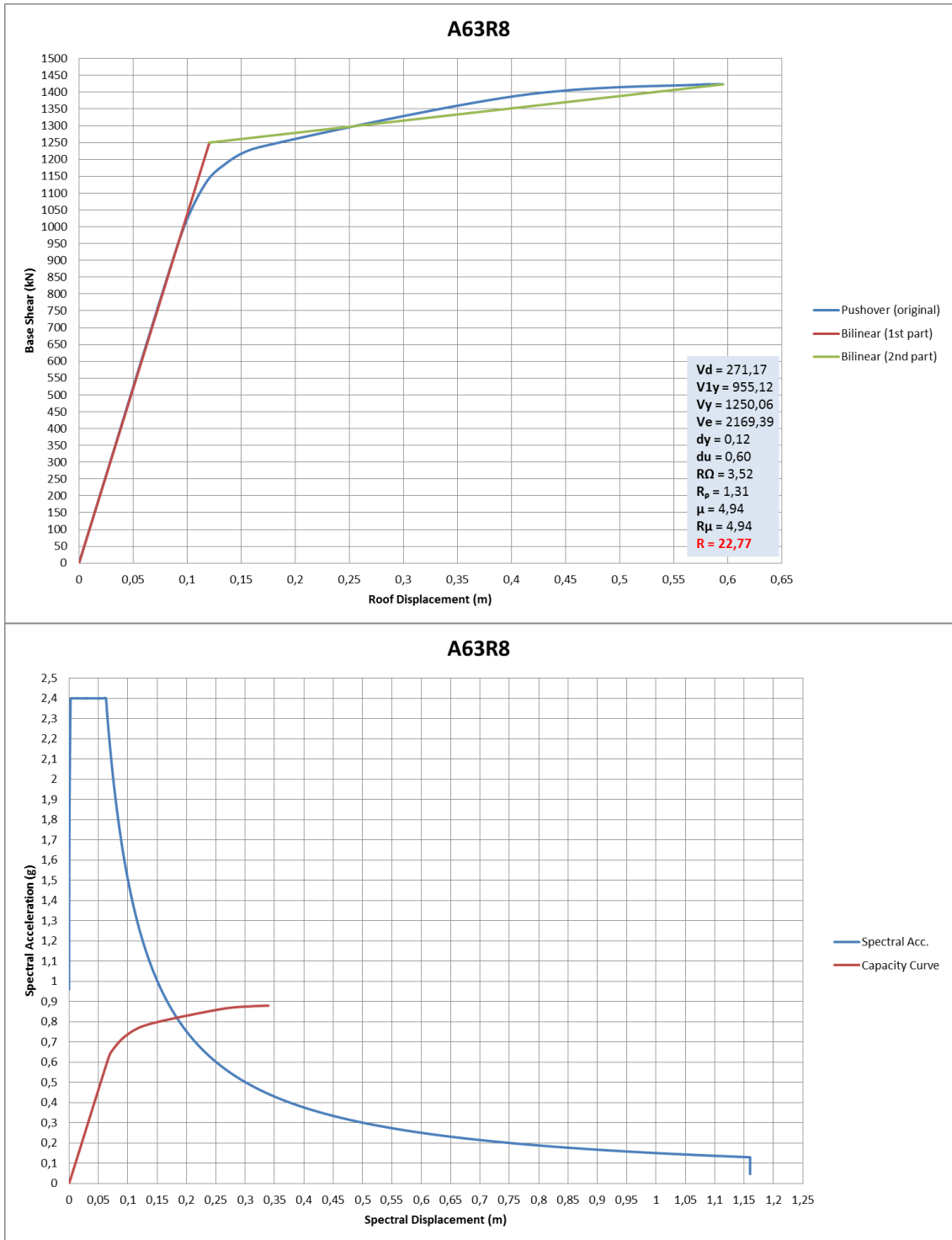


Figure B.20 Frame A63R8 Idealized pushover curve and spectral capacity curve

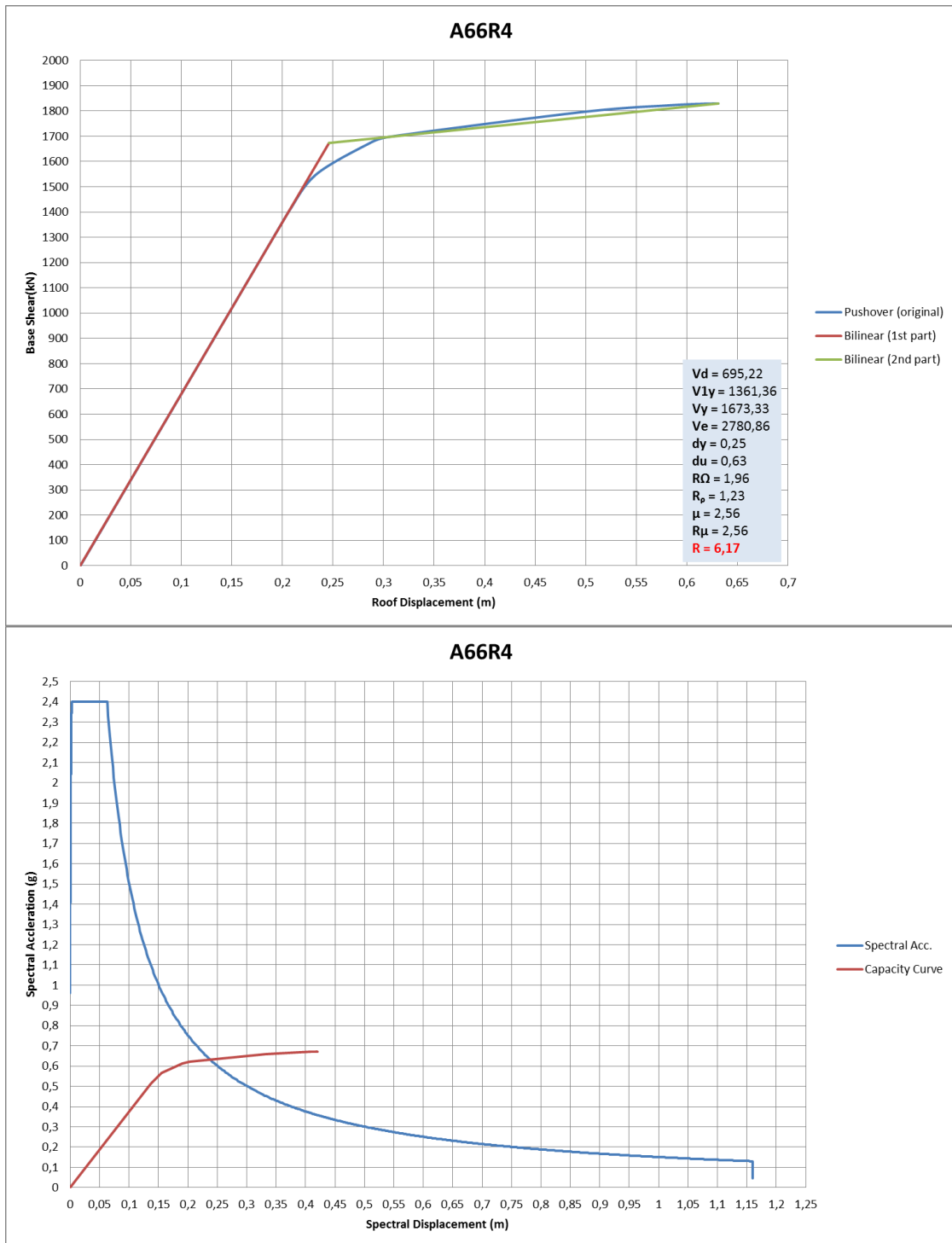


Figure B.21 Frame A66R4 Idealized pushover curve and spectral capacity curve

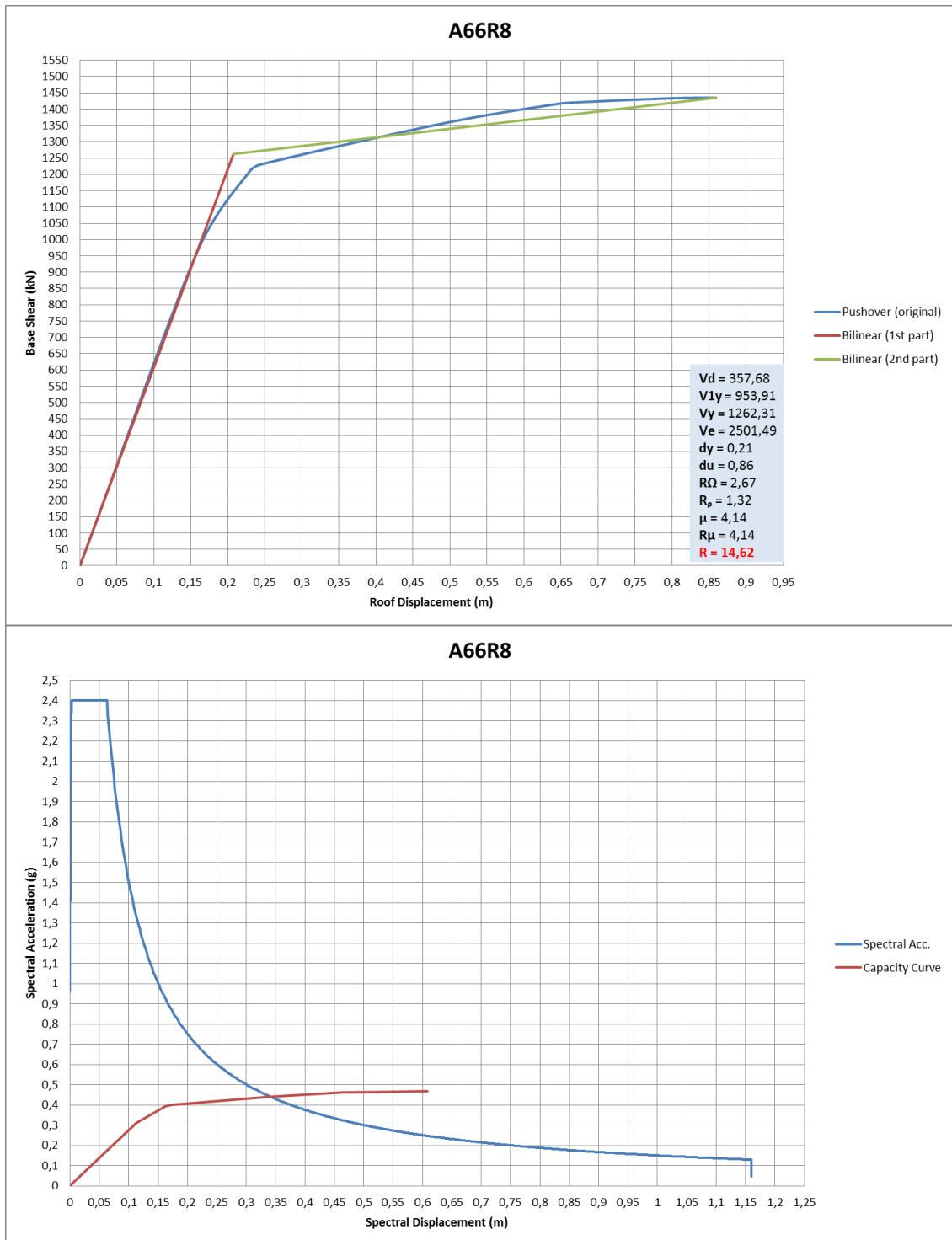


Figure B.22 Frame A66R8 Idealized pushover curve and spectral capacity curve

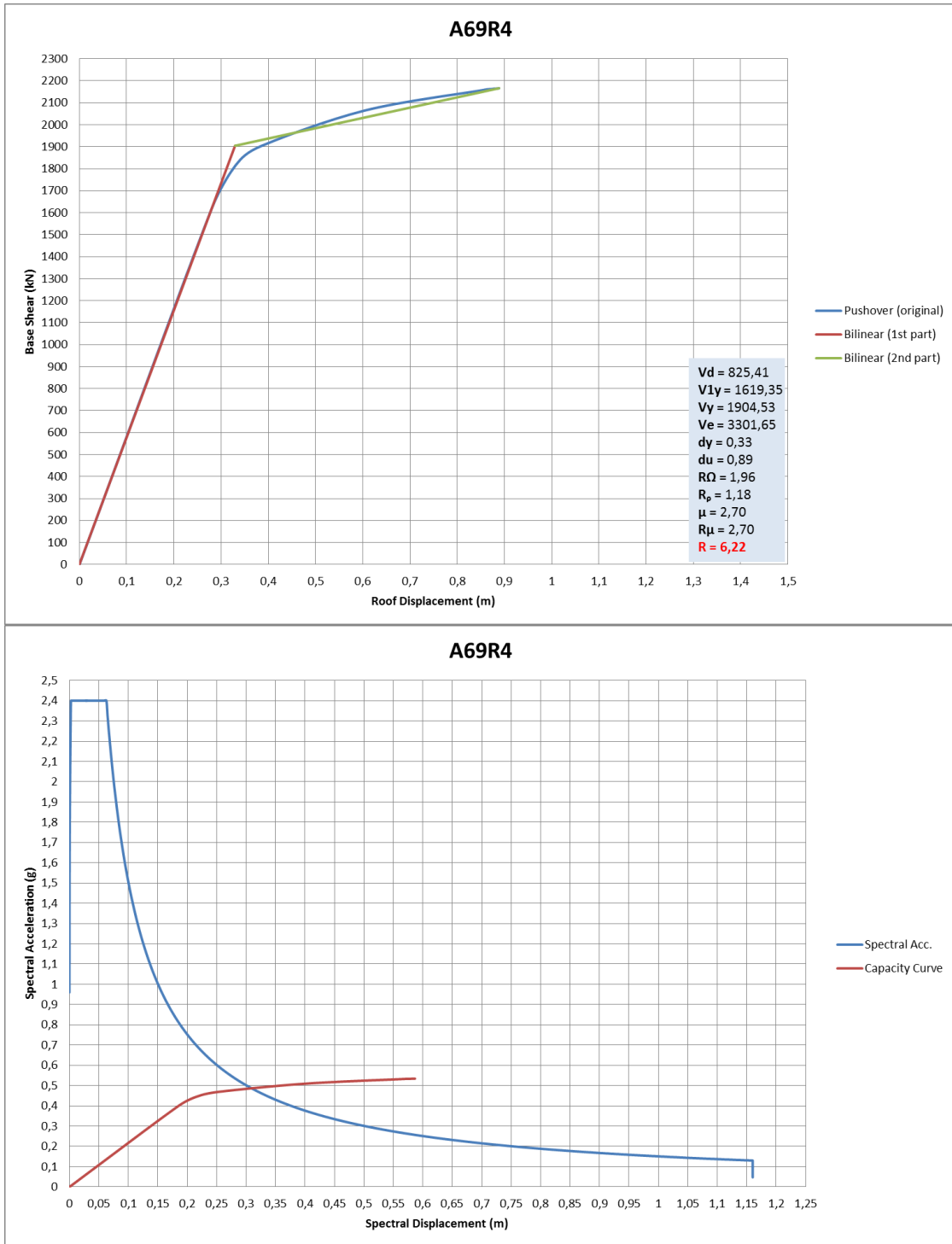


Figure B.23 Frame A69R4 Idealized pushover curve and spectral capacity curve

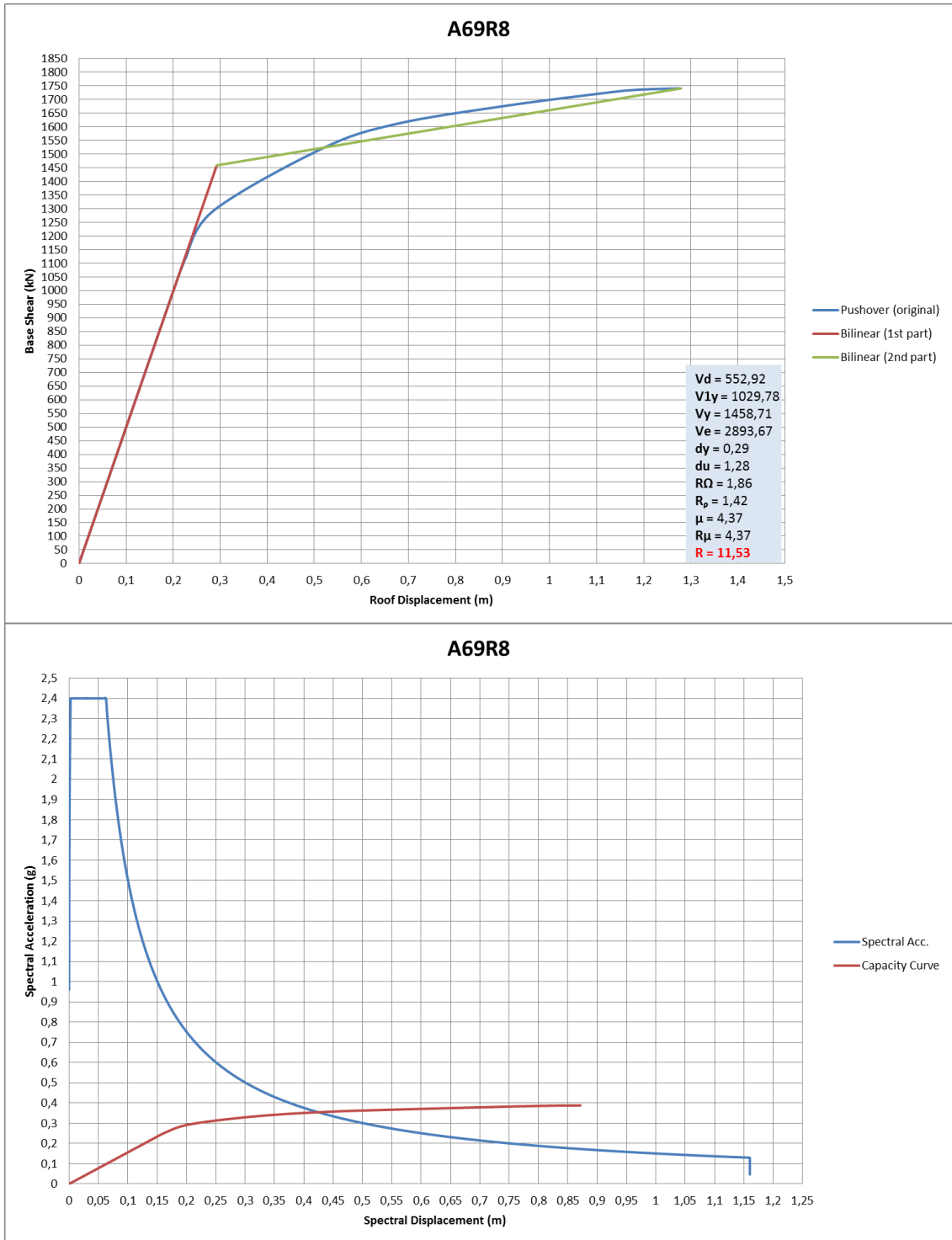


Figure B.24 Frame A69R8 Idealized pushover curve and spectral capacity curve

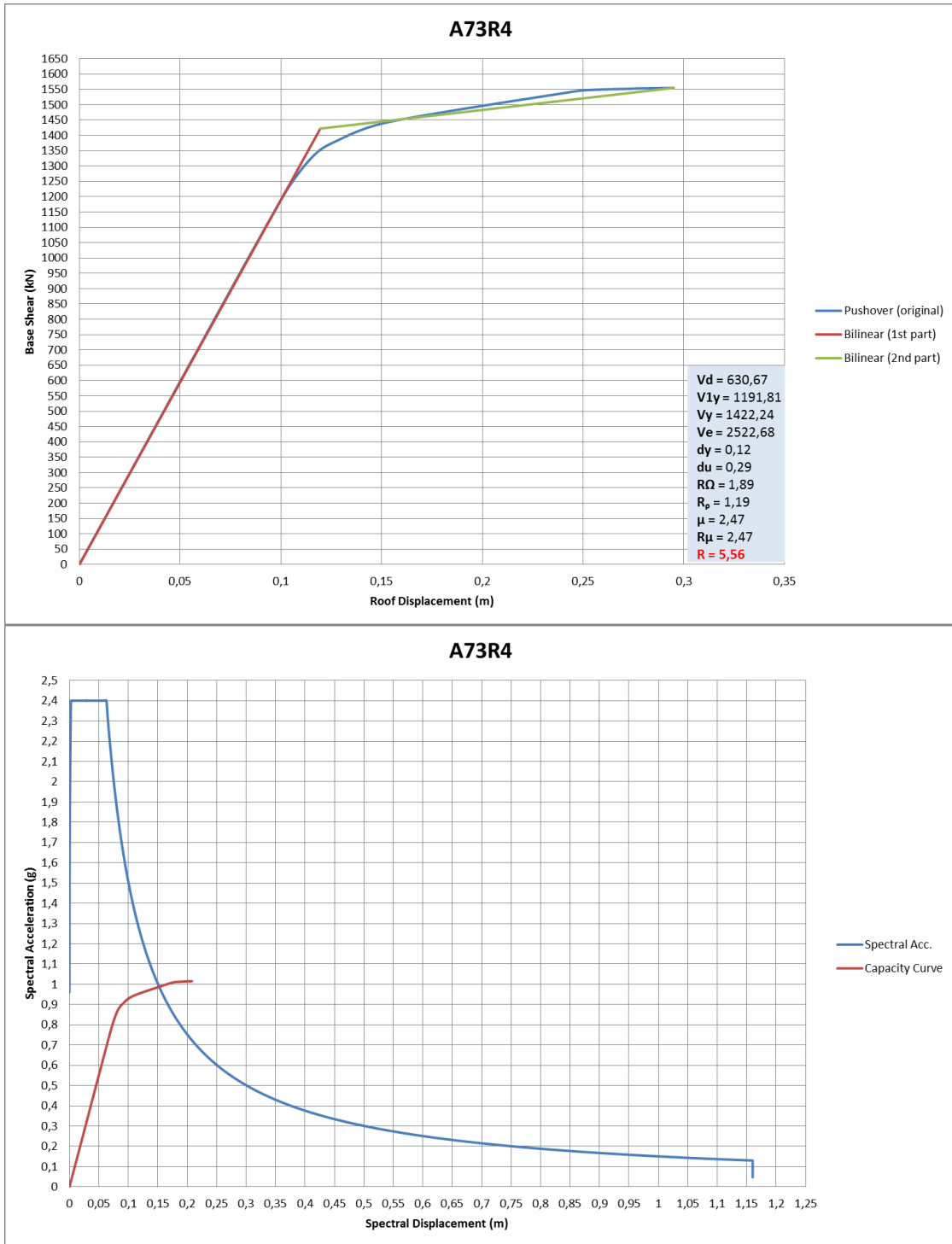


Figure B.25 Frame A73R4 Idealized pushover curve and spectral capacity curve

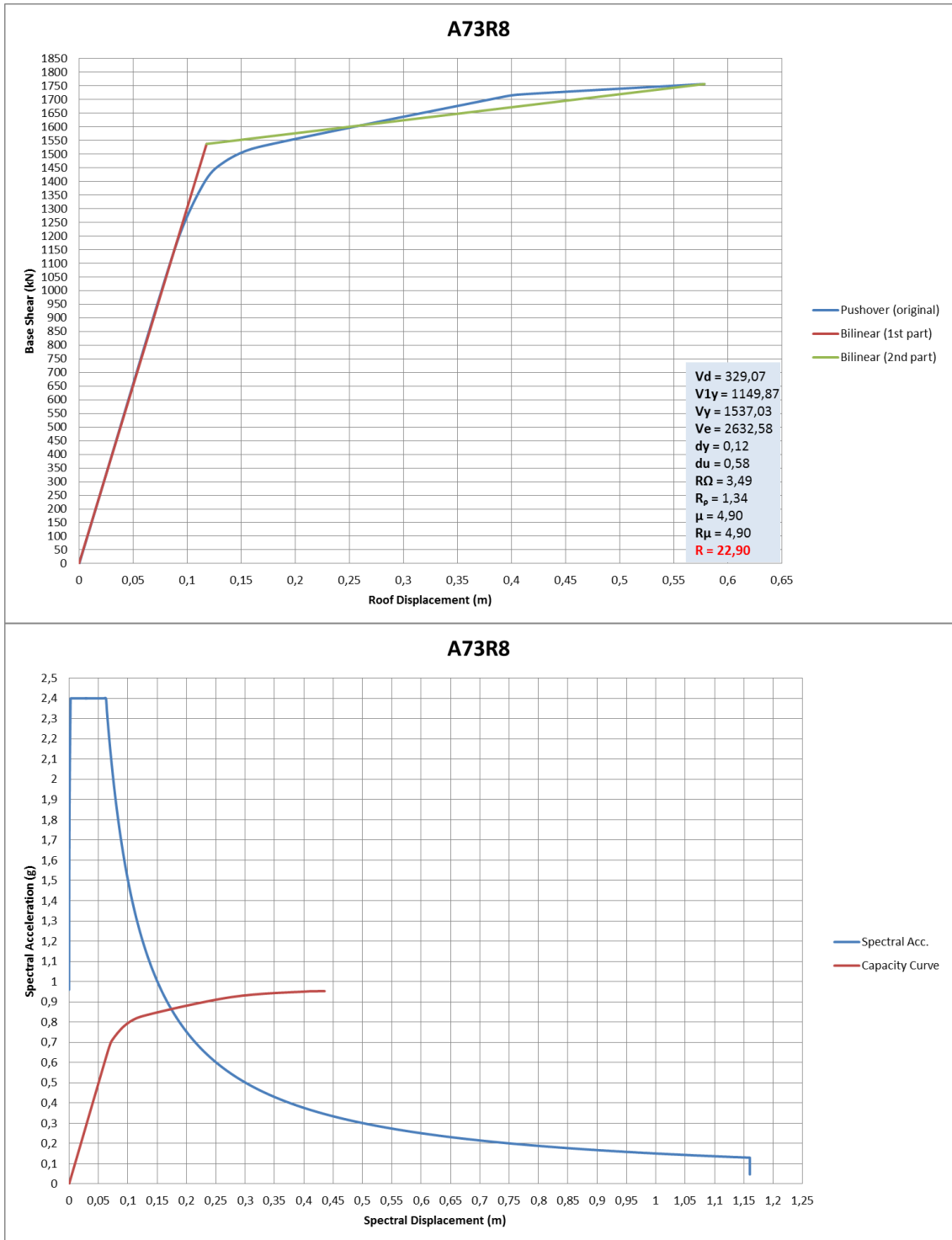


Figure B.26 Frame A73R8 Idealized pushover curve and spectral capacity curve

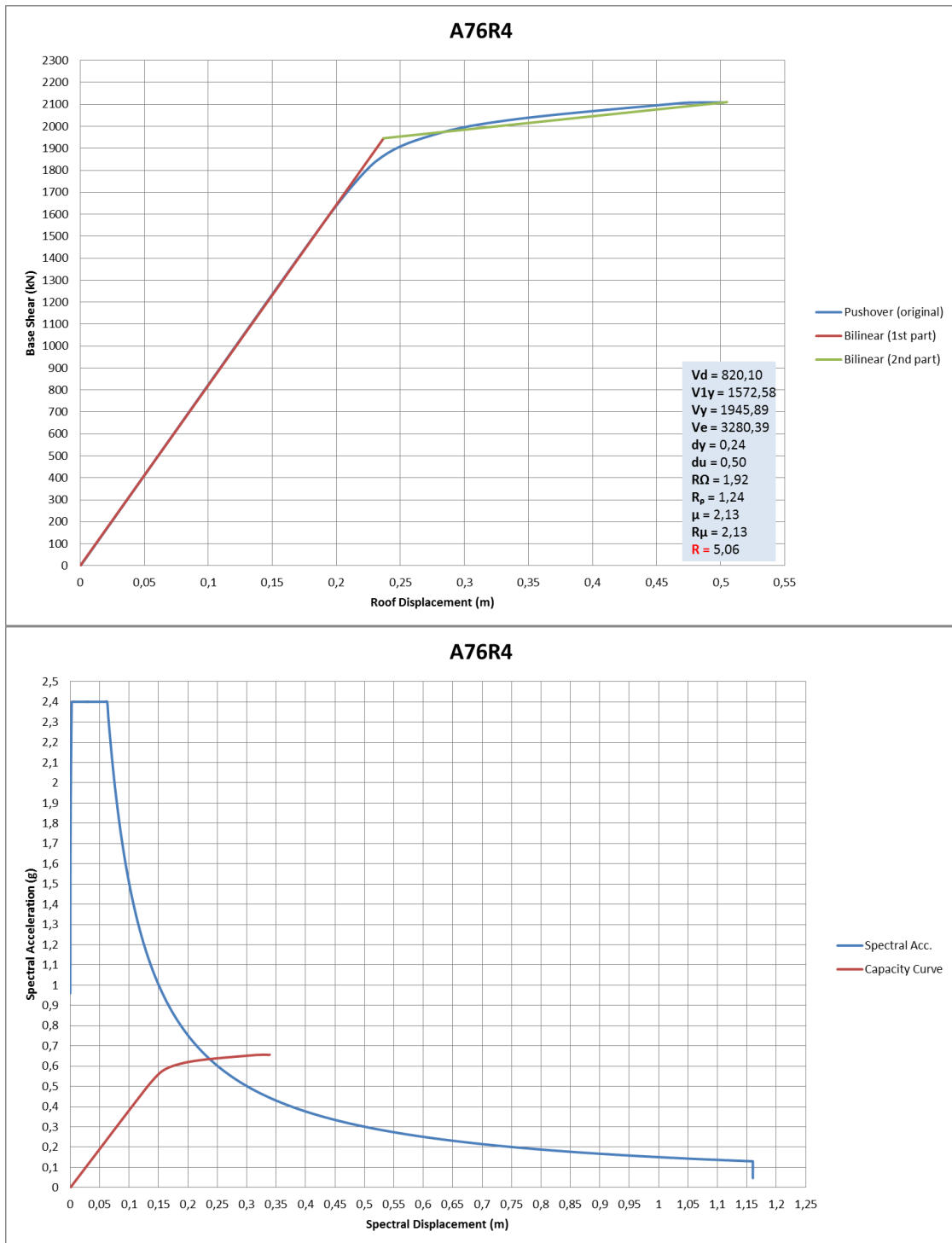


Figure B.27 Frame A76R4 Idealized pushover curve and spectral capacity curve

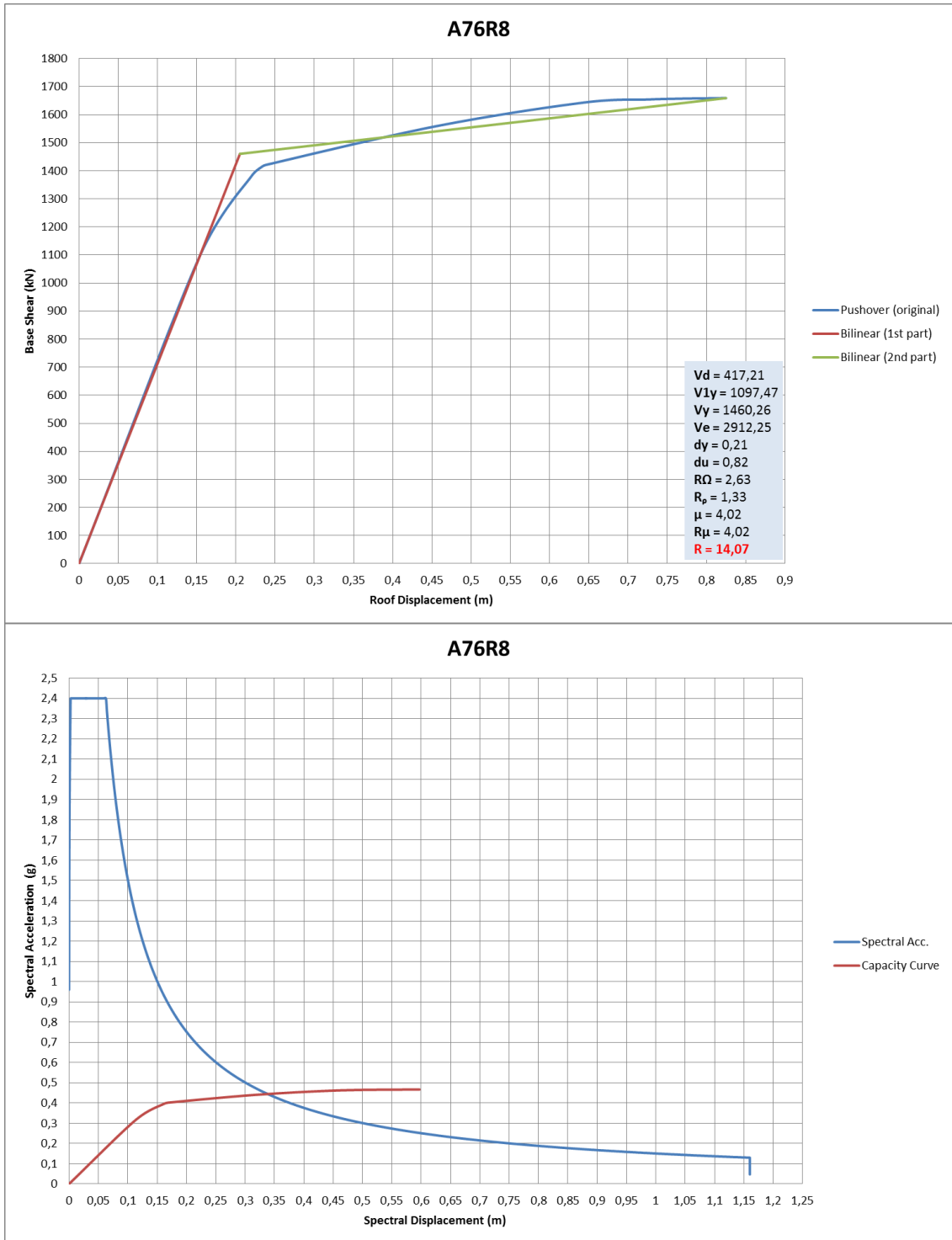


Figure B.28 Frame A76R8 Idealized pushover curve and spectral capacity curve

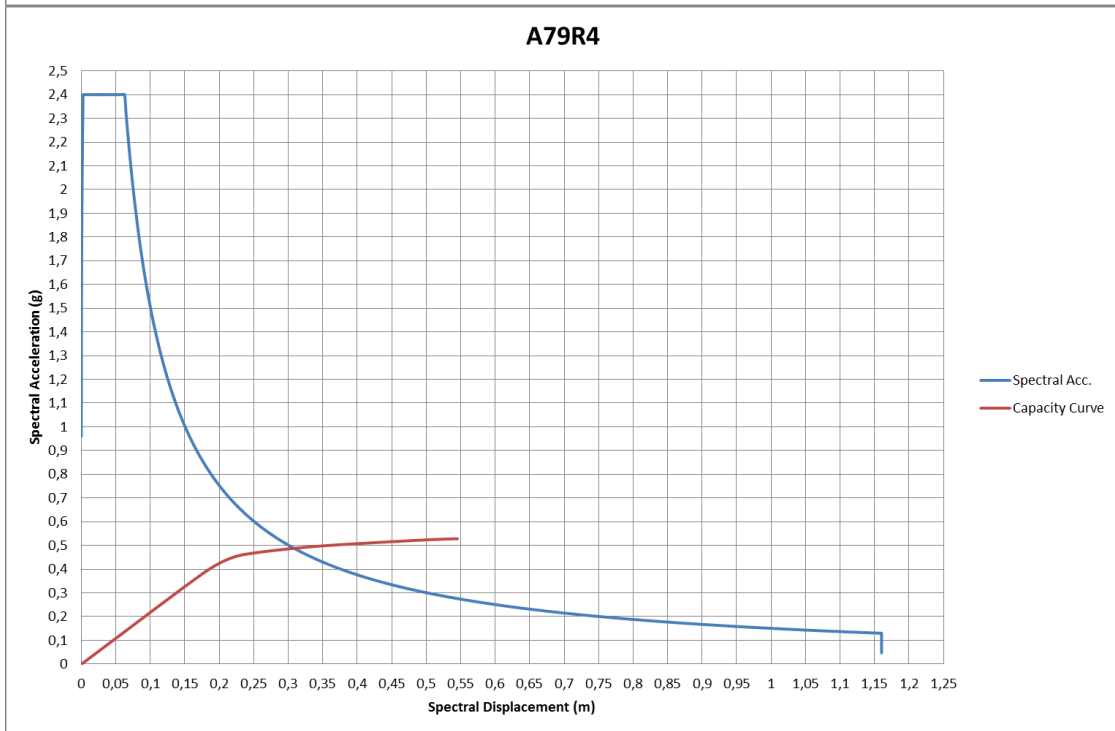
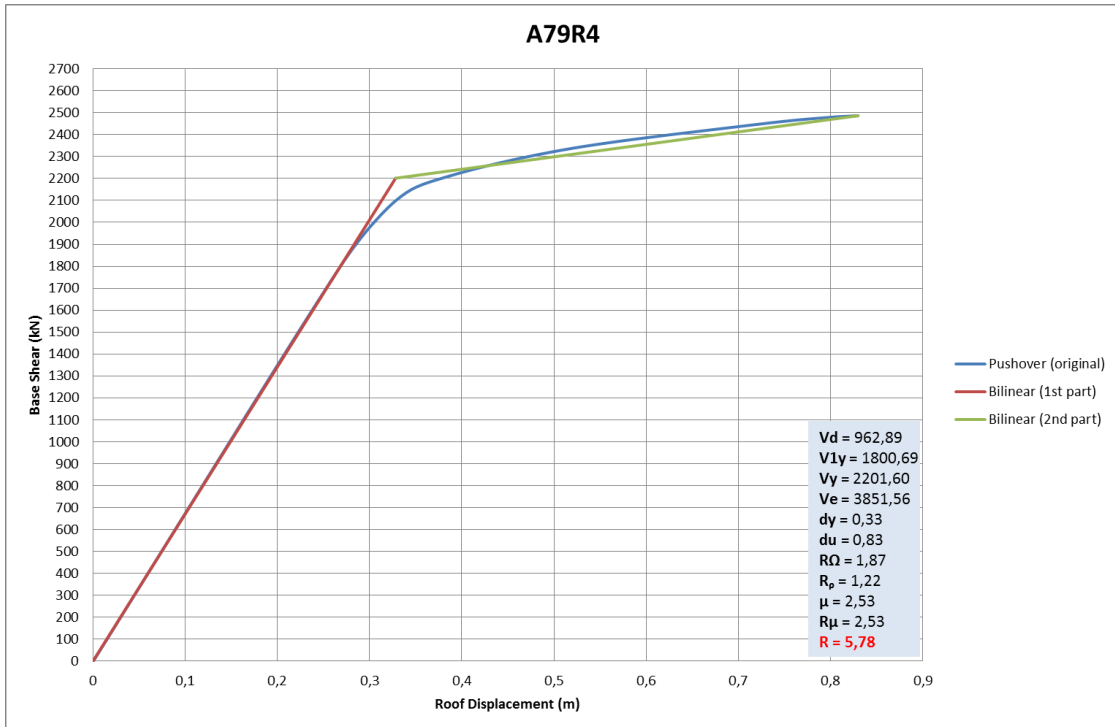


Figure B.29 Frame A79R4 Idealized pushover curve and spectral capacity curve

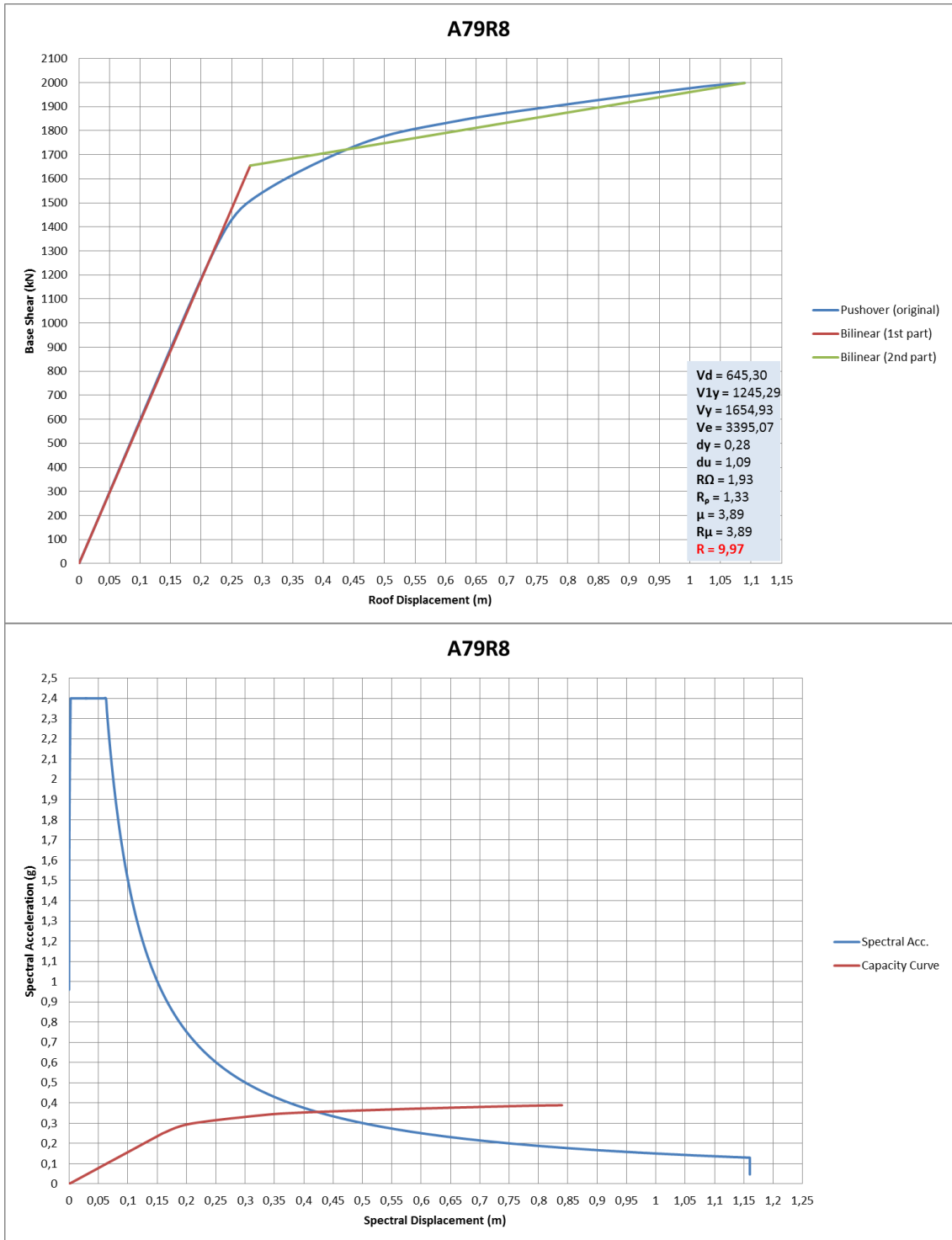


Figure B.30 Frame A79R8 Idealized pushover curve and spectral capacity curve

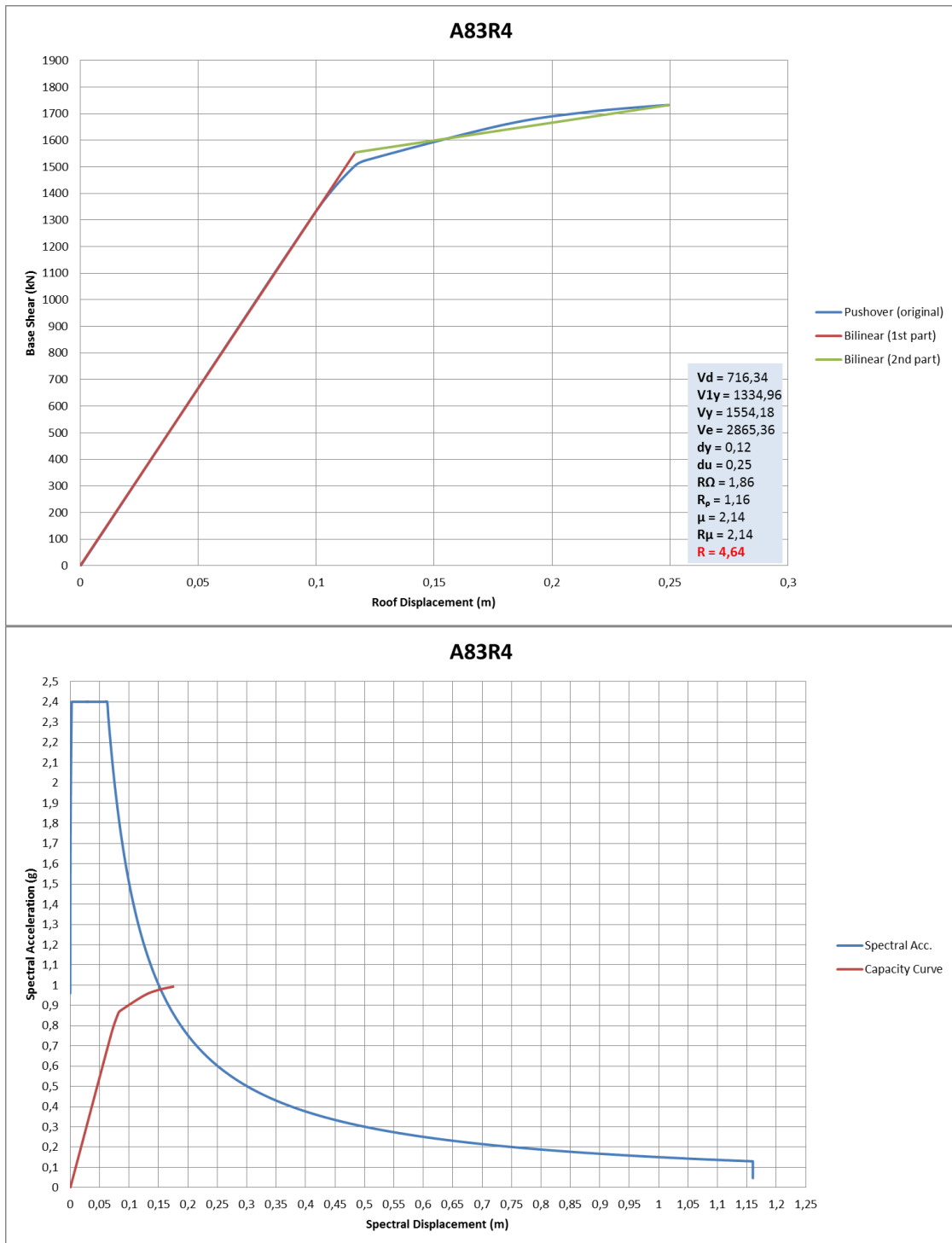


Figure B.31 Frame A83R4 Idealized pushover curve and spectral capacity curve

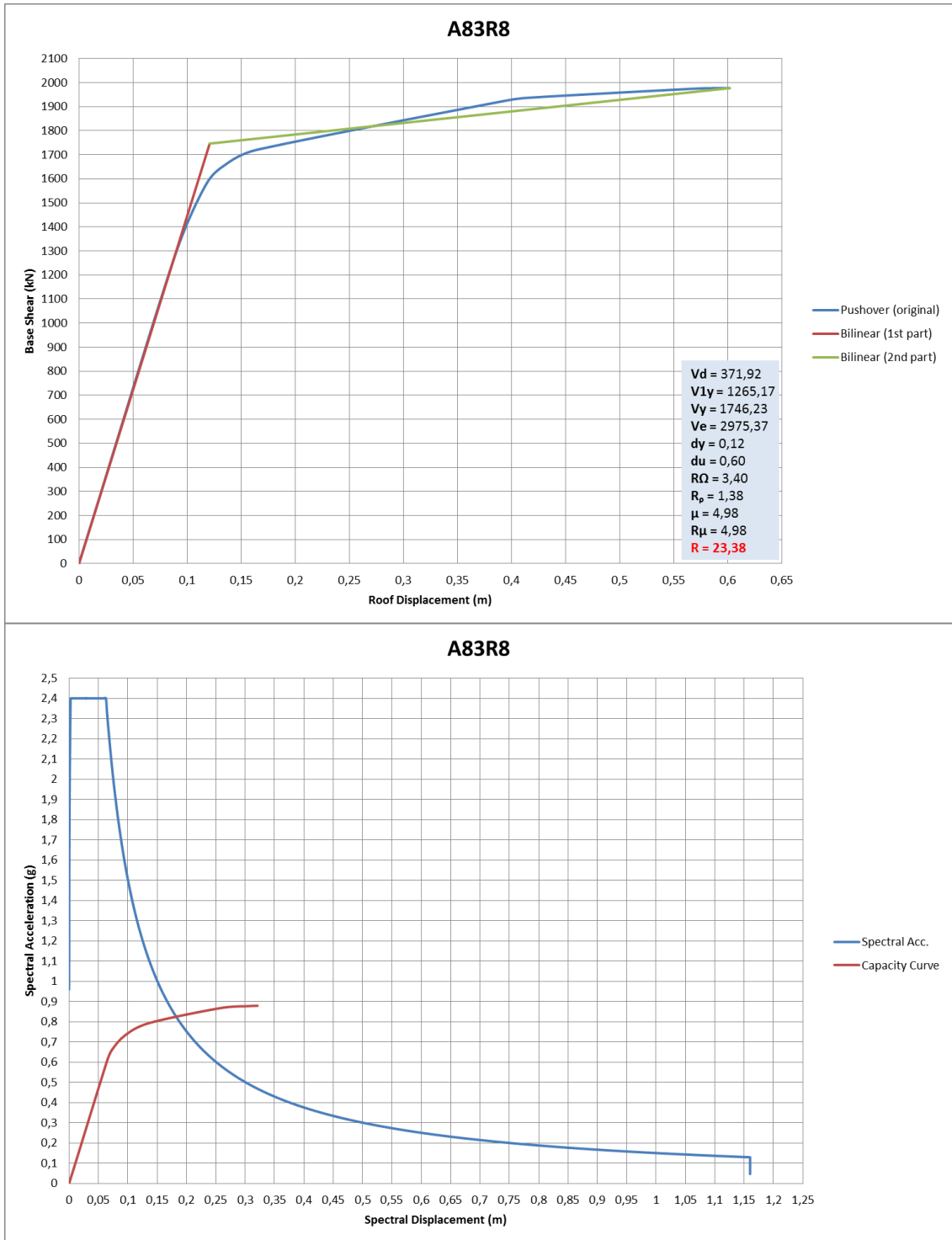


Figure B.32 Frame A83R8 Idealized pushover curve and spectral capacity curve

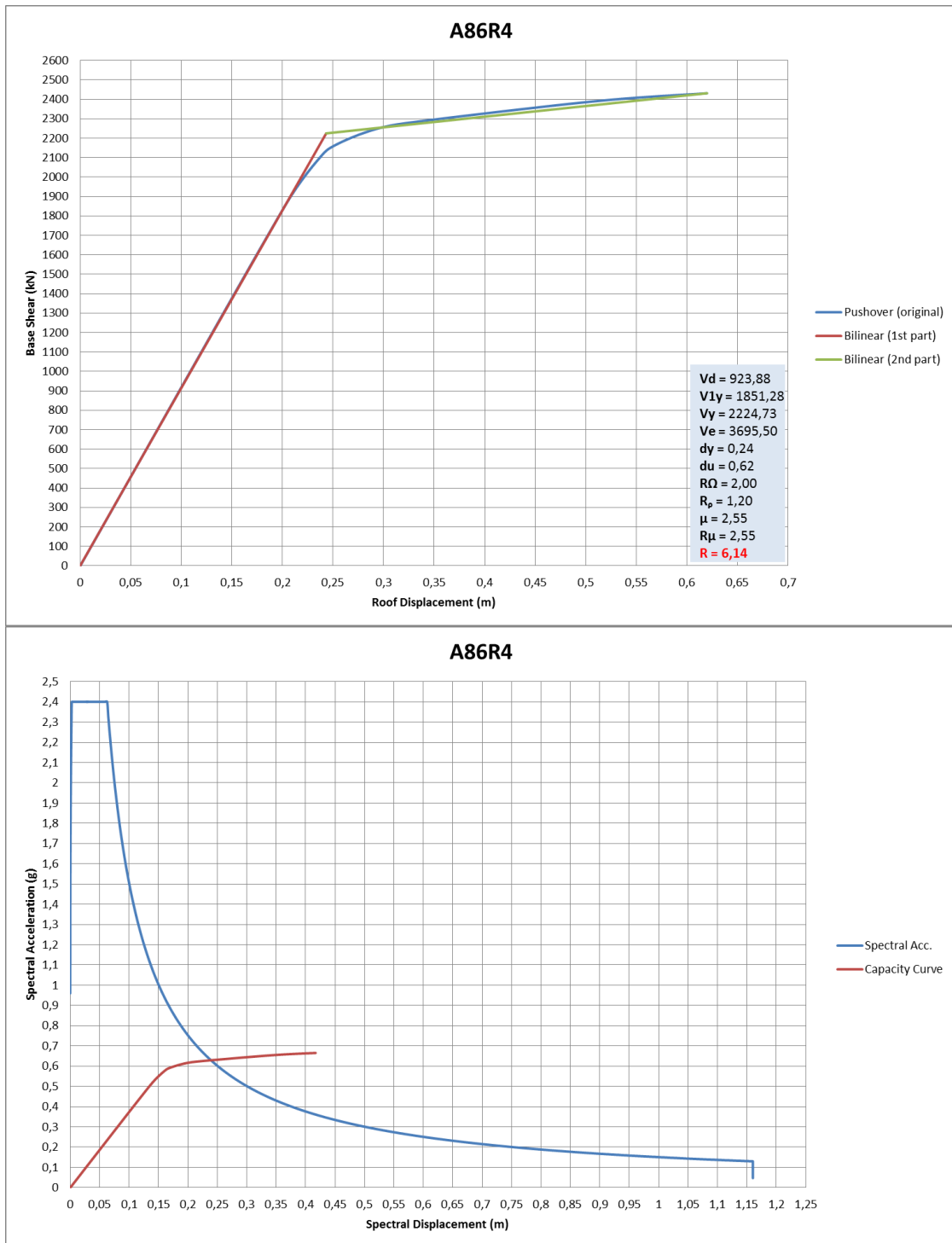


Figure B.33 Frame A86R4 Idealized pushover curve and spectral capacity curve

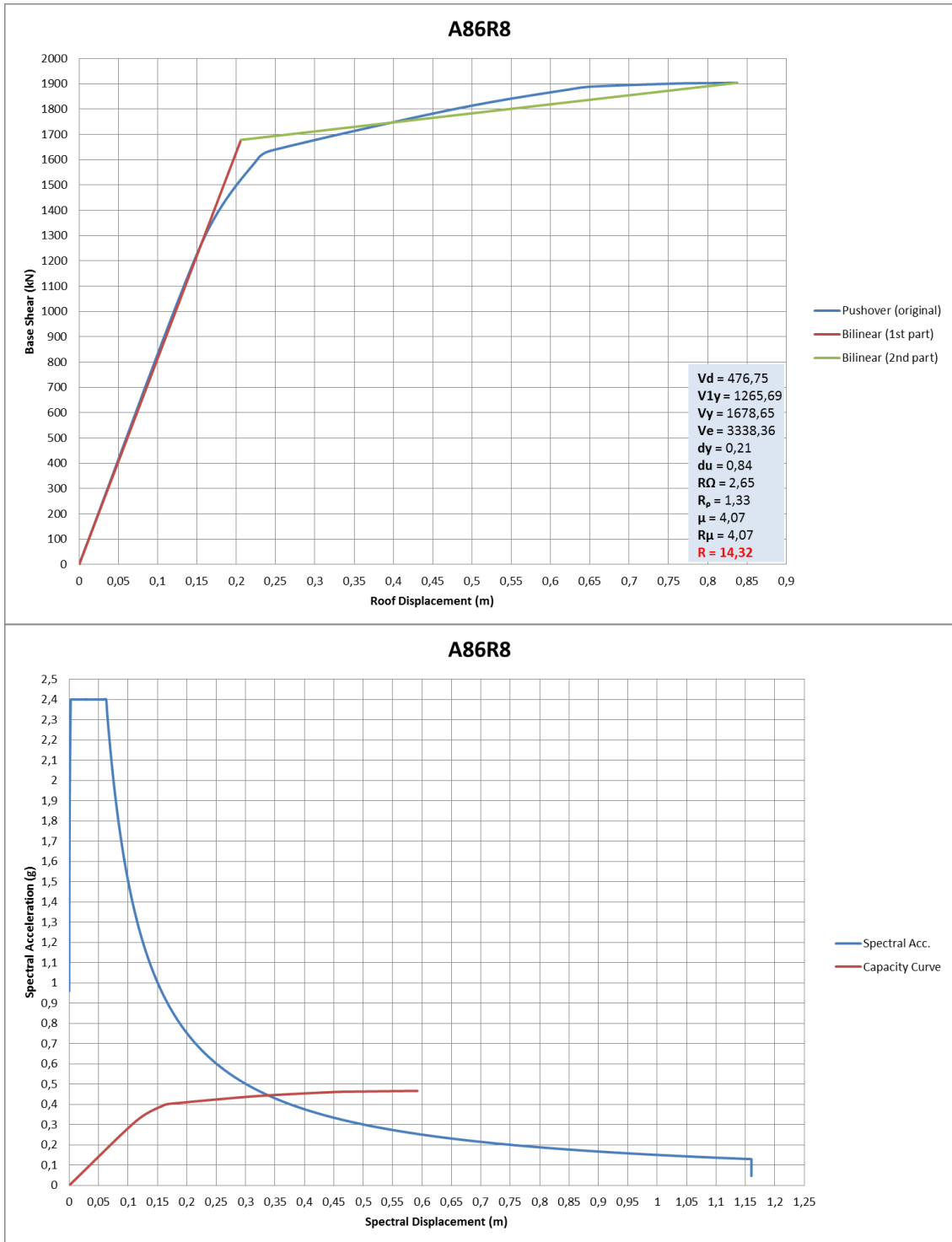


Figure B.34 Frame A86R8 Idealized pushover curve and spectral capacity curve

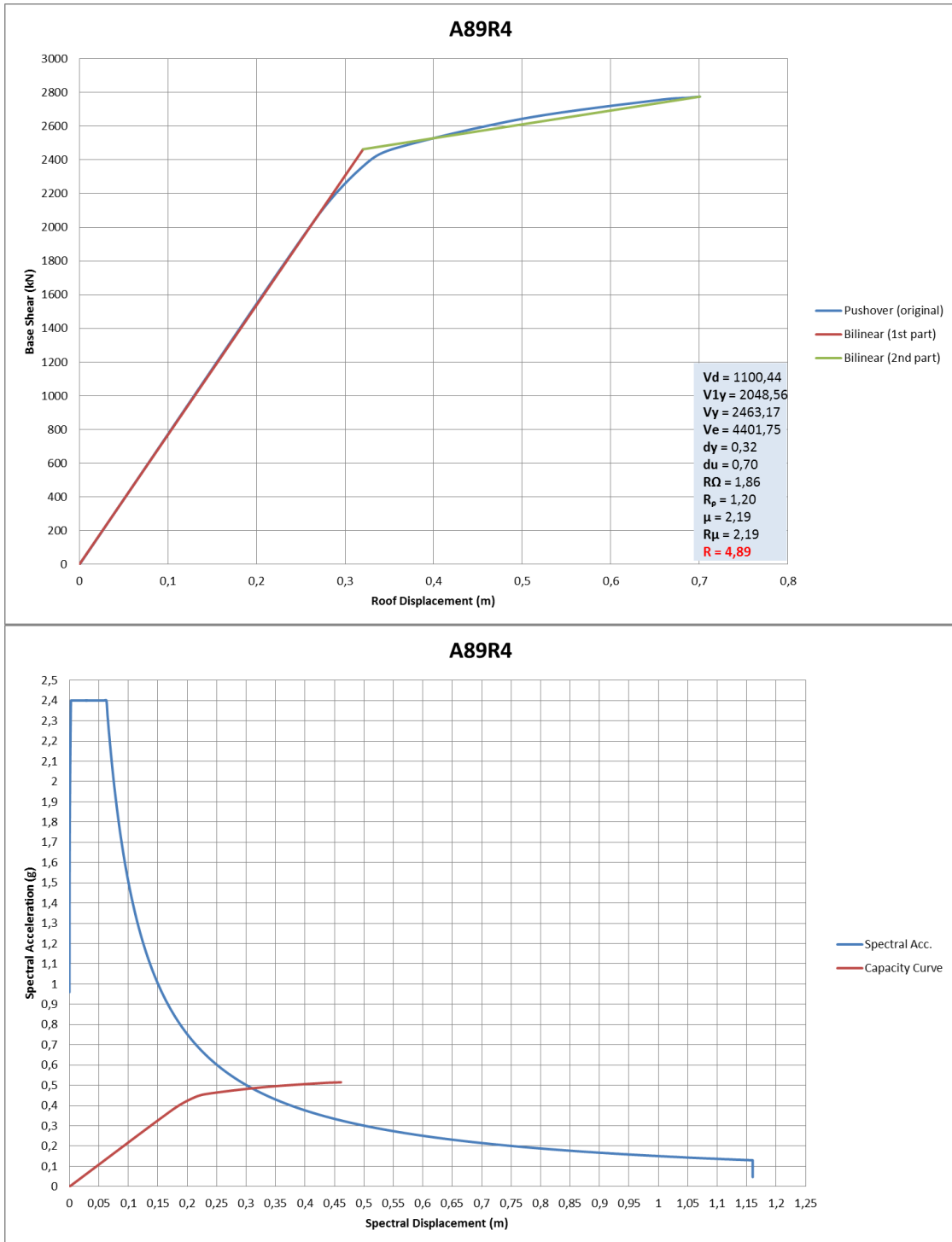


Figure B.35 Frame A89R4 Idealized pushover curve and spectral capacity curve

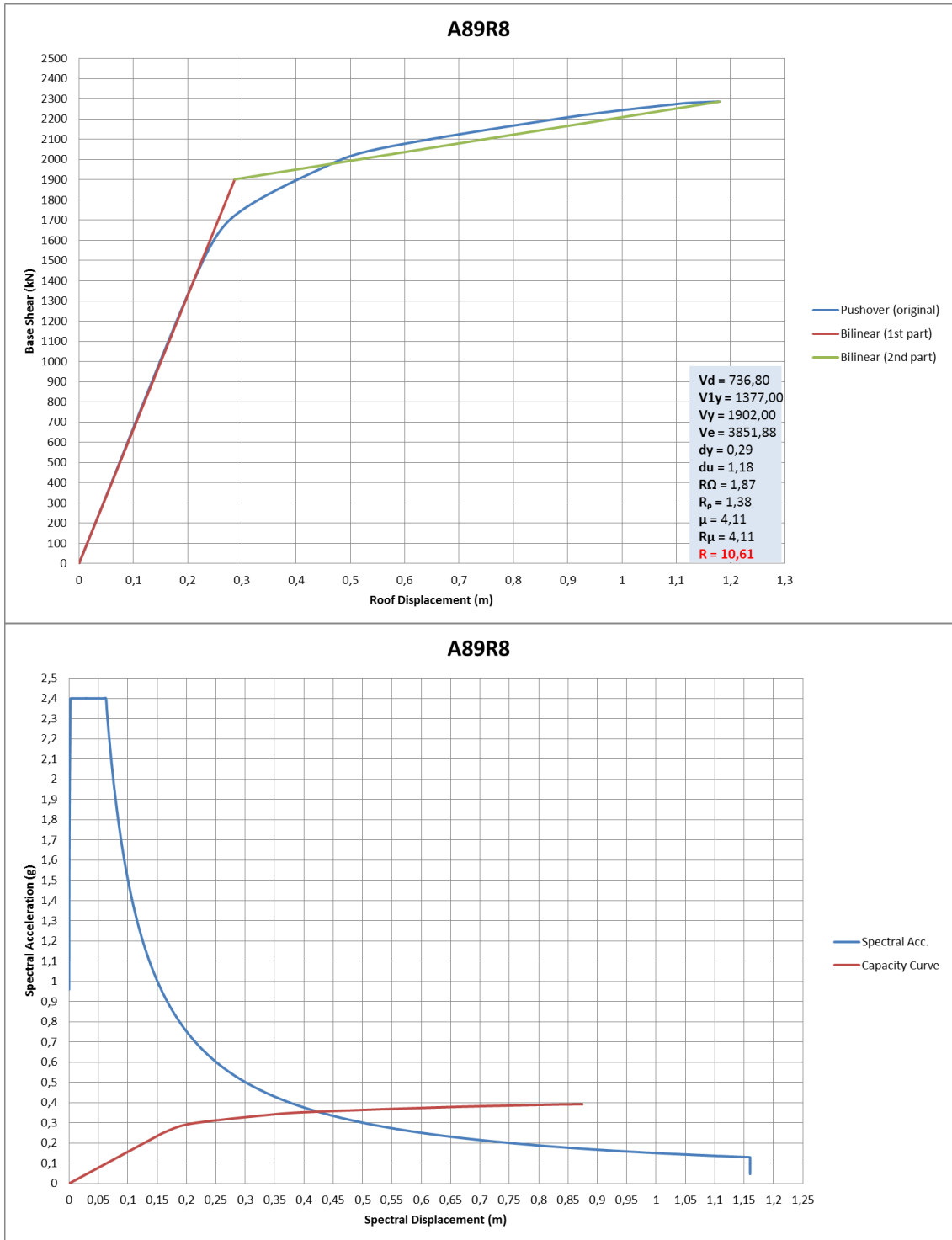


Figure B.36 Frame A89R8 Idealized pushover curve and spectral capacity curve

## APPENDIX C

### SUPERIMPOSING CAPACITY CURVES FOR OMRF AND SMRF

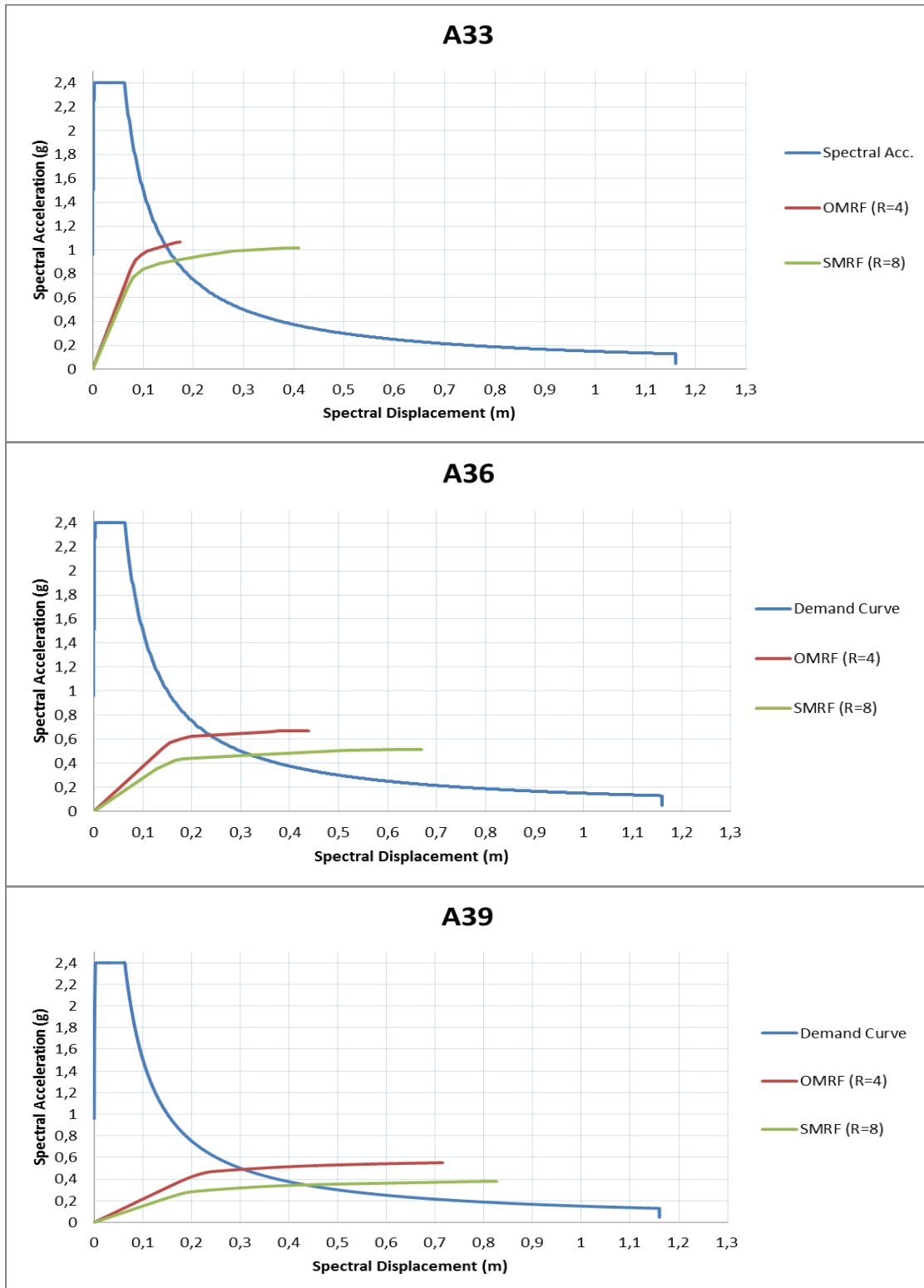


Figure C.1 Superimposing spectral capacity curves for 3-Span Frames

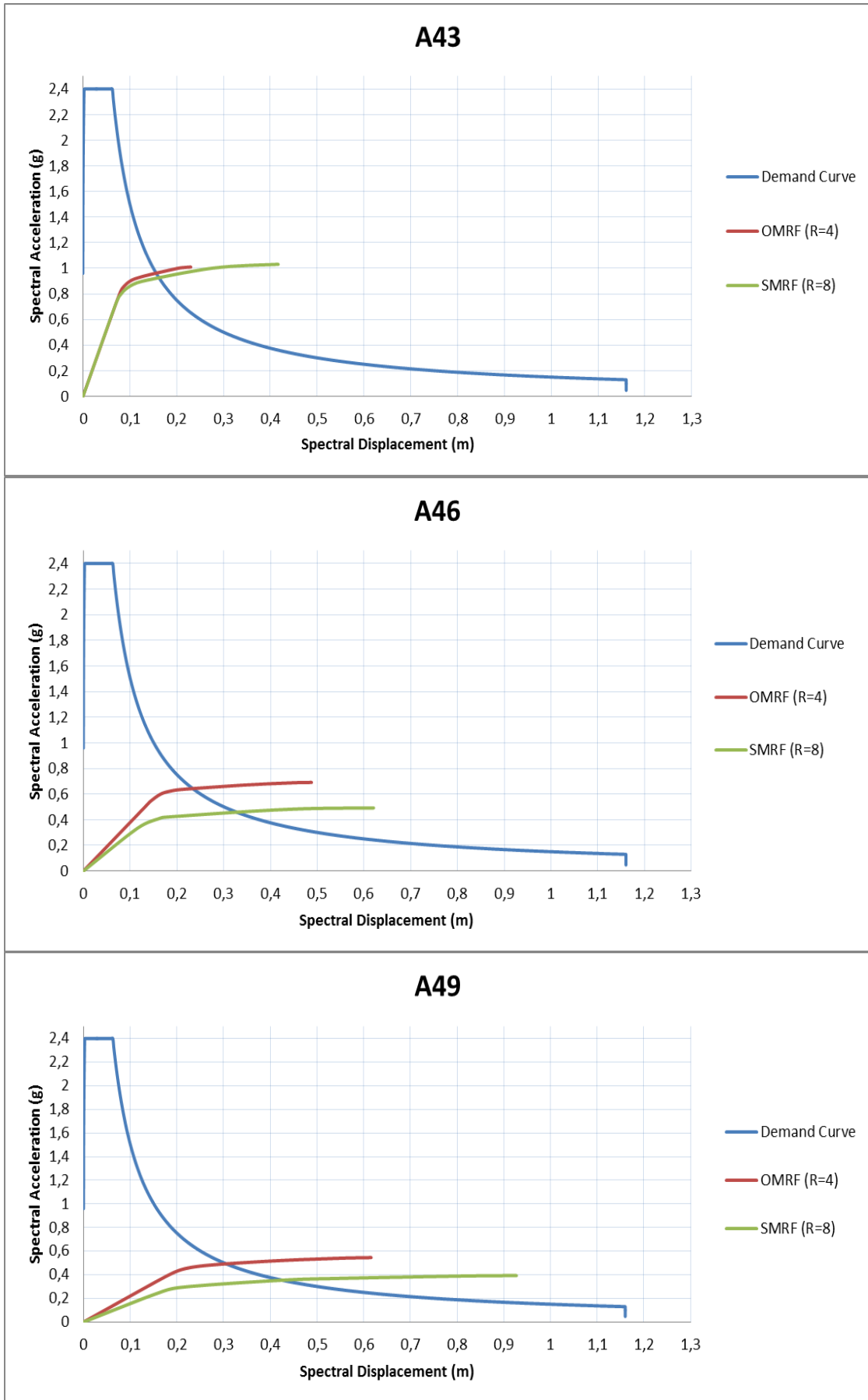


Figure C.2 Superimposing spectral capacity curves for 4-Span Frames

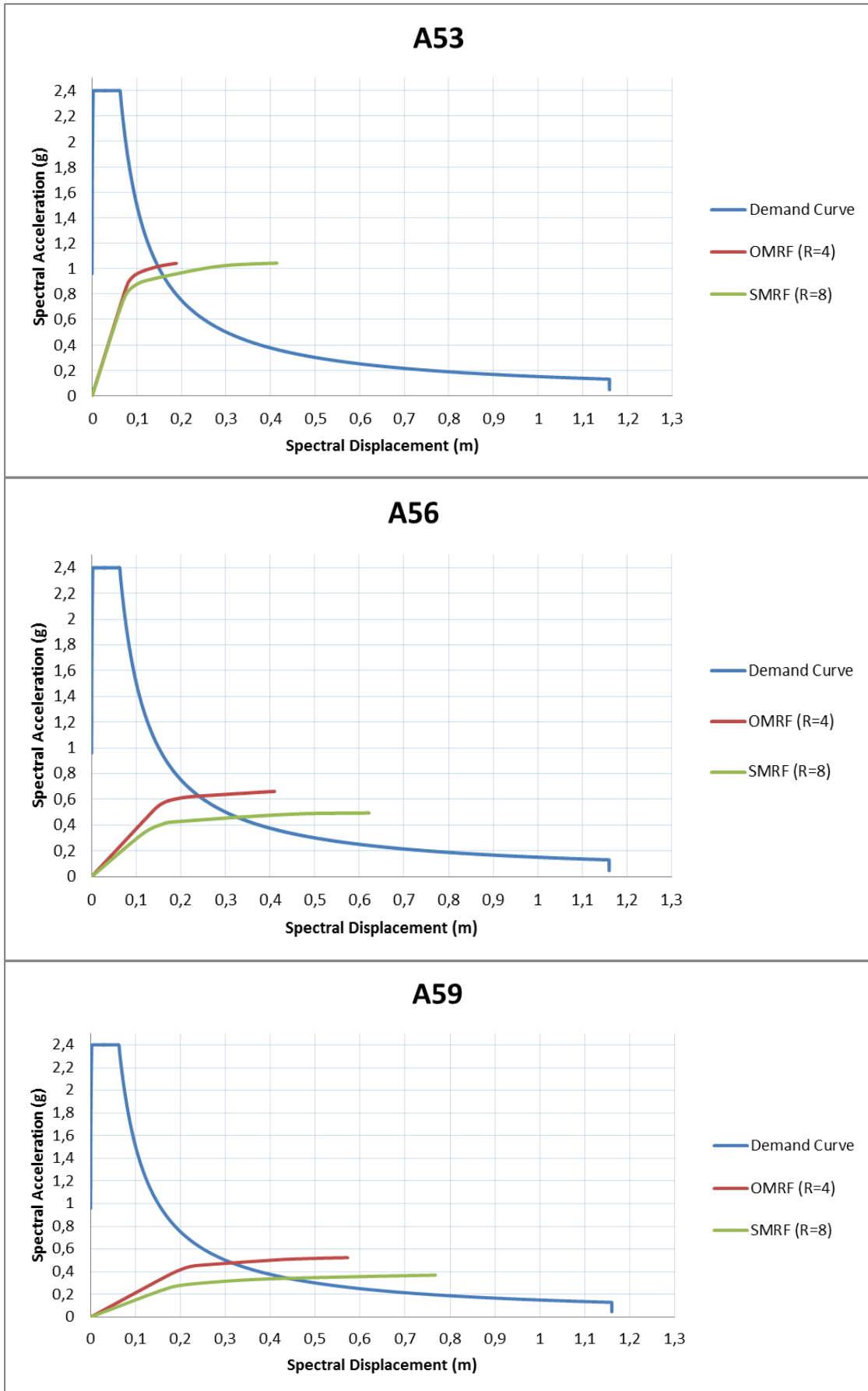


Figure C.3 Superimposing spectral capacity curves for 5-Span Frames

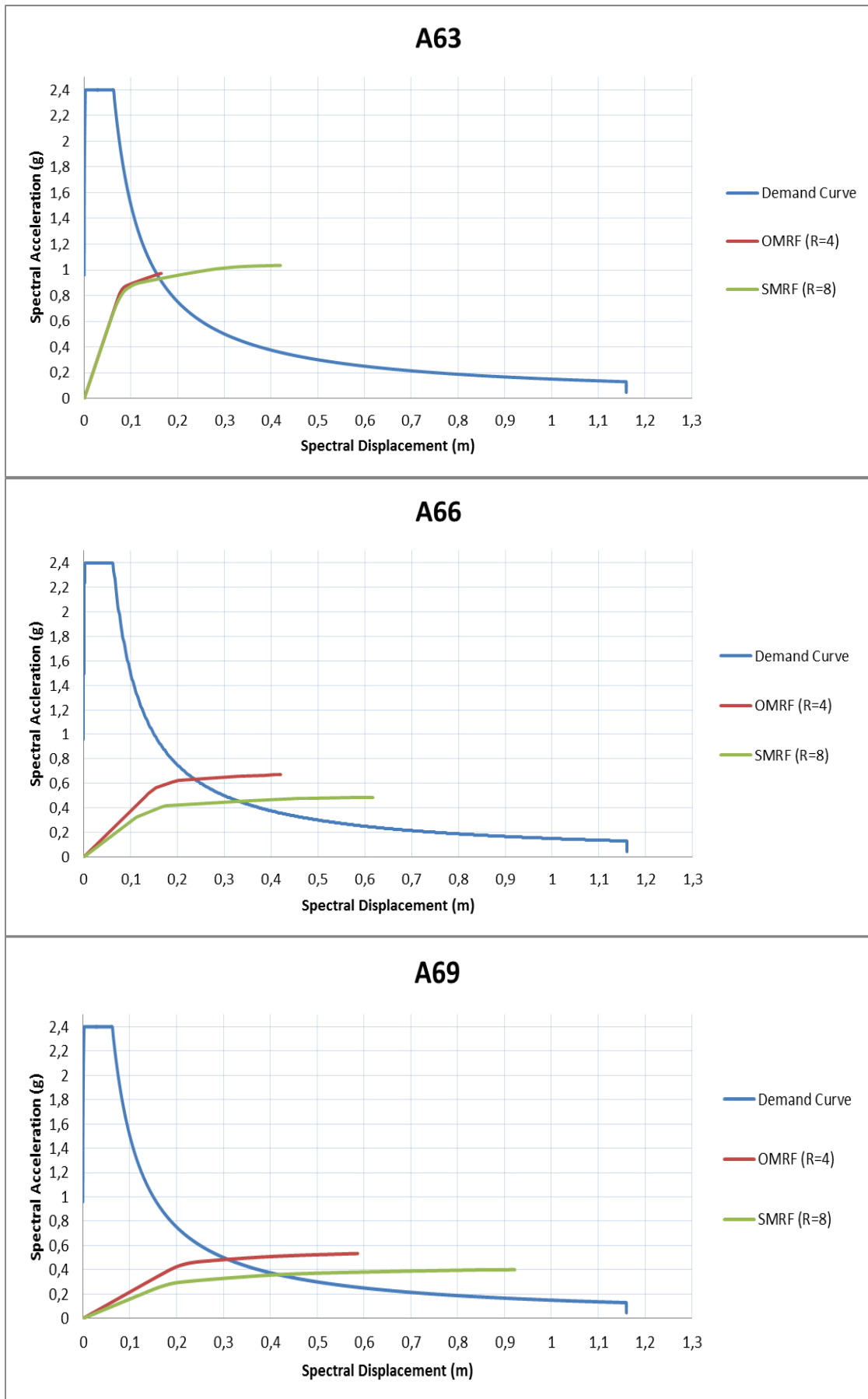


Figure C.4 Superimposing spectral capacity curves for 6-Span Frames

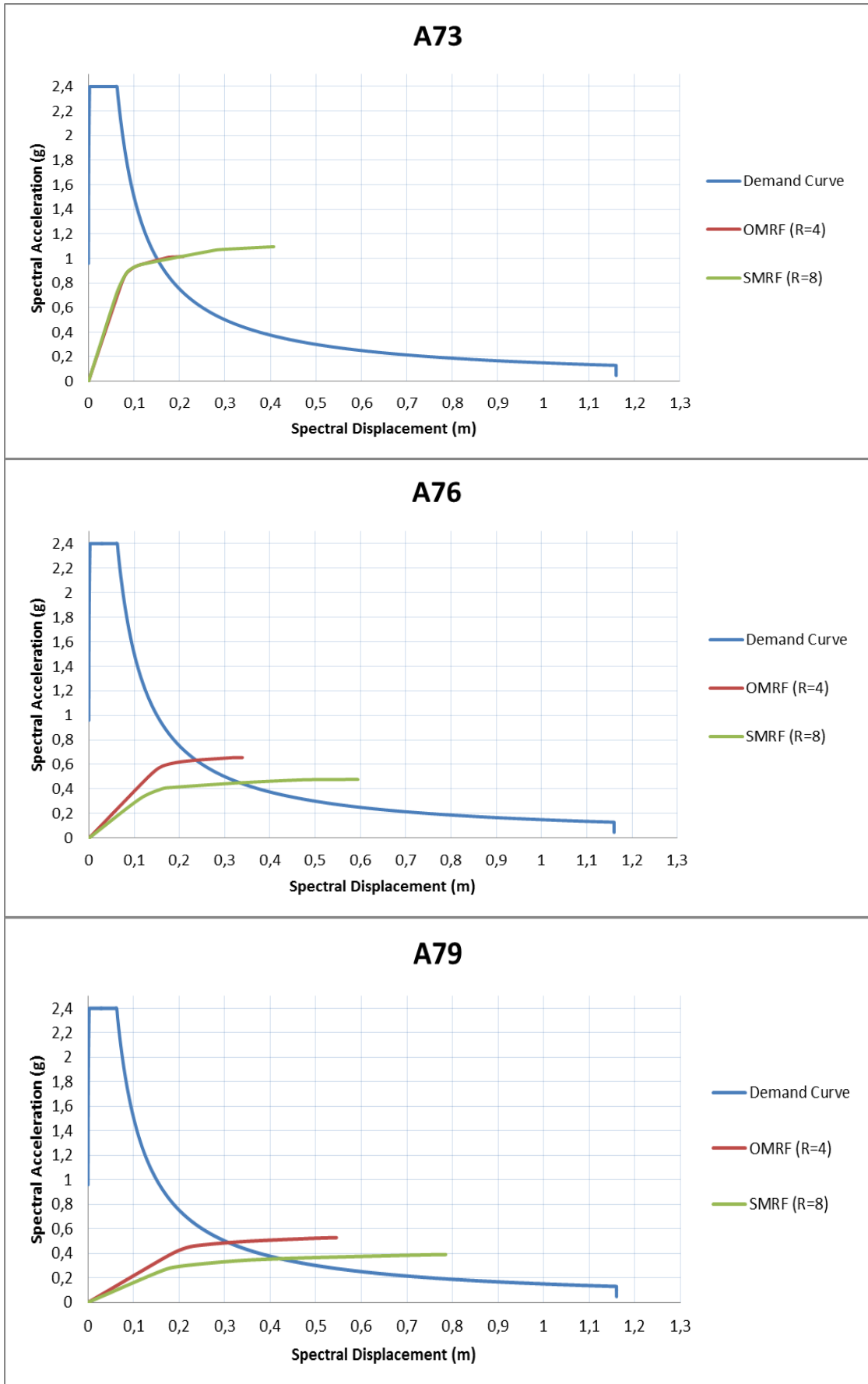


Figure C.5 Superimposing spectral capacity curves for 7-Span Frames

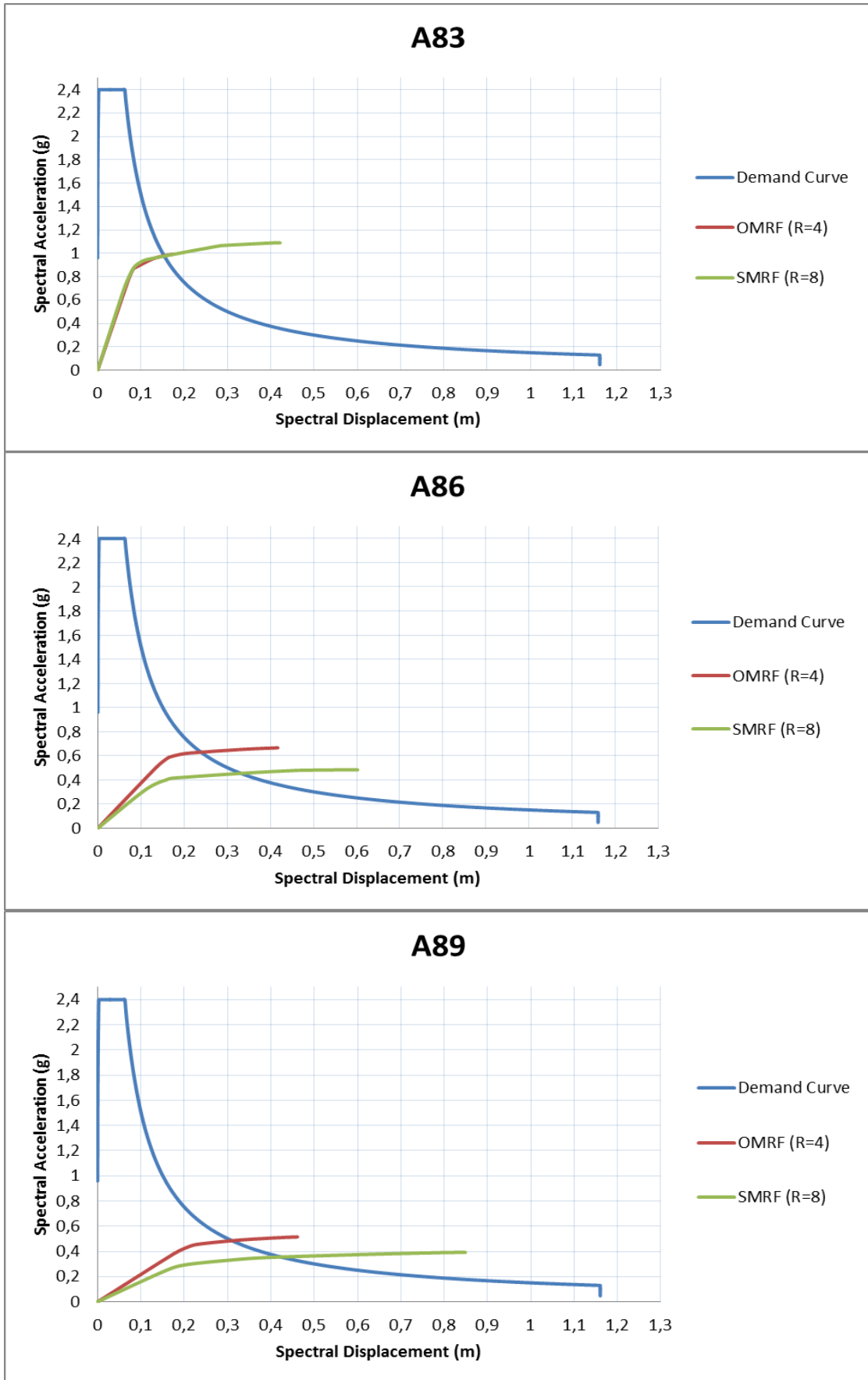


Figure C.6 Superimposing spectral capacity curves for 8-Span Frames